Development of a Control System for a Series-Parallel Plug-In Hybrid Electric Vehicle

DEVELOPMENT OF A CONTROL SYSTEM FOR A SERIES-PARALLEL PLUG-IN HYBRID ELECTRIC VEHICLE

BY

ALEXANDER MEYER LEBEL, B.Eng.

A THESIS

SUBMITTED TO THE DEPARTMENT OF COMPUTING & SOFTWARE

AND THE SCHOOL OF GRADUATE STUDIES

OF MCMASTER UNIVERSITY

IN PARTIAL FULFILMENT OF THE REQUIREMENTS

FOR THE DEGREE OF

MASTER OF APPLIED SCIENCE

Master of Applied Science (2017) McMaster University
(Software Engineering) Hamilton, Ontario, Canada

TITLE: Development of a Control System for a Series-Parallel Plug-In Hybrid Electric Vehicle

AUTHOR: Alexander Meyer Lebel
B.Eng., (Mechatronics Engineering)
McMaster University, Hamilton, Ontario, Canada

SUPERVISOR: Dr. Mark Lawford, Dr. Alan Wassyng

NUMBER OF PAGES: xxiii, 186

Lay Abstract

Compared to conventional combustion vehicles, an automobile with an electrified propulsion system has the potential to reduce fuel consumption and emissions due to the presence of an energy storage system and one or more electric machines. These benefits, however, come at the cost of increased control system complexity.

The question of how and when to use alternative energy sources – whether it be electrical or fuel energy – in a hybrid vehicle is at the epicenter of research and development initiatives in the automotive industry. Traditional heuristic methods have proven to be unstable due to their sensitivity to driving conditions and that optimal control policies require prior knowledge of the vehicle's route and destination, and therefore, are not suitable in most applications. Strategies which attempt to instantaneously minimize a vehicle's fuel or energy consumption, however, can overcome these aforementioned obstacles. As such, this area of research and development has received much interest.

The objective of this research was twofold: the first being to develop a control system for a series-parallel plug-in hybrid electric vehicle in a rational and systematic manner, and, secondarily, to evaluate the benefits of instantaneous minimization

methods for energy management.

Abstract

This thesis outlines the development of a control system for a series-parallel plug-in hybrid electric vehicle. The vehicle, developed at McMaster University for the EcoCAR 3 Advanced Vehicle Technology Competition, was produced in an effort to provide a Chevrolet Camaro with a high-performance, fuel efficient, hybrid powertrain.

A rational design methodology was adopted and guided the development of the control system and the implementation of its respective algorithms. A simulation tool was created using MATLAB and Simulink which, in turn, allowed for the effectiveness of the supervisory control logic to be evaluated by approximating the vehicle's energy consumption, fuel consumption, and emissions. The impact of hybridizing the vehicle's powertrain was similarly assessed by comparing it against its un-electrified counterpart, the 2016 Chevrolet Camaro LT.

A solution to the vehicle's energy management problem was proposed in the form of an Adaptive Equivalent Consumption Minimization Strategy (A-ECMS) which was then evaluated against more common heuristic approaches as well as non-adaptive instantaneous minimization methods. An artificial neural network was

selected as the strategy's adaptation mechanism and it was used to identify specific vehicular driving patterns in real-time. The neural network addresses many issues that arise due to the sensitivity of algorithms that attempt to solve the energy management problem without prior knowledge of the driving cycle.

The methods used during the process of the control system's verification and calibration are also discussed in this thesis and, in addition, encompass the use of software representations of the vehicle's Electronic Control Units (ECUs), the development of test cases, and the supervisory control software's evaluation in the Model-in-the-Loop (MIL), Software-in-the-Loop (SIL), and Hardware-in-the-Loop (HIL) environments.

Acknowledgements

This research was undertaken, in part, thanks to funding from the Natural Sciences and Engineering Research Council (NSERC), the Canada Excellence Research Chairs (CERCs) Program, and General Motors (GM).

I would like to thank my supervisors, Dr. Mark Lawford and Dr. Alan Wassyng, as well as Dr. Ali Emadi, for giving me the opportunity to pursue this research and making my stay at McMaster University an enriching one.

I would like to extend my gratitude to the members of the McMaster Engineering EcoCAR 3 Team and the McMaster Formula Hybrid Team, both past and present, for a remarkable three years. My time amongst you has changed me beyond what I could have possibly hoped for from my university experience. Not only have you all made me a better engineer, but you have you ignited in me a passion for learning, discovery, and innovation. Thank you.

Finally, I thank my parents, Pierre and Pauline Lebel, my friends, and my extended family for their continual guidance, support, and words of encouragement. None of this would have been possible without you.

Notations and Abbreviations

A-ECMS Adaptive Equivalent Consumption Minimization Strategy

ANL Argonne National Laboratory

AVTC Advanced Vehicle Technology Competition

BEV Battery Electric Vehicle

BMM Battery Management Module

CAFE Corporate Average Fuel Economy

CAN Controller Area Network

CERC Canada Excellence Research Chair

CFD Computational Fluid Dynamics

CG Center of Gravity

CO Carbon Monoxide

DP Dynamic Programming

ECM Engine Control Module

ECMS Equivalent Consumption Minimization Strategy

ECU Electronic Control Unit

EIA Energy Information Administration

EPA Environmental Protection Agency

ESS Energy Storage System

EV Electrified Vehicle

FCEV Fuel Cell Electric Vehicle

FMEA Failure Mode and Effects Analysis

FTA Fault Tree Analysis

GHG Greenhouse Gas

GM General Motors

GPS Global Positioning System

GREET Greenhouse Gas, Regulated Emissions and Energy Use in Transportation

HESS Hybrid Energy Storage System

HEV Hybrid Electric Vehicle

HIL Hardware-in-the-Loop

HSC Hybrid Supervisory Controller

HWFET Highway Fuel Economy Test

ICE Internal Combustion Engine

IEEE Institute of Electrical and Electronics Engineers

LHV Lower Heating Value

MABXII MicroAutoBox II

MCM Motor Control Module

MIL Model-in-the-Loop

MIS Module Interface Specification

NHTS National Household Travel Survey

NOx Nitrogen Oxide

NSERC Natural Sciences and Engineering Research Council

OOL Optimal Operating Line

OOP Optimal Operating Point

PCM Phase Change Material

PEU Petroleum Energy Use

PHEV Plug-In Hybrid Electric Vehicle

PID Proportional-Integral-Derivative

SAE Society of Automotive Engineers

SFTP Supplemental Federal Test Procedure

SIL Software-in-the-Loop

SOC State of Charge

SoftECU Software Representation of an Electronic Control Unit

STPA Systems Theoretic Process Analysis

TCM Transmission Control Module

THC Total Hydrocarbons

UCE Upstream Criteria Emission

UCMM Ultracapacitor Management Module

UDDS Urban Dynamometer Driving Schedule

UF Utility Factor

UMCM Ultracapacitor Master Control Module

VTS Vehicle Technical Specifications

WOT Wide-Open Throttle

WTW Well-to-Wheels

Contents

List of Tables

List of Figures

Chapter 1

Introduction

As global climate change continues to significantly affect the environment, presenting heightened environmental, socioeconomic and political concerns, demands from various governmental agencies, and several environmental advocacy groups are challenging industries and communities to reduce the causative and contributing factors to global warming and Greenhouse Gas (GHG) emissions.

For several generations, highly developed transportation networks have presented major innovations, improvements and resultant benefits in the movement of people and goods around the world. The rapid increase in transportation technologies during the last century, as well as the strong growth witnessed within the automotive industry, has had a negative affect on the environment. One of the greatest challenges facing today's society is the full understanding, appreciation, and unified response to the problem of climate change.

The past decade has witnessed governments, environmental regulatory agencies and the global community challenging the automotive industry to reduce petroleum consumption, and in turn, limit the volume of emissions produced by vehicles. Mandatory emissions and environmental controls present an opportunity to reduce further harm to the planet.

Through participation in the EcoCAR 3 Advanced Vehicle Technology Competition (AVTC), the McMaster Engineering EcoCAR 3 Team is working on the electrification of a Chevrolet Camaro in order to reduce its fossil fuel consumption. The purpose of this research was to develop the supervisory control system for said vehicle. This initiative, in part, will support the movement towards reducing the environmental impact of petroleum usage.

1.1 Vehicle Fuel Economy and Emissions Targets

It is undisputed that motorized vehicles collectively contribute to a number of important and pressing socioeconomic problems. In 2005, it was reported that the United States and China accounted for 25% and 15%, respectively, of the world's petroleum usage. Oil consumption within the United States has increased by approximately 40% since 1982; while the consumption of China and India has more than doubled over the same period [1]. The demand for petroleum is also expected to increase as new markets emerge and existing markets in developing countries expand. In addition, motorized vehicles are a major source of air pollution and a significant contributor to climate change, accounting for a large, and growing, share of GHG emissions worldwide. Much of the effort in reducing the fuel consumption and emissions of automobiles has been in the form of increasingly strict standards on new vehicles sold in developed countries.

In response to the growing concerns involving climate change, the Obama administration enacted, on May 29, 2009, a new program which adopted uniform federal standards to regulate both fuel economy and GHG emissions. This initiative has required that all vehicles with a model year between 2012 and 2016 meet an average fuel economy standard of 35.5 mpg by 2016. This was a significant increase from the former average of 25 mpg [2].

This program proved to be just the beginning of a major reform as President Obama announced on July 29, 2011 that an agreement with thirteen large automotive manufacturers had been made to increase the average fuel economy of cars and light-duty trucks to 54.5 mpg by the 2025 model year. Ford, General Motors (GM), Chrysler, BMW, Honda, Hyundai, Jaguar/Land Rover, Kia, Mazda, Mitsubishi, Nissan, Toyota, and Volvo, which together account for over 90% of all vehicles sold in the United States, all pledged to meet these new fuel economy targets [3]. This agreement brought about new Corporate Average Fuel Economy (CAFE) regulations for the 2017 to 2025 vehicle model years. It is anticipated that these new fuel economy standards will result in the conservation of billions of barrels of oil, the reduction of air pollution, and enable long-term planning for automakers. Table 1.1 specifies the projected fleet-wide emissions compliance targets as stated in the United States Environmental Protection Agency (EPA) Regulatory Announcement [4].

	2016	**2017**	**2018**	**2019**	**2020**	**2021**	**2022**	**2023**	**2024**	**2025**
Passenger Cars (g CO_2/km)	140	132	126	119	113	107	102	98	93	89
Light Trucks (g CO_2/km)	185	183	177	172	167	155	147	140	133	126
Combined Cars and Trucks (g CO_2/km)	155	151	144	138	132	124	118	112	106	101
Combined Cars and Trucks (mpg)	35.5	36.6	38.3	40	41.7	44.7	46.8	49.4	52	54.5

Table 1.1: Projected Fleet-Wide Emissions Compliance Targets

The regulatory pressure evidenced in North America has extended to other countries. Legislative policy makers continue to call for stricter limits placed on vehicle fuel economy, while countries such as India and China have proposed targets similar to those seen by the CAFE regulations. The enacted, and anticipated, fuel economy targets of several global regions are illustrated in Figure 1.1 [5]. The results are normalized to the standardized CAFE dynamometer test cycle.

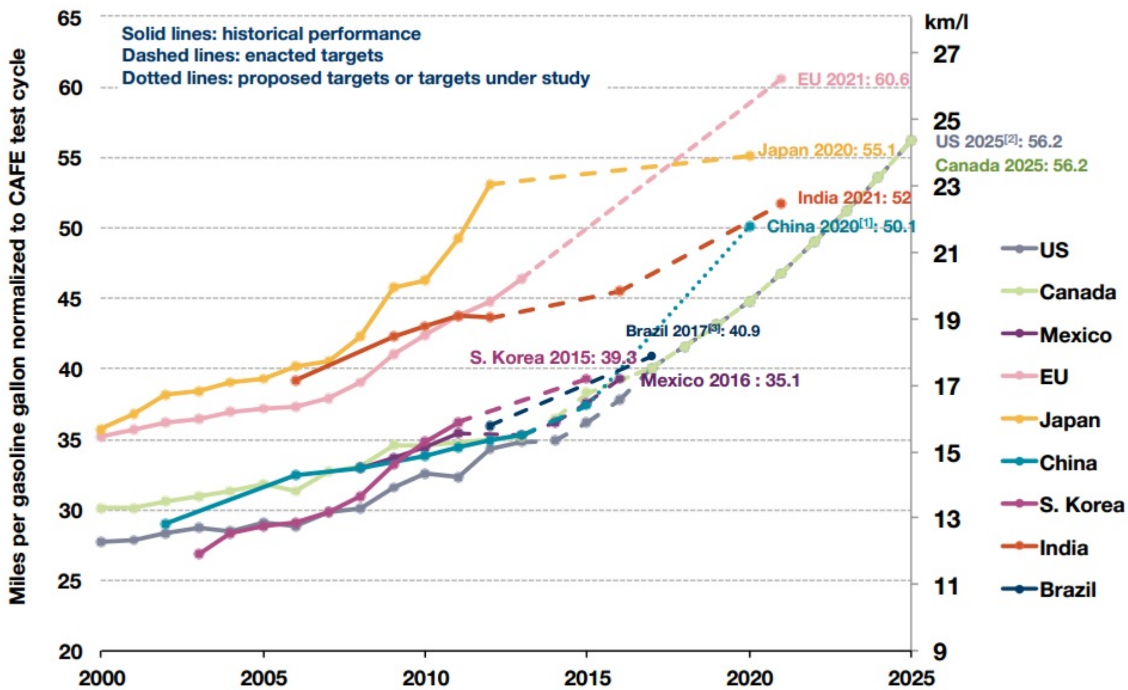

Figure 1.1: Global Fuel Economy Standards

Regulatory bodies have also enacted similar requirements for vehicle tailpipe emissions. A study conducted by the Energy Information Administration (EIA) found that the United States, a nation where 4% of the world's population resides, accounts for 24% of total global GHG emissions [1]. It is for this reason that criteria pollutants such as Total Hydrocarbons (THC) (similar to non-methane organic gases), Carbon Monoxide (CO), and Nitrogen Oxide (NOx) are explicitly controlled. The focus on improving a vehicle's fuel economy and reducing its emissions have led, in great part, to the research and development of Electrified Vehicles (EVs).

1.2 Current Automotive Electrification Trends

Legislation calling for lower emissions, the ever increasing cost of fuel, growing consumer expectations, and the realization that petroleum is a finite resource, have all led to a major reform in the automotive industry in the form of vehicle electrification. Although EVs have been around in some capacity for more than one hundred years, it was not until the last decade that the world has considered them to be a viable alternative to the traditional combustion vehicle. Currently, there are several variations of electrified transport, including: all-electric or Battery Electric Vehicles (BEVs), Hybrid Electric Vehicles (HEVs), Plug-In Hybrid Electric Vehicles (PHEVs), and Fuel Cell Electric Vehicles (FCEVs).

1.2.1 Battery Electric Vehicle

All-electric vehicles or BEVs use electric machines and the chemical energy stored in rechargeable battery packs instead of an Internal Combustion Engine (ICE) to provide tractive power. As no fuel is consumed in the operation of the vehicle, zero tailpipe emissions are produced (although emissions may be created in the generation of the electrical energy). BEVs often provide good dynamic performance (acceleration) but the lower specific energy of batteries compared to that of carbon-based fuels means that BEVs require battery packs that contribute significantly to the vehicle's mass and still provide a relatively low range. The perceived "range anxiety" of consumers has led to a slow adoption of BEVs and the investigation by automotive manufacturers into other, intermediate, technologies.

1.2.2 Hybrid Electric Vehicle

A HEV combines a conventional ICE with an electric propulsion system. The inclusion of the electrified powertrain is intended to achieve either better fuel economy of better performance than a combustion vehicle. HEVs may use their engine as a generator to produce electrical energy to either recharge their batteries or to power their electric machines. Significantly less emissions are produced by a HEV than a comparable combustion vehicle due to a number of efficiency-improving technologies. Since the ICEs within these vehicles are typically not used to provide tractive power they are smaller in size and geared to operate at maximum efficiency. Idle emissions may also be reduced through the use of start-stop systems where the ICE is shutdown and restarted as required. HEVs may also make use of regenerative-braking which converts the vehicle's kinetic energy into electrical energy, instead of it being wasted as heat as is the case with conventional brakes. This recovered energy may, in turn, be used to power the electric propulsion system. HEVs eliminate the issue of "range anxiety" associated with BEVs as the ICE may function as a range extender when the batteries are depleted.

1.2.3 Plug-In Hybrid Electric Vehicle

A PHEV shares many of the characteristics of a HEV, having a powertrain that incorporates both a conventional ICE and electric machines; and of a BEV, as it is able to recharge its Energy Storage System (ESS) by plugging it into an external power source. PHEVs share the same disadvantage with BEVs in that they require a large battery pack; but because of it, PHEVs can achieve a better fuel economy than a HEV. Like the HEV, PHEVs were developed in order to alleviate the concerns that consumers have concerning the limited range of BEVs.

1.2.4 Fuel Cell Electric Vehicle

A FCEV makes use of an electrified powertrain, accompanied by a fuel cell and an ESS. Fuel cells generate electricity, generally using oxygen from the air and compressed hydrogen, in order to power the vehicle's electric machines. The only byproducts of the chemical reaction are pure water and heat, meaning zero tailpipe emissions are produced. FCEVs are, however, not as effective as a BEV seeing as they consume twice a much energy due to the inefficacies involved with the electrolysis and storage of hydrogen [6].

Although a wide range of electrification technologies and ideologies exist, EVs of any sort will play a crucial role in decarbonizing the transport sector. In fact, the EPA estimates that if the adoption of electric or hybrid electric vehicles reaches a penetration of 30% market share by 2025, it could account for 25% of the total reduction in GHG emissions required from the United States transportation industry [1].

1.2.5 Vehicle Electrification for Dynamic Performance

Among the general public, automobile electrification is often synonymous with low dynamic performance. Many individuals are not willing to compromise their vehicle's top speed, or ability to accelerate and corner to improve its fuel economy. This belief, however, is a misconception. Due to the capacity of electric machines to provide near-instantaneous torque, BEVs are capable of achieving some of the fastest accelerations among any production vehicle. The Tesla Model S P100D, for instance, is capable of accelerating from rest to 100 km/h in less than 2.3 seconds [7].

BEVs do, however, have several features that detract from the obvious performance benefits of electric machines. To sustain their operation, BEVs are often equipped with large, and heavy, ESSs. These ESSs are capable of achieving weights in excess of 500 kg, which in conjunction with heavy electric motors and inverters, add a significant load to the vehicle [8]. In addition, many of the electric machines used in consumer automobiles are not capable of producing enough power to achieve top speeds that rival those of high performance combustion vehicles.

HEVs and PHEVs are, however, able to realize the benefits of both electric machines and the ICE for achieving high levels of dynamic performance. In these vehicles, electric motors are used to facilitate fast accelerations and the engine is capable of producing the power necessary for top speeds not achievable by BEVs. The McLaren P1, Porsche 918 Spyder, and Ferrari LaFerrari are three of the highest performing vehicles that are commercially available, and each is either a HEV or a PHEV. The technical specifications of the Tesla Model S P100D, McLaren P1, Porsche 918 Spyder, and Ferrari LaFerrari are provided below in Table 1.2 [7] [9] [10].

	Vehicle			
Specification	**Tesla Model S P100D**	**McLaren P1**	**Porsche 918 Spyder**	**Ferrari LaFerrari**
Engine	N/A	3.8 L Bi-Turbo V8	4.6 Litre V8	6.3 Litre V12
Total Power	507 kW	673 kW	661 kW	708 kW
Total Torque	1072 Nm	979 Nm	1274 Nm	899 Nm
Curb Mass	2,219 kg	1,395 kg	1,634 kg	1,345 kg
Acceleration, IVM – 100 km/h	2.3 s	2.8 s	2.5 s	2.9 s
Top Speed	249 km/h	344 km/h	349 km/h	351 km/h

Table 1.2: Performance Vehicle Technical Specifications

1.3 EcoCAR 3 Competition

One of the earliest, and most prestigious, programs in the automotive industry to address environmental concerns is the AVTCs program. At the core of AVTCs is the effective collaboration of the United States government, the automotive sector, and a number of North American academic institutions. The primary focus has been to provide a realistic training platform for university students across a multitude of disciplines to apply modern technology and implement innovative concepts into a re-engineered production vehicle. Through participation in AVTCs, students learn how to work in interdisciplinary teams, on real-world problems, in order to comply with future market demands. These demands include, but are not limited to, stringent emission standards, cost targets, safety regulations, consumer appeal, energy consumption, and performance requirements [11].

The current AVTC, EcoCAR 3, was launched in the fall of 2014 and marks the 26$^{\text{th}}$ anniversary of the program. Sixteen North American universities participated in the competition with the objective of re-engineering a 2016 Chevrolet Camaro LT so that it may meet future market requirements such as energy efficiency, cost, and performance. The overarching goal was to maintain the Camaro's powerful muscle car image by implementing high performance electrification technologies, while minimizing its environmental impact through the implementation of an advanced and more efficient powertrain [11].

The EcoCAR 3 competition was held over a period of four years and was designed to follow a very similar vehicle development process to that which is commonly used in the automotive industry. This format introduced students to the process of how vehicles are designed before they are brought to market. By using the 2016 Chevrolet Camaro LT's performance as a benchmark, each team's goals for their respective vehicle were determined early in the process and the timeline was set using major milestones for each year of the competition. In its second year, teams received their Camaro with the goal of integrating their vehicle's powertrain as designed in year one of the competition. The third year of EcoCAR 3 focused on the refinement of the mechanical, electrical and control systems such that the vehicle is in a near-complete state. By the end of the fourth year it is intended that the vehicle should operate as envisioned and be tested as if it were being prepared for production [12].

McMaster University was honoured for its acceptance as one of the two Canadian institutions to compete in the EcoCAR 3 competition. Since the 1980s, McMaster University has participated in a variety of Society of Automotive Engineers (SAE) challenges such as Formula SAE, Formula Hybrid, Mini Baja, and Solar Car. With the Canada Excellence Research Chair (CERC) in Hybrid Powertrain Program that was launched in 2011 at McMaster University, the institution has experienced a transition to increased undergraduate student development and experiential learning in addition to research excellence [13]. As a result, McMaster's automotive research efforts shifted towards leadership in advanced electrified powertrain development. The new orientation led to rapid recognition from the automotive industry and established professional engineering societies such as the SAE and the Institute of Electrical and Electronics Engineers (IEEE). With McMaster University's acceptance to the premier North American advanced vehicle competition, the McMaster Engineering EcoCAR 3 Team intended to create the next generation of technical leaders in vehicle electrification and showcase the ingenuity of Canadian engineering.

1.4 Research Objective and Scope

The objective of this thesis was to develop the control system for the McMaster Engineering EcoCAR 3 Team's Camaro E/28 (the team's entry to the EcoCAR 3 competition) and to investigate the impact of the vehicle's powertrain and control strategies on its fuel economy and performance. The contributions made as a result of this research include:

1. The development of the vehicle model that was used to evaluate the Camaro E/28's fuel and energy consumption, production of emissions, and dynamic performance.
2. The selection of the Electronic Control Units (ECUs) that support the vehicle's hybrid powertrain architecture.

3. The re-design of the 2016 Chevrolet Camaro LT's control system's communication/control network to allow for the introduction of additional ECUs.
4. The development of the Camaro E/28's supervisory control software, including:
   - i A novel implementation of the Adaptive Equivalent Consumption Minimization Strategy (A-ECMS) using an artificial neural network as an adaptation mechanism.
   - ii Startup procedures featuring concurrent operations that allow for rapid attainment of propulsion readiness.
   - iii Logic that identifies the vehicle's ideal mode of operation for meeting efficiency, performance, drivability, and safety objectives.
   - iv Logic that determines an efficient power split for each of the vehicle's modes of operation.
   - v The optimization of the vehicle's gear selection schedules.
5. The development of Software Representations of Electronic Control Units (Soft-ECUs), test cases, and several other model-based design techniques to facilitate the verification and calibration of the vehicle's supervisory control software in several testing environments.
6. An analysis of the A-ECMS and its impact on the vehicle's fuel and energy consumption, and production of emissions.
7. An analysis of the impact that electrification technologies had on the fuel and energy consumption, production of emissions, and dynamic performance of the 2016 Chevrolet Camaro LT.
8. A comparison of the Camaro E/28's dynamic performance to that of the 2016

Chevrolet Camaro LT and the 2015 Chevrolet Camaro Z/28.

This thesis also includes discussions on the the selection of the Camaro E/28's hybrid powertrain architecture but it should not be considered within the scope of the author's research.

The development of the Hybrid Energy Storage System (HESS) model, as described in Chapter 4, was a result of the joint research efforts of Tyler Stiene and the McMaster Engineering EcoCAR 3 Team. For additional information concerning the model, please refer to Stiene's thesis: "Analysis of a Hybrid Energy Storage System and Electrified Turbocharger in a Performance Vehicle" [14].

Chapter 2

Literature Review

The design of the control system for any vehicle is a complex task that requires extensive forethought, discipline, and iterative development. The need for some form of rational design process and development cycle is, therefore, essential. In addition, as the impact that control algorithms have on a vehicle's performance has become more apparent over time, the automotive industry has responded by adopting a model-based design approach which allows for the development and testing of software to be conducted in simulation environments. The implementation, calibration, and validation of these algorithms outside of the vehicle has thereby drastically reduced development time and costs.

2.1 Rational Design Process

Ideally, engineers should design systems in a rational and systematic way, however, this is rarely the case. Designers will typically start with a clear statement of desired objectives, behaviours, and implementation constraints but they subsequently make a series of design decisions without explanation for their rationale. David Parnas and Paul Clements, in their definitive paper "A Rational Design Process: How and Why to Fake It," explain that the design process will never proceed in a "rational" manner, due to the following reasons [15]:

- The individuals who commission a system are unsure of their desires or are unable to convey all that they know.
- Even if the requirements are established, many details only become known as progress is made during implementation.
- It is impossible to fully comprehend the plethora of details that must be taken into account in order to design and build a system correctly.
- All but the most trivial projects are subject to change for external reasons and some of these changes may invalidate previous decisions.
- Human errors can only be avoided if one can avoid the use of humans.
- Designers are often burdened by preconceived ideas.
- For economic reasons, designs may be reused from some other project. These designs were, therefore, not developed based on the requirements alone.

An engineer being able to derive a design in a rational, error-free way from a statement of requirements, therefore, appears to be unrealistic. Good engineering practices, however, demand that there is still merit to attempting to follow an ideal design process and to produce the documentation that makes it appear as though they have. For the following reasons, a rational design process should be "faked" [15]:

- Designers need guidance.
- A rational design will be more achievable if the process is followed rather than produced on an ad hoc basis.
- A well documented design makes it possible to transfer people, ideas, and software between projects.
- It becomes simpler to measure the progress of a project if an ideal process is agreed upon.

Designing a system in a rational way is a difficult, nearly impossible, process. Doing so will, however, result in a product that can be easily understood, maintained, and reused. For these reasons, automotive manufacturers continue to adhere to, or at the very least attempt to fake, an ideal software design process as described below:

1. Establish and Document Requirements
2. Design and Document the Modular Structure
3. Design and Document the Module Interfaces
4. Design and Document the Uses Hierarchy
5. Design and Document the Module Internal Structures
6. Implement Software
7. Maintain Software

2.2 V-Model Development Cycle

The V-Model defines the necessary steps to successfully design, develop, and validate a control system. Unlike the traditional “waterfall” approach, the V-Model demonstrates the relationships between each phase of the development life cycle and its associated phase of testing [16]. Figure 2.1, below, provides a graphical representation of the V-Model development cycle.

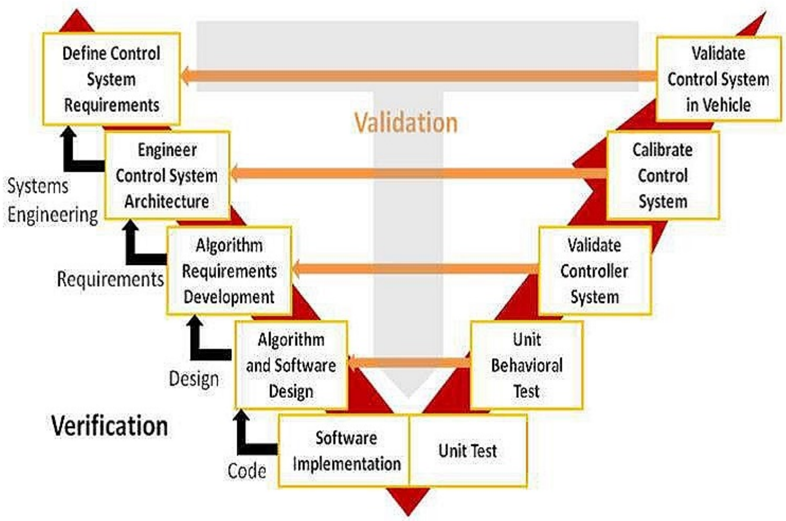

Figure 2.1: V-Model Development Cycle

The horizontal and vertical axes represent time or project completeness (left-to-right) and the level of abstraction (coarsest-grain abstraction uppermost), respectively. The left-hand side of the model consists of defining requirements, designing subsystems, and implementation, while the right-hand side involves the testing and validation for each of these steps.

The secondary process workflows, designated by the black and orange arrows in Figure 2.1, are of particular importance to the V-Model development cycle. The black arrows represent the verification process, or the comparison of each step to the defining requirements of the step that preceded it. For instance, after a control algorithm has been developed during the *Algorithm and Software Design* phase is must first be verified that it meets the requirements that were set forth at the *Algorithm Requirements Development* step before proceeding to *Software Implementation*. The orange arrows, on the other hand, denote the process of validation. The algorithms that were developed during the *Algorithm and Software Design* phase must be validated using a *Unit Behaviour Test* before preceding to the *Validate Controller System* stage. If this process fails, the algorithm must be redesigned and all subsequent tasks must be performed once again.

The V-Model development cycle is an industry accepted practice and has been a staple in the development of control systems for many years.

2.3 Model-Based Design

Model-Based design is a process that enables fast and cost-effective development of dynamic systems, including control systems. In model-based design, a plant model is at the center of the development process, from requirements specification through design, implementation, and testing.

Model-Based design has forever changed the way engineers work by allowing for design tasks to be relocated from the lab or field to the desktop. Software is no longer required to be handwritten in C or Assembler code but may be developed using a graphical language such as MATLAB/Simulink, Statemate, LabView, or similar tools [17] [18] [19]. The executable binaries may then be automatically generated for embedded deployment and verified using simulated test benches, thereby saving time and engineering costs. Additionally, model-based design environments support the separation of concerns and improves the modularity and reusability of software by allowing for the development to occur at a higher level of abstraction [20].

The advantages of the model-based design paradigm are numerous, and include [21]:

- The ability to link design directly to requirements.
- The use of a common design environment that facilitates communication, analysis, and testing between various development groups.
- Design reuse for derivative systems.
- The ability to automatically generate embedded software and documentation.
- Verification without threat to the system and environment through the use of simulation-based testing.

Large software intensive systems, such as automobiles, are notoriously difficult to test given their dynamic reactions and safety-critical behaviour. The use of model-based design's simulated environments allows for the verification and validation of a system by systematically assessing its performance and robustness through various testing environments. The testing applied to control systems developed using a model-based design methodology are commonly referred to as: Model-in-the-Loop (MIL) simulation, Software-in-the-Loop (SIL) simulation, and Hardware-in-the-Loop (HIL) simulation. These testing environments support the (V-Model) development cycle as illustrated by Figure 2.2 [22].

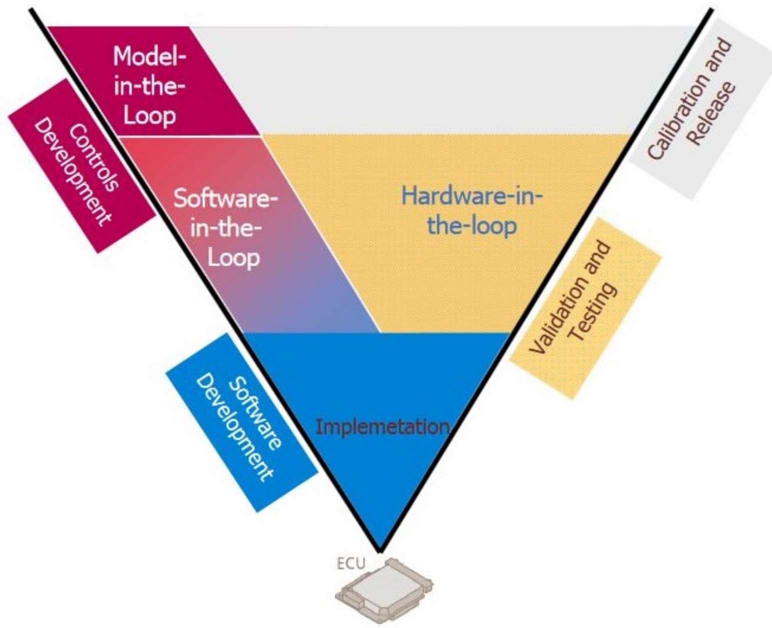

Figure 2.2: Model-Based Development Cycle

2.3.1 Model-in-the-Loop Simulation

MIL simulation is a technique that is used in the development of a model of a physical system and is unconstrained by hardware or computer processing power. The purpose of MIL simulation is to verify the validity of a model and to judge its approximation to the physical system. MIL simulation may include high fidelity plant models that require extensive computing resources, since there is no requirement for the simulation to be executed in real-time.

2.3.2 Software-in-the-Loop Simulation

SIL simulation is a technique used to validate that an executable generated from a controller model is able to govern the simulated system as intended. The model remains unconstrained by hardware and processing power, as was the case in MIL simulation, but additional characteristics of the physical system are included such as: message latency, electrical noise, and non-idealized input and output signals. The software's algorithms, fault detection and mitigation, and ability to control the plant model are all evaluated using a variety of test cases. SIL simulation is an ideal approach when attempting to determine that the software under development meets its designated requirements.

2.3.3 Hardware-in-the-Loop Simulation

HIL simulation is a technique used to validate that an executable generated from a controller model performs as desired when running on its intended platform. The software under test is now subject to the constraints of the physical hardware it has been designed to run on. Both the simulated physical system and its control logic are required to execute in real-time and are constrained by the computing resources available to them. The HIL simulation setup will typically involve a HIL simulator and an ECU. The purpose of HIL simulation is to identify issues with software, and with its interfaces to the physical system, early in the development cycle, thereby respecting quality requirements and time-to-market restrictions.

2.4 Impact of Supervisory Control

Compared to conventional vehicles, an automobile with an electrified powertrain has the potential to reduce fuel consumption and emissions due to the presence of a bidirectional ESS and one or more electric machines. The addition of these devices allows for the reduction of idle emissions through start-stop systems, regenerative braking, and the potential for engine downsizing. These benefits, however, come at the cost of increased control complexity.

In a HEV or PHEV, the driver's power demand may now be met by one, or a combination of, the vehicle's on-board energy sources. The dilemma of how to split the power demand between the ICE and the electric machines, with the intent of minimizing fuel consumption and emissions without compromising drivability, is what has become known as the "energy management problem" [23].

The energy management problem seeks to determine the power flows from a vehicle's engine and electric machines so as to maximize its performance as defined over a period of time. Several methods have been proposed for determining an efficient power split and may be classified according to the following techniques [24]:

- Numerical methods for global optimization
- Numerical methods for local optimization
- Analytical optimization methods
- Instantaneous minimization methods
- Heuristic methods

The achievable improvement in fuel economy due to vehicle electrification depends strongly on the degree of electrification and on the driving cycle. Realistic estimates range from below 10% for mild hybrids to more than 30% for highly hybridized vehicles [23]. This potential can be realized only with a sophisticated control system that attempts to optimize for the energy management problem.

2.5 Summary of Literature Review

Within the last several years, the share of software controlled innovations within the automotive industry have increased drastically, and continues to increase. With the widespread adoption of EVs and the advent of autonomous vehicle technologies, the impact that software will have on industry, transportation and general public life is immeasurable. The need for a rational design process and an established development cycle when designing control systems has never been more apparent. Fortunately, the widespread adoption of model-based design techniques has improved the safety of these systems while allowing automobile manufactures to introduce "greener" vehicles more quickly and to satiate the consumer's desire for new and exciting technologies.

Chapter 3

Vehicle Architecture

The McMaster Engineering EcoCAR 3 Team's design philosophy was to redefine the American Muscle car by producing a high performance, hybrid electric, Chevrolet Camaro. The Camaro E/28 was designed as a performance vehicle with the capability of achieving the economic benefits expected of a hybrid. The Camaro E/28, as the name suggests, was designed to be the hybrid electric equivalent of GM's "ultimate track-capable Camaro" [25], the Chevrolet Camaro Z/28.

When asked about fuel economy, Al Oppenheiser, chief engineer of the 2016 Chevrolet Camaro, stated, "On the list of top ten reasons why people buy Camaros, fuel economy is 23. For a Z/28 buyer it's probably at about 30 or 40" [26]. This was meant in jest, but it does truly reflect the public perception of performance versus fuel efficiency. Consumers believe that in order to have fuel efficiency with an electrified powertrain, a vehicle needs to be underpowered. Exotic sports car manufacturers like Porsche (918 RSR), McLaren (P1), Ferrari (LaFerrari) and BMW (i8) are proving that EVs are able to not only achieve high levels of efficiency, but also incredible performance.

Just as the Chevrolet Camaro Z/28 served as a testament to the expertise of Chevrolet, the McMaster Engineering EcoCAR 3 Team hoped to demonstrate that, like exotic sports car manufacturers, even “old school” American Muscle can be brought into the twenty-first century. By implementing a high power, high torque, electrified powertrain, the team hoped to achieve Vehicle Technical Specifications (VTS) that approach that of the Chevrolet Camaro Z/28.

3.1 Consumer Market Research

During Year 1 of the EcoCAR 3 competition, the McMaster Engineering EcoCAR 3 Team conducted a consumer market research report in which it was determined that for the Camaro to remain viable in the near future the fuel economy would need to be greatly improved without sacrificing its dynamic performance. A hybridized Camaro could meet the stringent CAFE fuel economy targets well into the future; however, vehicle electrification results in a significant price premium over its equivalent conventional counterpart. To make the vehicle both viable from a regulatory and a consumer point of view, an electrified Camaro must, therefore, offer something more than improved fuel economy. It was concluded that a hybrid Camaro could be designed with technical specifications approaching that of the Chevrolet Camaro Z/28 which would offer consumers high performance without paying for it at the pump.

3.2 Vehicle Technical Specifications

While selecting the powertrain for the Camaro E/28, a VTS was generated by simulating a vehicle model over multiple driving cycles, with varying parameters, to better understand the requirements of certain architectures. The team also used the target VTS specified by the EcoCAR 3 rules as a baseline reference. The result was a VTS with similar energy and fuel consumption targets to those specified by the competition but with a focus on significantly better vehicle performance. The VTS targets for the Camaro E/28 are provided by Table 3.1. The first two columns of the table illustrate the minimum requirements and desired specifications for the vehicle, as designated by the EcoCAR 3 competition, while the third column lists the targets set forth by the McMaster Engineering EcoCAR 3 Team.

	EcoCAR 3		Camaro E/28
Specification	**Requirement**	**Target**	**Target**
Acceleration, IVM – 100 km/h	7.9 s	5.9 s	5.0 s
Acceleration, 80 – 110 km/h	9.9 s	7.3 s	2.5 s
Braking, 100 – 0 km/h	41 m	39 m	39 m
Acceleration Torque Split (Front/Rear)	49% F, 51% R	0% F, 100% R	0% F, 100% R
Lateral Acceleration	0.80 G	0.85 G	0.85 G
Double Lane Change	84 km/h	88 km/h	88 km/h
Highway Gradeability	6% at 100 km/h	6% at 100 km/h	6% at 100 km/h
Curb Mass	2010 kg	1910 kg	1900 kg
Starting Time	15 s	2 s	2 s
Total Vehicle Range	240 km	–	320 km
Electric-Only Range	N/A	–	20 km
UF-Weighted Fuel Energy Consumption	N/A	–	550 Wh/km
UF-Weighted Electric Energy Consumption	N/A	–	150 Wh/km
UF-Weighted Total Energy Consumption	840 Wh/km	700 Wh/km	700 Wh/km
UF-Weighted WTW Petroleum Energy Use	750 Wh PE/km	420 Wh PE/km	420 Wh PE/km
UF-Weighted WTW Greenhouse Gas Emissions	250 g GHG/km	225 g GHG/km	225 g GHG/km

Table 3.1: Vehicle Technical Specification Targets

In order to achieve the performance goals, the team designed a P1-P2 series-parallel hybrid electric vehicle architecture. The Camaro E/28's powertrain consisted of two YASA-P400 HC electric motors in the P1-P2 parallel positions and a GM 2.0 litre LTG turbocharged inline-4 engine fueled with E85. The P1 position signifies the first electric motor's placement on the accessory side of the ICE while the P2 designation indicates that the second machine is located prior to the input of the transmission. The electric motors were powered via a combination of ultracapacitors and batteries referred to as a HESS. The Camaro E/28's powertrain architecture is illustrated below in Figure 3.1 and an image of its final assembly is presented in

Figure 3.2.

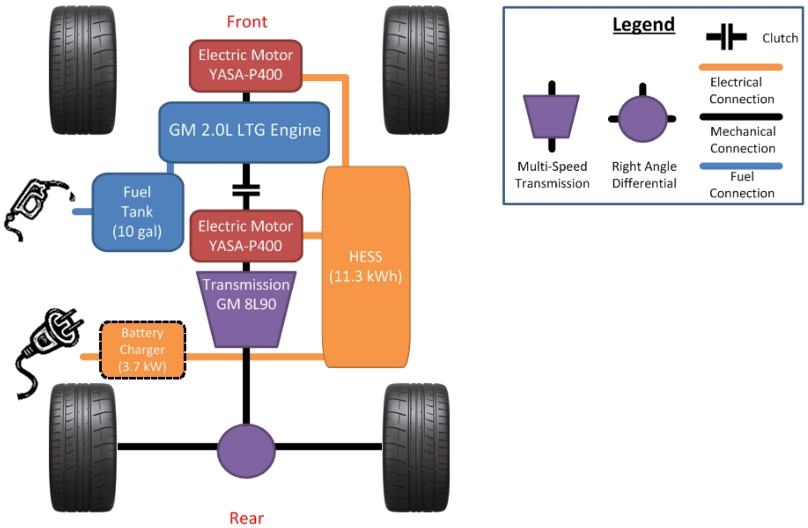

Figure 3.1: P1-P2 Series Parallel Powertrain Architecture

Figure 3.2: Camaro E/28 Assembled Powertrain

3.3 Powertrain Components

Component selection was a crucial task in the development of the powertrain architecture, and only industry leading components and technologies were capable of achieving the vehicle's desired performance.

3.3.1 YASA-P400 HC Electric Motors and PM150DZR Inverters

The hybrid architecture of the Camaro E/28's powertrain required two YASA-P400 HC electric motors in a P1-P2 parallel configuration. The P2 motor served as the vehicle's primary source of tractive power in the electric and series modes of operation (henceforth referred to as "drive modes"). It also provided the vehicle with regenerative braking capabilities. The P1 electric motor, on the other hand, was used to start and stop the engine, aid the engine in matching the speed of the P2 motor when transitioning into the parallel drive mode, and to recover electric energy while in the series drive mode. While the vehicle was in the parallel drive mode, both the P1 and P2 electric motors provided tractive power along with the ICE. An image of the YASA-P400 HC electric motor is provided below in Figure 3.3.

Figure 3.3: YASA-P400 HC Electric Motor

YASA motors and generators are the smallest and lightest in their class. Based on YASA's unique yokeless and segmented armature topology, the motors use fewer materials and operate more efficiently in order to provide higher torque and power densities than any comparable motor or generator [27]. The YASA-P400 HC makes use of both rotor and stator cooling allowing for higher peak and continuous delivery of torque and power. A performance summary of the YASA-P400 HC at 350 V_{DC} and 450 A_{RMS} is provided by Table 3.2 [28].

Characteristic	**Performance**
Power	
Peak	145 kW
Continuous	100 kW
Torque	
Peak	390 Nm
Continuous	300 Nm
Speed	0 RPM – 8,000 RPM

Table 3.2: YASA-P400 HC Performance Summary

The inverters that were selected to control the YASA-P400 HC motors are the PM150DZR from Rinehart Motion Systems. The PM family of propulsion inverters are specifically designed for on and off-road EVs or HEVs and the PM150DZR is intended for motorsport and other high performance vehicle applications such as LeMans LMP prototype racing, Formula 1, and Formula E [29]. Table 3.3 provides a summary of the PM150DZR's capabilities [30].

Characteristic	**Performance**
Operating Voltage	50 V_{DC} – 800 V_{DC}
Motor Current	
Peak	300 A_{rms}
Continuous	225 A_{rms}
Output Power	
Peak	150 kVA

Table 3.3: Rinehart Motion Systems PM150DZR Performance Summary

3.3.2 GM LTG Internal Combustion Engine

The GM LTG is a 2.0 litre, turbocharged, four-cylinder Ecotec engine designed for greater efficiency. The turbocharger is capable of generating up to twenty pounds of boost and its twin-scroll design helps eliminate turbo lag while supplying a broad power band. This permits the LTG to respond rapidly to throttle input, a quality often associated with higher displacement, naturally aspirated, engines [31]. The GM LTG ICE is illustrated in Figure 3.4.

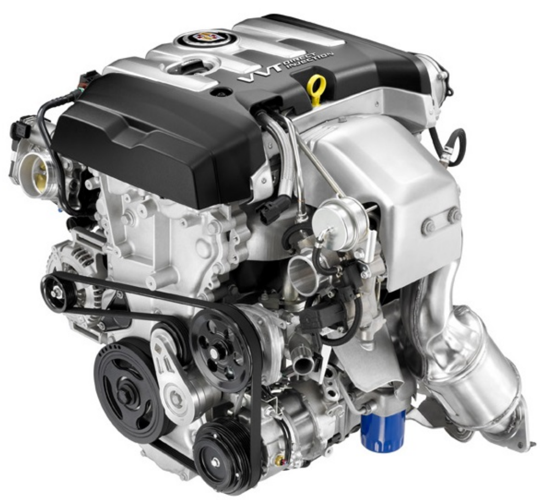

Figure 3.4: GM LTG Internal Combustion Engine

The LTG is rated at 247 horsepower at 5,400 RPM and 400 Nm at 2,500 RPM. The engine's torque curve is broad and flat, delivering 90% or its peak torque between the speeds of 1,700 RPM and 5,500 RPM. The torque and power curves of the GM LTG ICE are provided below in Figure 3.5.

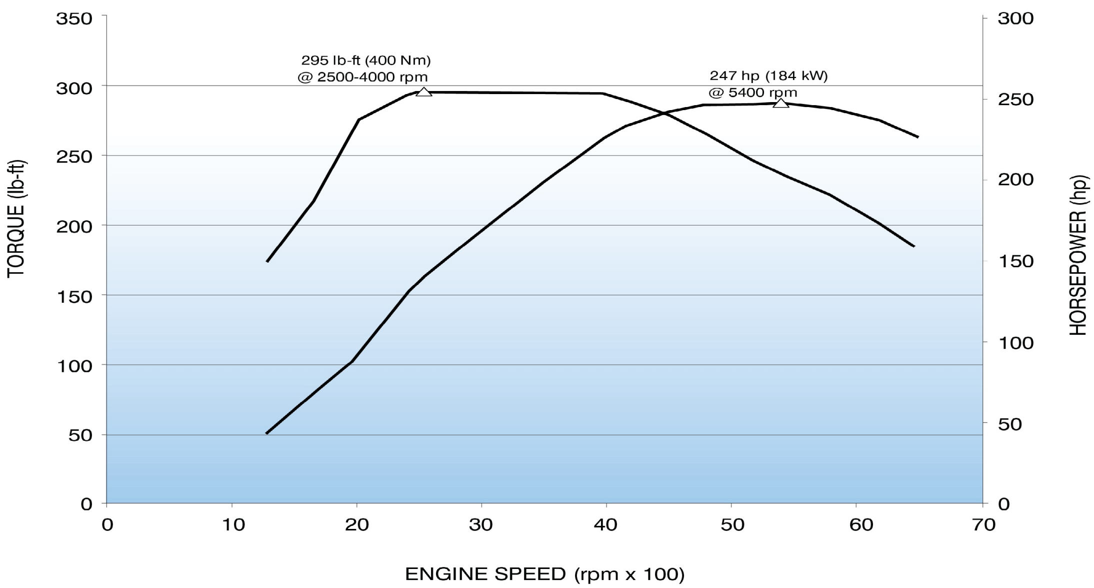

Figure 3.5: GM LTG Torque and Power Curves

The Camaro E/28 was designed with the intention of being a flexible-fuel automobile. A flexible-fuel vehicle (colloquially called a flex-fuel vehicle) is equipped with an ICE designed to run on more than one fuel, usually gasoline blended with either ethanol or methanol. Flex-fuel engines are capable of burning any proportion of the resulting blend up to 85% (E85) [32]. As such, the Camaro E/28's LTG ICE has been converted to allow for flex-fuel capabilities. When fueled with E85, the engine is capable of producing 390 horsepower and 490 Nm [33].

3.3.3 GM 8L90 Transmission

The Hydra-Matic 8L90 is an electronically controlled eight-speed automatic transmission developed and produced by GM for use in rear and rear-biased all-wheel-drive vehicles with a longitudinal powertrain orientation. The 8L90 transmission is expected to contribute up to 5% greater efficiency, when compared with a six-speed automatic [34]. An image of the GM 8L90 transmission is presented in Figure 3.6.

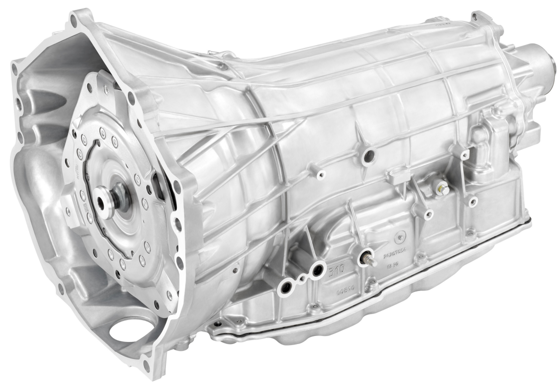

Figure 3.6: GM 8L90 Transmission

Smaller steps between subsequent gearing ratios allows the vehicle's powertrain to operate at optimal points within its speed band, making the most of its power and torque, to improve performance and efficiency. The gearing ratios for the GM 8L90 transmission are provided by Table 3.4.

Gear	**1**	**2**	**3**	**4**	**5**	**6**	**7**	**8**	**Reverse**
Ratio	4.56	2.97	2.08	1.69	1.27	1	0.85	0.65	3.82

Table 3.4: GM 8L90 Gear Ratios

The 8L90 uses variable force solenoids and other control components to monitor clutch pressures with optimum accuracy. The result is faster and more precise shifts that rival the dual-clutch/semi-automatic transmissions found in many supercars. The 8L90 has an impressive torque capacity of 1000 Nm and matched that of the Camaro E/28's powertrain.

3.3.4 Hybrid Energy Storage System

In lieu of a conventional ESS, in which a single battery type or capacitor is used to store energy, a HESS attempts to combine two or more energy storage technologies, with supplementary operating characteristics (such as energy and power density, self-discharge rate, efficiency, lifetime, etc.), in order to achieve a solution not feasible by any one component [35].

For most applications, a HESS will combine Li-ion batteries with ultracapacitors. Compared to batteries, ultracapacitors have a high power density (but a lower energy density) and superior low-temperature performance [36]. Additionally, the life of an ultracapacitor is much longer than that of a battery, exceeding over one million cycles [37]. The combination of the two inherently offer better performance as each offsets the other's weaknesses. In addition, since a HESS offers higher power densities than a conventional ESS, it will allow for the implementation of smaller battery packs which can drastically reduce the weight and cost of the system. Figure 3.7, below, features a Ragone Chart, which illustrates the comparison of energy and power densities of conventional batteries to that of ultracapacitors [38].

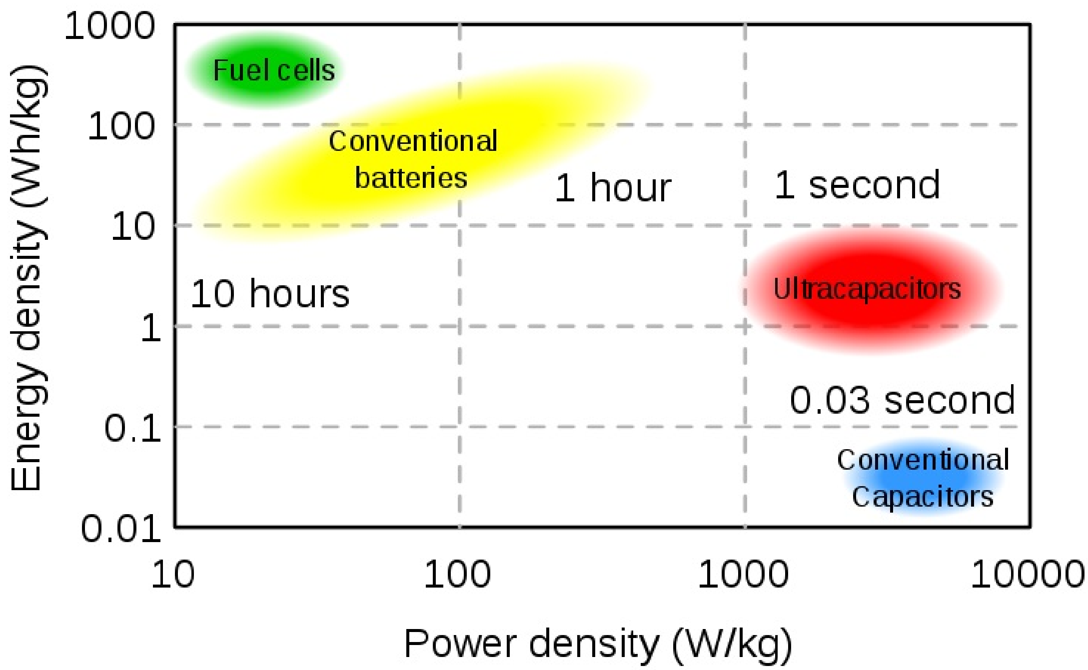

Figure 3.7: Ragone Chart Comparing Conventional Batteries to Ultracapacitors

Several configurations for HESS designs have been proposed with varying levels of complexity. Based on the use of power electronic converters in the configurations, a HESS can be classified into two types: passive or active. Conventional active methods use one or more DC/DC converters to interface the energy storage devices to the DC bus [36]. The topology of the Camaro E/28's HESS is the battery/ultracapacitor active parallel configuration illustrated in Figure 3.8.

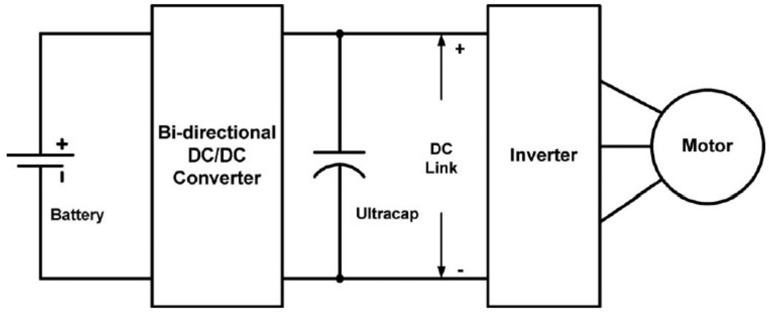

Figure 3.8: Active Parallel HESS Topology

In this type of active parallel topology, the battery pack is connected through a DC/DC converter to the ultracapacitor bank which is, in turn, linked to the DC bus. In this case, since the battery pack is decoupled from the DC link, a battery with a lower voltage may be used. This HESS configuration also allows the use of a smaller DC/DC converter since the battery pack supplies most of the constant power. The ultracapacitors act as a low-pass filter, minimizing the number of cycles that the battery pack will experience, thereby extending the system's overall life. It is important to note that the State of Charge (SOC) of the ultracapacitors determine the operating voltage of the vehicle's primary DC bus.

The Camaro E/28's HESS combines Nickel Manganese Cobalt Li-ion batteries from LG Chem with a novel lithium-doped ultracapacitor technology from JM Energy [39] [40]. A DC/DC converter from BRUSA Elektronik is used to transfer energy between the two energy storage components [41]. Table 3.5, below, lists the specifications of the Camaro E/28's HESS.

	Battery Pack	**Ultracapacitor Pack**	**HESS**
Cells	LG Chem 18650 HG2	JSR Prismatic 3300c	
Configuration	84s12p (6x14s12p)	108s (9x12s)	
Chemistry	NMC	Li-Ion Ultracapacitor	
Voltage	352 – 168 V	410 – 237 V	400 – 237 V
Current	240 A	360 A	600 A
Pack Resistance	0.189 Ω	0.144 Ω	
Energy	10.8 kWh	440 Wh	11.3 kWh
Power	62 kW	117 kW	180 kW
Energy Density	228 Wh/kg	11.0 Wh/kg	130 Wh/kg
Power Density	1311 W/kg	2932 W/kg	2064 W/kg
Cell Mass	47.3 kg	39.9 kg	87.2 kg

Table 3.5: Hybrid Energy Storage System Specifications

The Camaro E/28's battery pack makes use of a Phase Change Material (PCM) to provide each cell with both structural support as well as passive thermal management. The material undergoes a unique solid-to-solid phase change process after reaching its melting point in which it absorbs a large amount of latent heat energy without increasing in temperature. The melting point of the PCM exists below the thermal operating limits of the cells and well above the average ambient temperature. These characteristics improve the utility of the battery pack by allowing for more energy to be discharged at higher temperatures. Figure 3.9 demonstrates how each of the battery pack's cells are encased in PCM, while Figure 3.10 illustrates its thermal characteristics [42] [43].

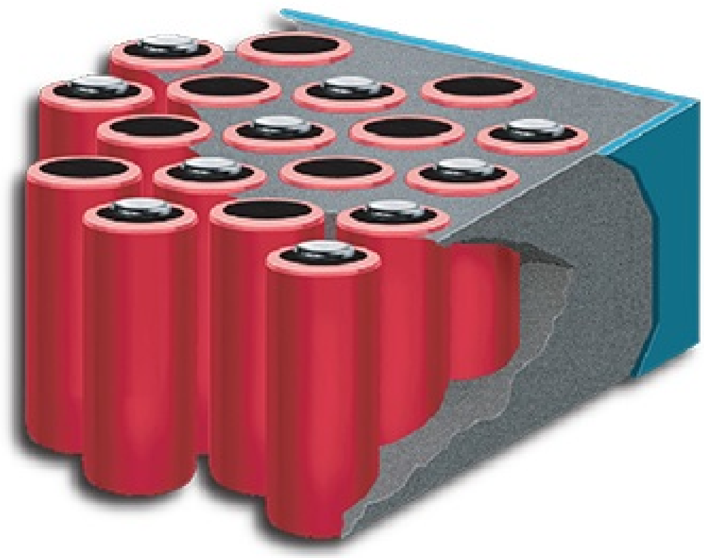

Figure 3.9: Battery Cells Encased in Phase Change Material

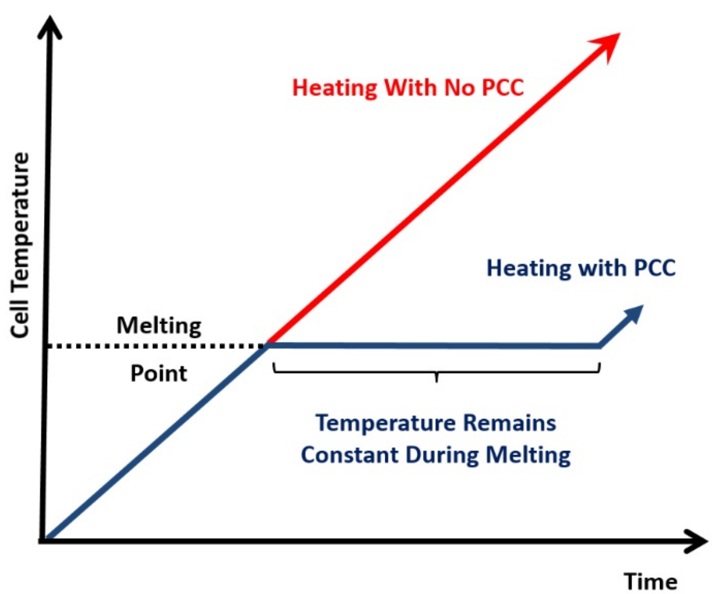

Figure 3.10: Phase Change Material Thermal Characteristics

3.4 Summary of Vehicle Architecture

The perception that electrified vehicles are "boring," "slow," and "underpowered" has significantly hindered their adoption. Consumers, however, need to look no further than the examples set by exotic sports car manufacturers like Porsche, McLaren, Ferrari, and BMW to see that this is not the case. The McMaster Engineering EcoCAR 3 Team hoped to demonstrate that even "old school" American Muscle may take advantage of the performance benefits offered by vehicle electrification technologies. The Camaro E/28, the team's entry to the EcoCAR 3 competition, sought to compete directly with the technical specifications of the Chevrolet Camaro Z/28 by introducing a P1-P2 series-parallel hybrid electric powertrain architecture to a 2016 Chevrolet Camaro LT. In this chapter, the Camaro E/28's vehicle architecture and technical specifications were introduced and the rationale behind their selection was discussed. In addition, the components that constitute the vehicle's powertrain were presented in detail, including and the Camaro E/28's revolutionary HESS.

Chapter 4

Vehicle Model Development

A vehicle model is a mathematical representation of an automobile that may be used to assess its performance given a prescribed scenario. These models are often used to aid in the selection of components, to evaluate control methods, and to determine its fuel and energy consumption. Vehicle models may vary in fidelity, but often include a representation of a chassis, a powertrain, and a driver.

Although there exist numerous software tools for the development of models, MATLAB and Simulink from MathWorks have received widespread adoption in the automotive industry for the simulation of vehicles and for the development of their supervisory control systems [44] [45]. Simulink is a graphical programming environment for the modelling and simulation of multidomain dynamic systems. Simulink's primary interface is a graphical block diagramming tool and operates on the principles of model-based design. MATLAB and Simulink provide numerous tools for analysis and optimization, and are capable of automatically generating embedded software for deployment on microprocessors.

MathWorks also provides products that enable the natural and rapid creation of mathematical models of physical systems. With Simscape, an extension of the Simulink environment, component models are created based on physical connections that directly integrate with block diagrams and other modelling paradigms [46]. By creating multidomain schematics based on physical connections, Simscape enables models to be developed without deriving and implementing the system-level equations.

To evaluate the performance of the Camaro E/28 and its supervisory control system, a model was developed using MATLAB and Simulink that would be able to simulate the vehicle's powertrain over several standard driving cycles. The plant model is divided into six separate component subsystems which encompass the:

1. Driver
2. Hybrid Supervisory Controller
3. Powertrain
4. Chassis
5. Sensors
6. Actuators

Figure 4.1, below, demonstrates the architecture of the vehicle model.

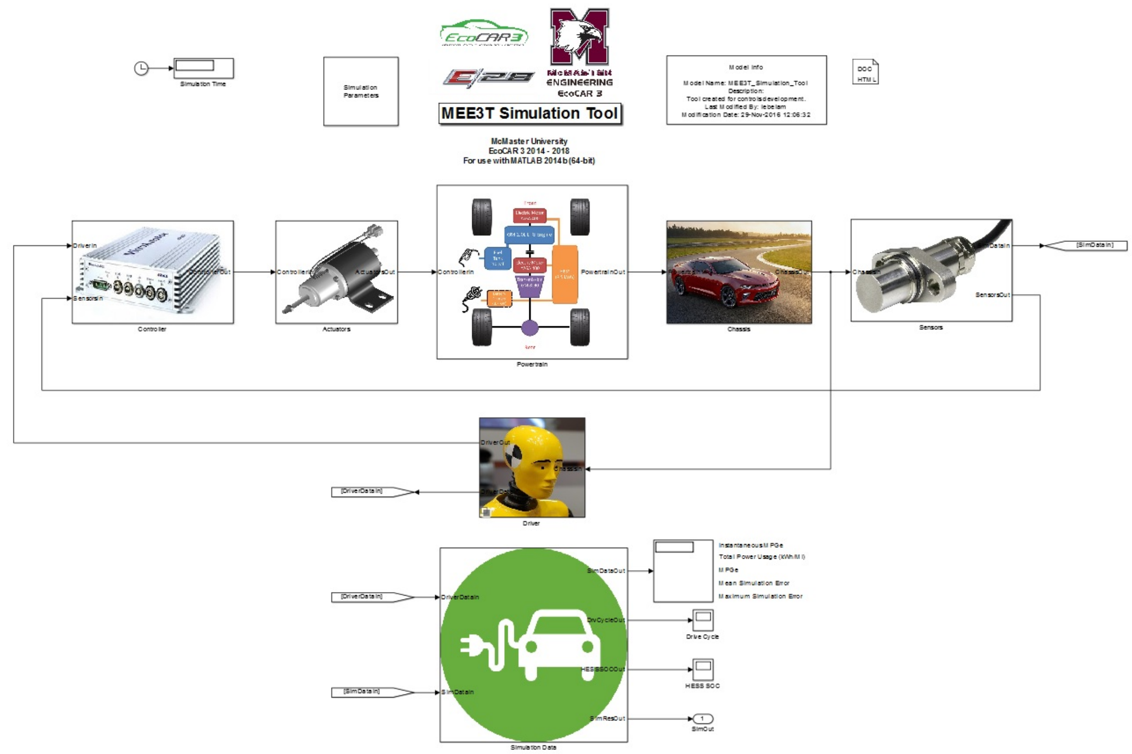

Figure 4.1: Vehicle Model Architecture

4.1 Driver Model

The driver model is meant to simulate the actions that a human being would take during the normal operation of the vehicle. It simulates the proper startup and shutdown procedures required for the Camaro E/28 as well as determines the position of the accelerator and brake pedal that will result in the vehicle's current velocity matching that of a predefined driving cycle.

The driver is modelled using a single Proportional-Integral-Derivative (PID) controller with all positive outputs resulting in a non-zero accelerator pedal position and all negative outputs resulting in a non-zero brake pedal position. Simulink Stateflow was used to simulate the startup and shutdown procedures the driver must take before and after a driving cycle has been executed, respectively.

Additional driver models were also developed with the intention of validating various aspects of the vehicle's control software. A "manual" driver model was created where the accelerator and brake pedal positions, the state of the gear selector, and the "Start" button were all controlled in real-time by the individual conducting the simulation. The vehicle's startup and shutdown logic, and the fault remediation software associated with it, may be validated using this model.

A "performance" driver model that accepts driving cycles in a velocity vs. distance format, as opposed to the more traditional velocity vs. time arrangement, was also developed. This variant allowed for the Camaro E/28's dynamic performance to be simulated and compared against other high performance vehicles.

The "automatic" driver model is presented in Figure 4.2, below.

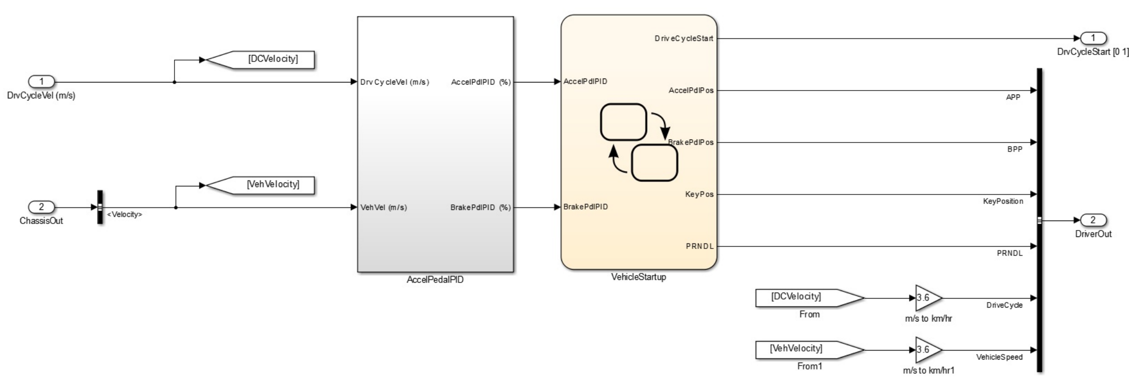

Figure 4.2: Automatic Driver Model

4.2 Hybrid Supervisory Controller Model

The Hybrid Supervisory Controller (HSC) model contains the logic used to interpret the requests issued by the driver model, and in turn, provides the vehicle's powertrain plant models with the appropriate torque commands. The HSC model, like the driver model, has several variants each of which performs a specific task. These variants include MIL, SIL, and HIL controllers.

The MIL controller model, which operates according to simple heuristic methods, determines the power split between the vehicle's two electric machines and the ICE in a purely thermal manner. The MIL controller was used extensively in determining the Camaro E/28's optimal powertrain architecture and in comparing its dynamic performance against that of other vehicles.

The SIL controller model, which incorporates additional control and diagnostic logic, is representative of the actual vehicle's software. The SIL controller also includes SoftECUs, or software representations of the vehicle's ECUs, which are now used to exert control over the vehicle's other plant models. The SoftECUs allow for the Camaro E/28's software to be validated in a safe and controlled simulation environment. The SIL controller model and a selection of its SoftECUs are illustrated in Figure 4.3.

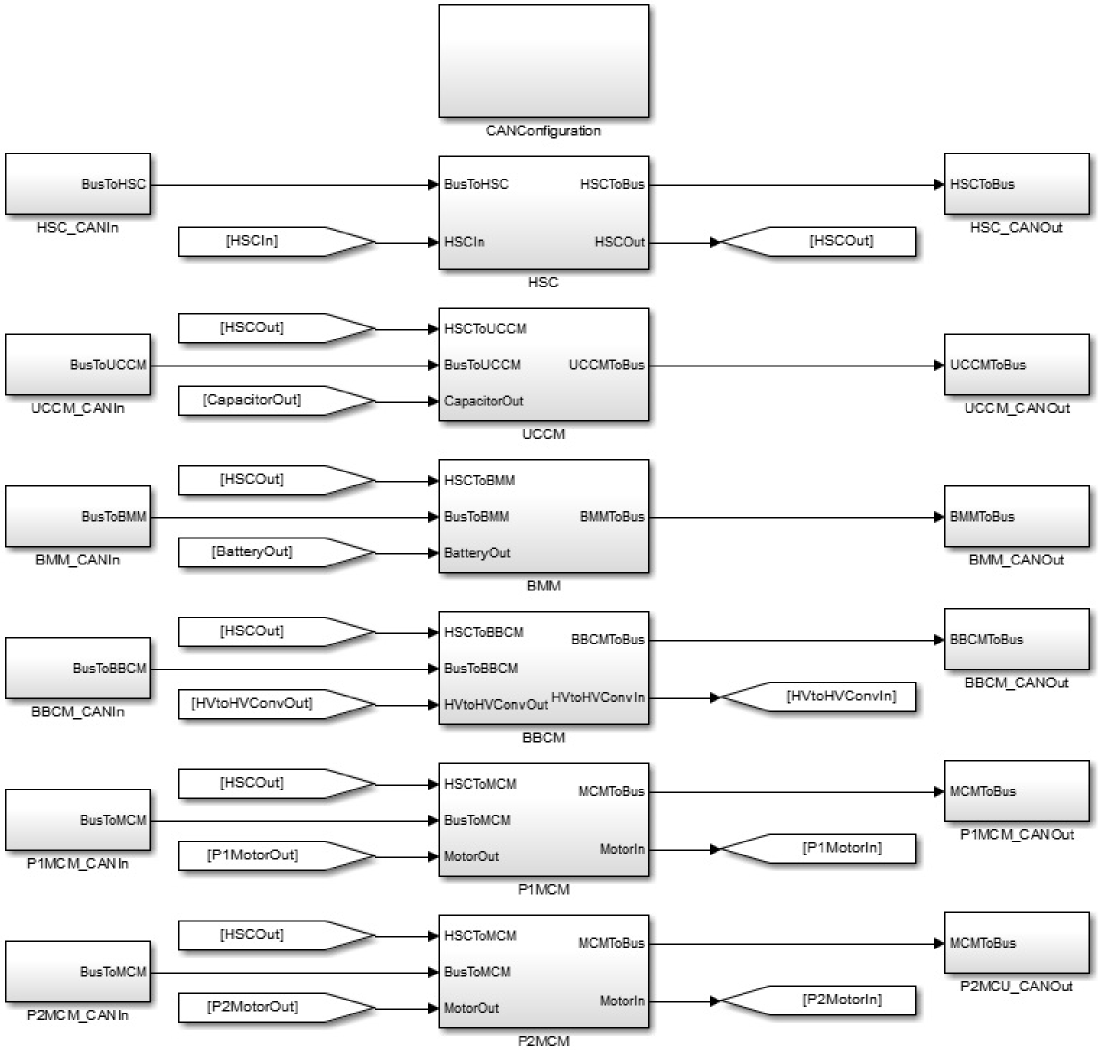

Figure 4.3: SIL Controller Model and SoftECUs

The HIL controller model maintains the SoftECUs used within the SIL controller, however, the Camaro E/28's supervisory control software is replaced with logic that allows the vehicle model to interface with a HIL simulator. The vehicle's software is instead compiled and run on its target platform. This controller allows for the testing and refinement of the vehicle's control system in the HIL environment.

4.3 Powertrain Model

The powertrain model encompasses several subsystems, each of which represents a torque producing, energy storage, or torque/speed manipulating component within the vehicle. The powertrain subsystem is divided into eight component plant models and include the:

1. P1 Electric Motor
2. Internal Combustion Engine
3. Clutch
4. P2 Electric Motor
5. Torque Converter
6. Transmission
7. Fuel Tank
8. Hybrid Energy Storage System

Figure 4.4, below, illustrates the architecture of the powertrain model.

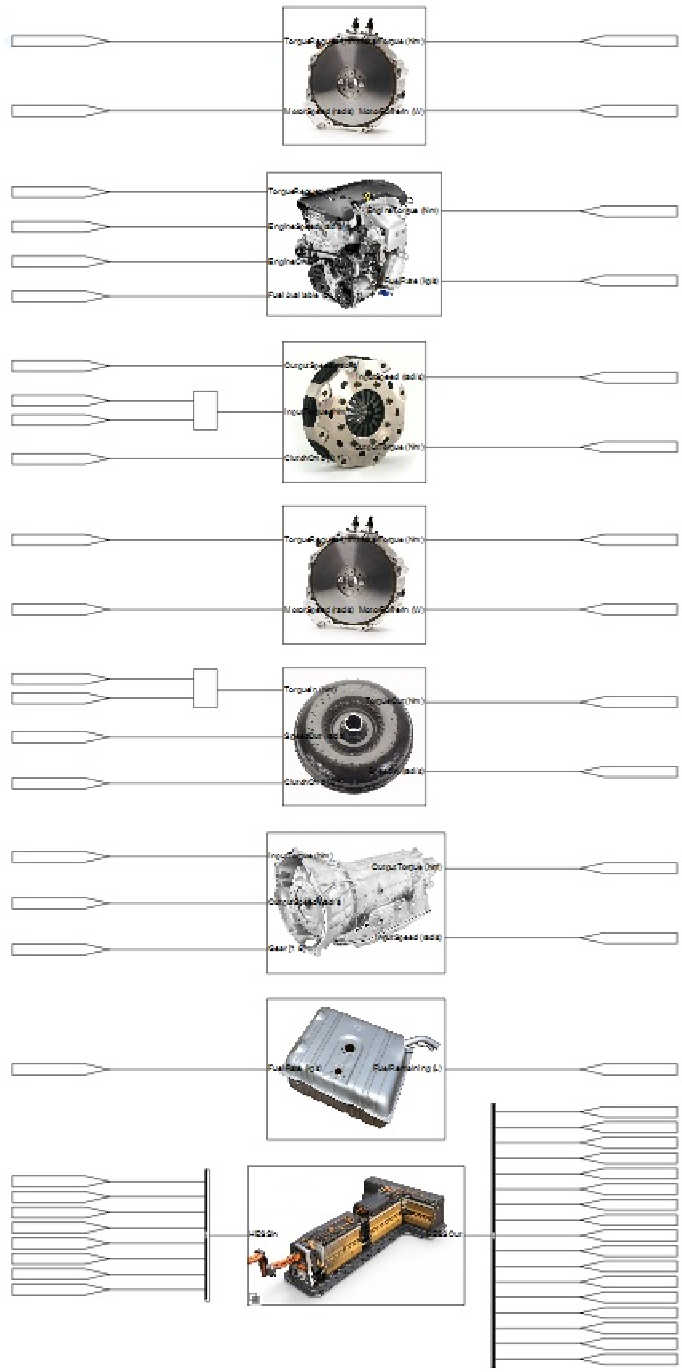

Figure 4.4: P1-P2 Series-Parallel Powertrain Model

4.3.1 P1/P2 Electric Motor Model

The plant model for the YASA-P400 HC electric motor and its inverter, the Rinehart PM150DZR, were developed from the datasheets provided by YASA and Rinehart Motion Systems, respectively. The datasheets for the YASA-P400 HC included plots of maximum and continuous motor torque versus speed at a variety of voltage and current (maximum) set points as well as efficiency maps for the motor at 400 V_{DC} and 300 V_{DC} (600 A_{RMS}) [28].

The plant model for the YASA-P400 HC electric motor used a combination of lookup tables, physics-based calculations, and Simscape blocks as a primary operating basis. The motor plant model is illustrated by Figure 4.5.

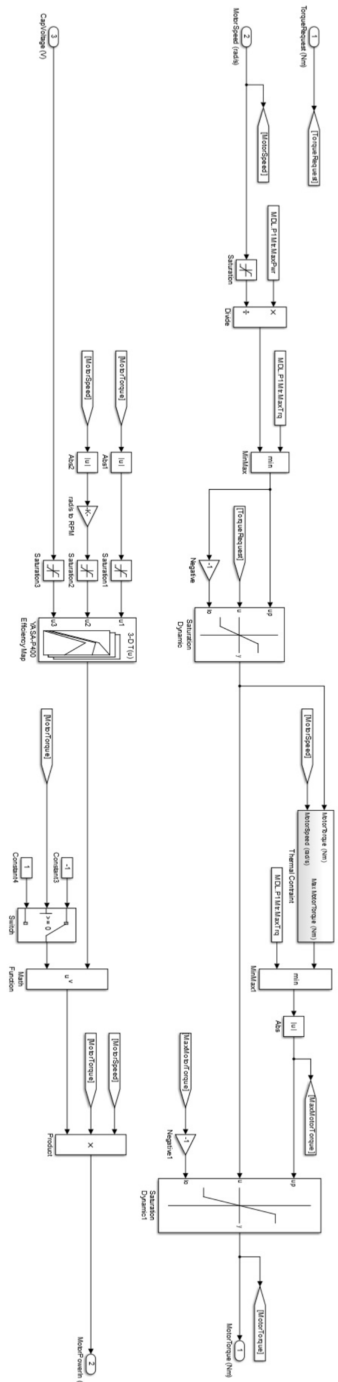

Figure 4.5: YASA-P400 HC Plant Model

The torque produced by the motor plant model was determined from the request sent from the HSC model, the voltage of the ultracapacitors within the HESS model, the motor's speed, as well as the temperatures of its rotor, core, windings, and the inverter. Using an algorithm, the maximum torque that the electric motor is expected to be able to produce is calculated from its speed and ultracapacitor voltage. Subsequently, the derating applied to the motor's performance was determined from the temperatures of its rotor, core, and windings, as well as the temperature of the inverter, using a series of lookup tables. The torque requested by the HSC model was then compared against the maximum torque that the motor is capable of producing, taking into account the temperature derating. The lesser of these two values is the torque that is actually produced by the plant model.

It is also within the YASA-P400 HC plant model where the temperatures of its rotor, core, and windings, as well as the inverter are determined. Simscape was used in the development of the plant model's thermal systems. Figure 4.6 demonstrates the thermal model for the YASA-P400 HC electric motor.

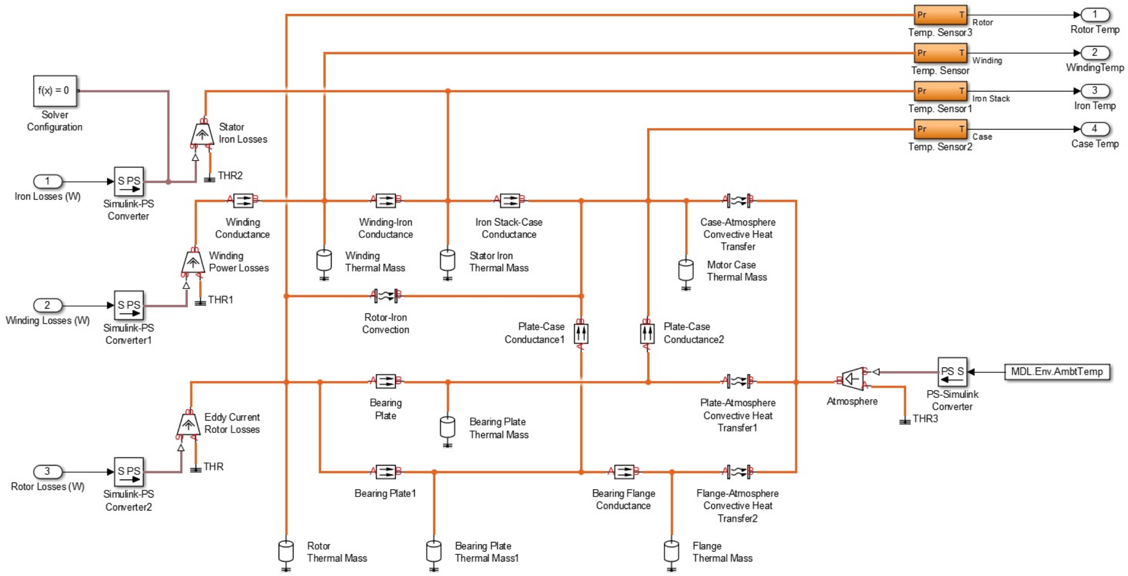

Figure 4.6: YASA-P400 HC Thermal Model

4.3.2 Internal Combustion Engine and Fuel Tank Models

The plant model of the GM LTG ICE was modelled using both physics-based calculations and a series of look-up tables. A Wide-Open Throttle (WOT) curve, a minimum torque curve, a pumping losses torque curve, and a fuel flow rate map were all obtained from a representative engine model in Autonomie. Autonomie is a powertrain and vehicle model architecture development environment based on Simulink. It contains many pre-defined plant models of components such as engines, electric motors, transmissions, etc [47]. An image of the ICE plant model is provided in Figure 4.7, below.

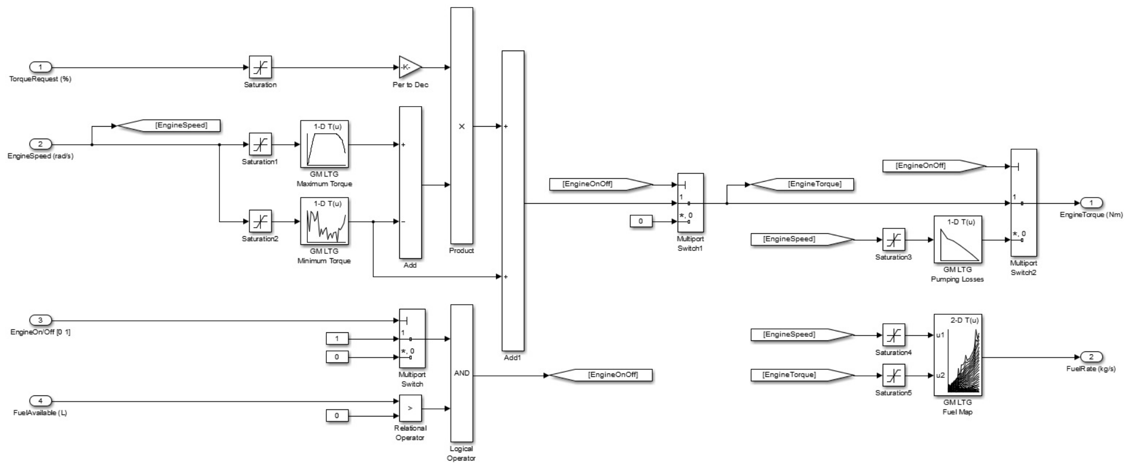

Figure 4.7: GM LTG Plant Model

The HSC model requests a torque from the ICE plant model by commanding the position of the throttle. It is assumed that the throttle's position is proportional to the maximum torque that the engine may produce at its current angular velocity. The torque that the plant model produces is determined by multiplying the throttle position, as a percentage of the WOT position, by the ICE's maximum output torque at its current speed. Subsequently, using the engine's current angular velocity and output torque, its instantaneous fuel consumption is calculated from the fuel flow rate look-up table.

Using the ICE model's instantaneous fuel consumption, a fuel tank model was produced to integrate this value over time and determine the amount of fuel remaining. If the engine depletes its fuel reserves (or if the fuel injection is shut off), the ICE model will instead produce the negative pumping losses for its current speed.

4.3.3 Clutch Model

The clutch used to transition the Camaro E/28's powertrain between the electric/series drive mode and the parallel mode is modelled using Simscape, MATLAB's physical system modelling toolbox. It is within this plant model that the inertial mass and friction of the two electric motors, the ICE, and the vehicle's driveline are accounted for. Figure 4.8 illustrates the powertrain clutch model. If it were not for the clutch model, and the inclusion of the inertial mass of the P1 electric motor and ICE, the simulation of the vehicle's series drive mode would not have been possible.

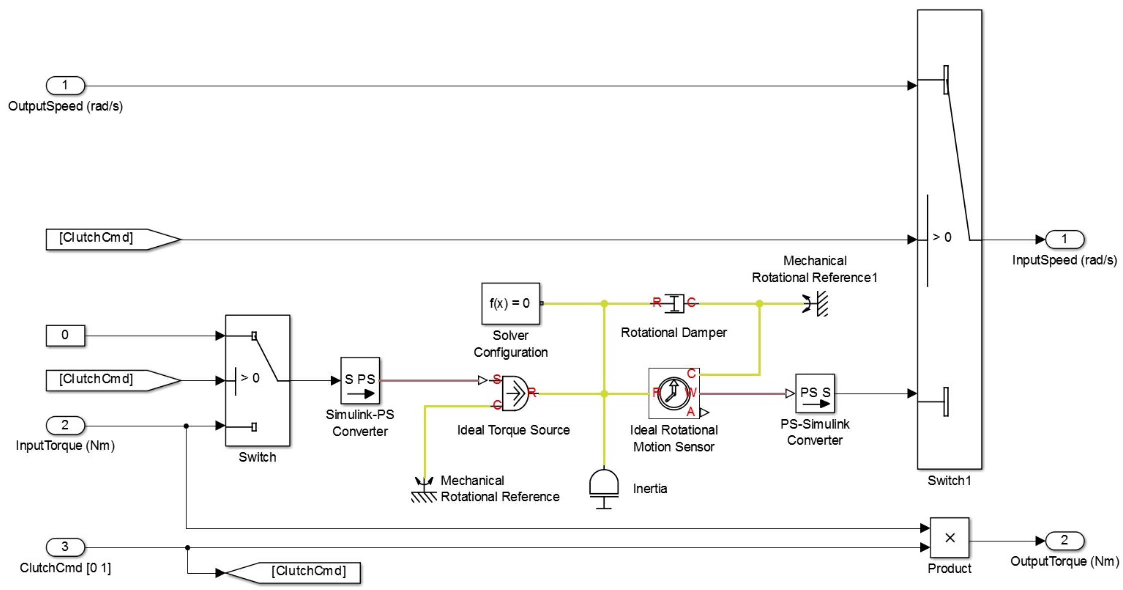

Figure 4.8: Powertrain Clutch Plant Model

4.3.4 Torque Converter Model

A torque converter, like a clutch, couples two independent driveline axes in such a way as to transfer angular motion and torque from an input to an output shaft. Unlike a clutch, however, a torque converter never locks and the output shaft never reaches the speed of the input (the torque converter transfers motion by hydrodynamic viscosity, not by surface friction). A torque converter, therefore, does not step through discrete stages and avoids the motion discontinuities inherent in friction clutches [48]. A clutch, however, was modelled alongside the torque converter so that the input and output shafts may be locked if it is commanded to do so by the HSC model. The torque converter was modelled using several look-up tables and the physics-based calculations which describe its traditional mechanics [49]. The torque converter plant model is illustrated by Figure 4.9.

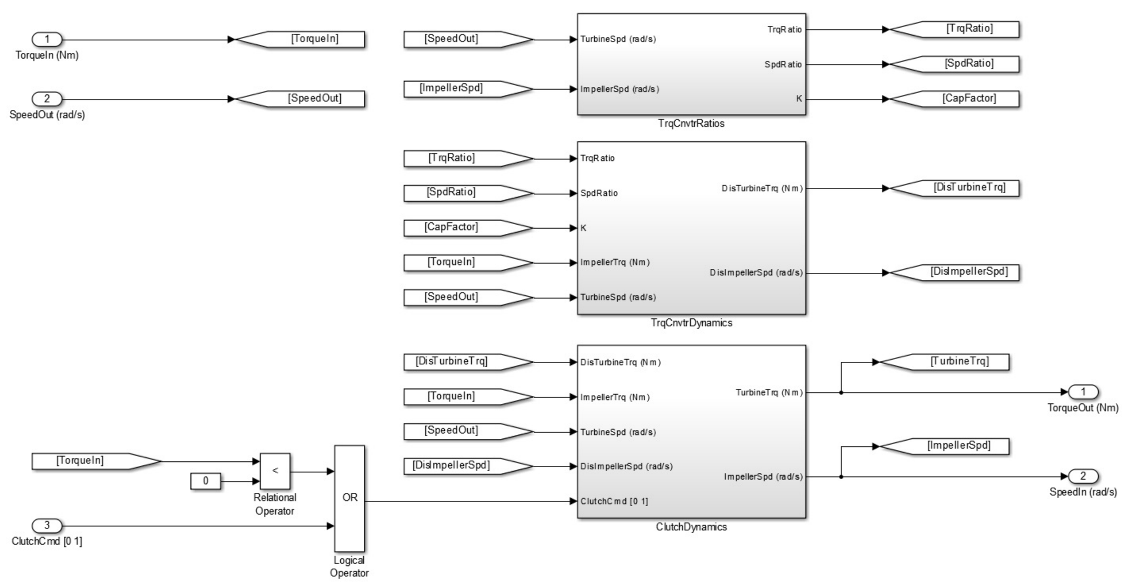

Figure 4.9: Torque Converter Plant Model

The torque converter model allows for the more accurate simulation of various vehicle functions. The ICE's idling behaviour, for instance, was able to be simulated due to its inclusion. This would not have been possible if the engine plant model was coupled directly to the transmission due to the way that the simulation tool calculates the driveline's angular velocity from the vehicle speed using a feedback method.

The torque converter model was also vital in the development of the software which has the P2 electric motor simulate the ICE's idling behaviour in the vehicle's electric and series drive modes. This was required so that the vehicle's "creep" function was available at all times and that the transmission had the necessary oil pressure to shift gears (the pump is driven from the input to the transmission).

4.3.5 Transmission Model

The transmission was modelled as a series of gear ratios which were then multiplied by the torque that the powertrain produced in order to determine the vehicle's axle torque (torque at the wheels). This ratio included that of the transmission's current gear as well as that of the differential. The driveline's angular velocity was then calculated by dividing the vehicle's speed by the tire radius and then translating that value back through the differential and transmission.

In order to increase the fidelity of the model, a delay of 0.25 seconds was introduced in order to simulate the time it took to change gears and a static efficiency of 92% was specified for the torque output in order to approximate the transmission losses. This value was based on dynamometer experiments carried out by Irimescu et.al [50]. Figure 4.10 provides an image of the transmission plant model's Simulink block diagram.

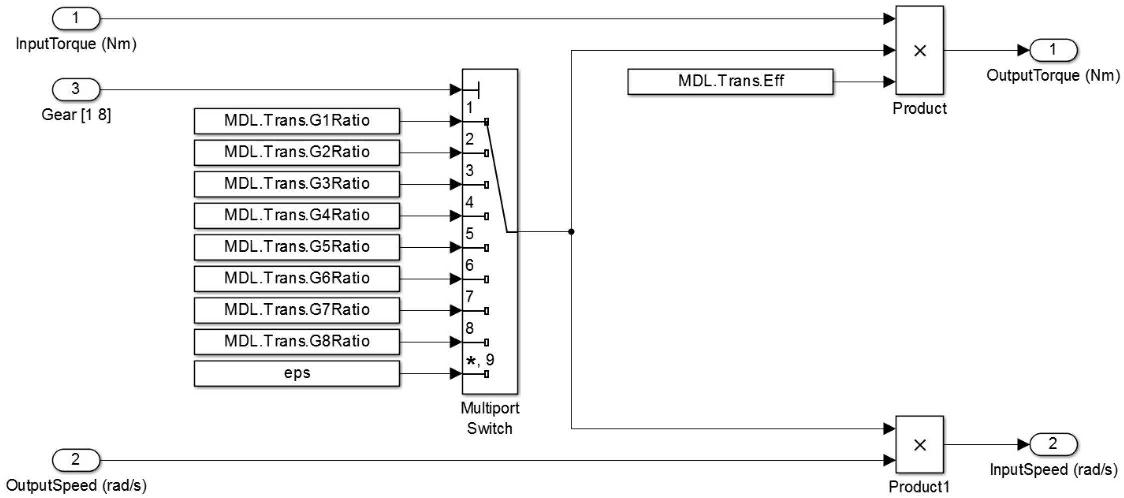

Figure 4.10: Transmission Plant Model

4.3.6 Hybrid Energy Storage System Model

The Camaro E/28's HESS was modelled using the Li-ion battery and ultracapacitor models provided by the Simscape Power Systems toolbox [51]. The two energy sources were interfaced with a Power Balance block which was used to simulate the HESS's DC/DC converter. A power balance block is commonly used to reduce model complexity and computation time. The contactors and fusing hardware found within the HESS's battery and ultracapacitor packs were also faithfully reproduced. These features prevented any power from being drawn from the HESS if the contactors had not been successfully closed or if the fuses had been compromised. This additional level of fidelity allowed for the verification and validation of the vehicle's control strategies relating to the management of its electrical systems.

Thermal models for the battery and ultracapacitor packs were also developed.

The battery modules provided by AllCell had several unique thermal properties due to their use of a PCM at the module's core. The material provided a great deal of thermal mass not only at its activation temperature but also throughout its entire operating range. The PCM, however, had poor thermal conductivity and the heat that the module absorbed took a considerable amount of time to remove through cooling efforts [43]. To better simulate the battery modules, a PCM Simscape block was developed and integrated into a one-dimensional resistive point mass thermal network. To parameterize the model, several Computational Fluid Dynamics (CFD) simulations were conducted using the NX Thermal Analysis Tool [52]. Figure 4.11 is an image of the CFD thermal simulation and Figure 4.12 demonstrates the thermal model for a single row of cells in the battery pack.

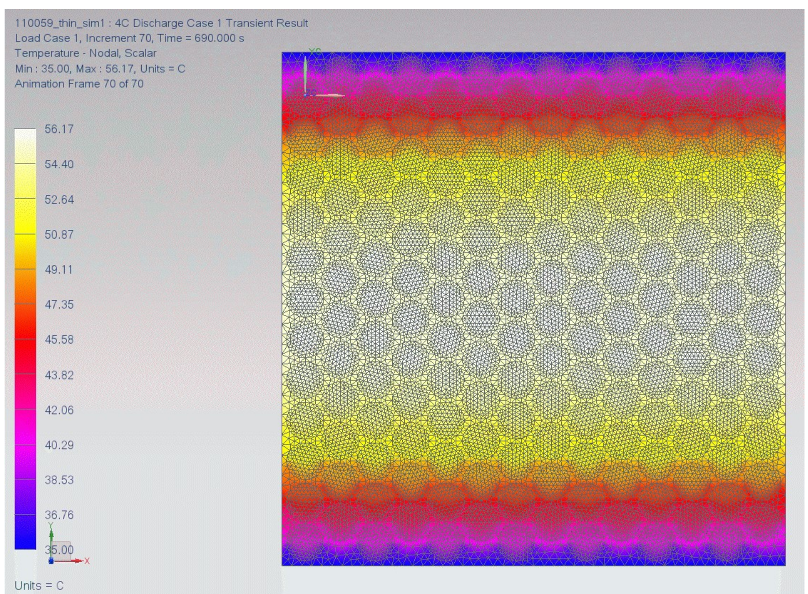

Figure 4.11: AllCell Module Thermal Simulation

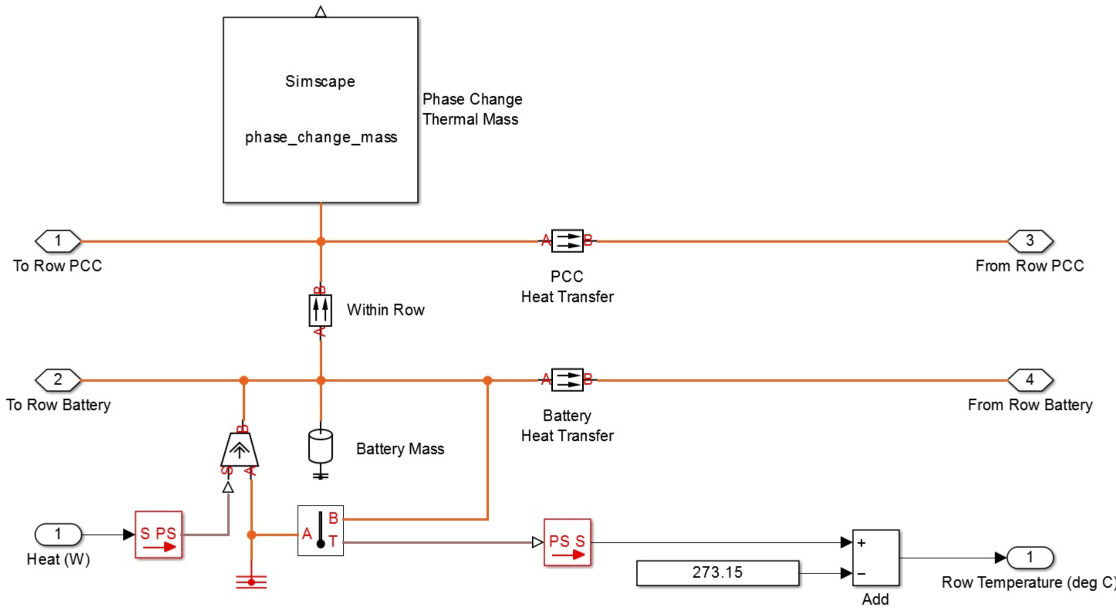

Figure 4.12: Battery Pack Thermal Model

The JM Energy ultracapacitor modules did not provide any effective means for liquid cooling, and therefore, were cooled using forced air drawn from the vehicle's cabin. The ultracapacitor thermal model consisted of a single thermal point mass and was parameterized with data from a test conducted by JM Energy using the MATLAB Statistics and Machine Learning Toolbox [53]. The model made the assumption that the same air flow conditions were experienced by all nine modules simultaneously. Figure 4.13, below, illustrates the thermal model of the HESS's ultracapacitor pack.

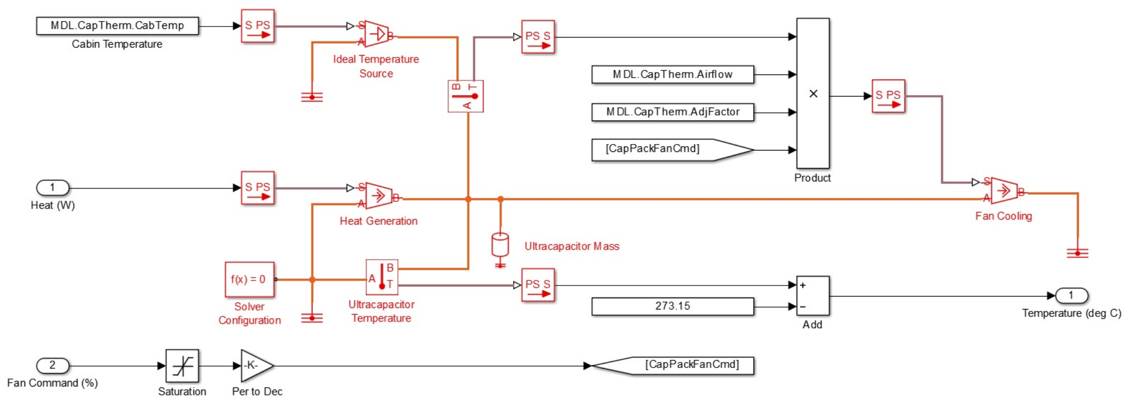

Figure 4.13: Ultracapacitor Pack Thermal Model

4.4 Chassis Model

The chassis plant model simulates a two-axle vehicle, with four equally sized wheels, moving forward or backward along its longitudinal axis. The chassis model only considers longitudinal dynamics, parallel to the ground and oriented along the direction of motion. The vehicle is assumed to be in pitch and normal equilibrium, and as such, the equations assume that the wheels never lose contact. A more complex dynamics model could have been created, which simulates the vehicle's suspension and individual tires, in order to better predict how the Camaro E/28's lateral movement and yaw affect the performance and drivability of the vehicle. This level of fidelity was deemed to be out of the scope of this research; seeing that the focus was on the development and testing of the Camaro E/28's control system and on how these algorithms affected the vehicle's fuel economy, energy consumption, and emissions.

The chassis model is derived from the first principles of one dimensional longitudinal dynamics. The chassis is considered to be an inertial mass and by applying Newton's Second Law of Motion the vehicle's instantaneous acceleration can be determined. The chassis' velocity and position can be further derived by integrating the vehicle's instantaneous acceleration over time. Equation 4.1 and Equation 4.2 show how the chassis's velocity may be calculated from the summation of the forces acting on it.

$$F_{net} = ma \tag{4.1}$$

$$V = \int a \, \mathrm{d}t \tag{4.2}$$

The vehicle's motion may be determined by analysing the net effect of all the forces and torques acting on it. The longitudinal tire forces push the vehicle forward and are opposed by aerodynamic drag, the rolling resistance of the tires, and the force needed to overcome any grade in the road surface. For simplicity, the weight of the vehicle and aerodynamic drag were assumed to act through the chassis' Center of Gravity (CG). Figure 4.14 illustrates the free body diagram of the vehicle and all of the forces acting on it and Table 4.1 defines the chassis model variables.

Symbol	**Description**	**Units**
F_{net}	Sum of all longitudinal forces acting on the vehicle	N
F_x	Tractive longitudinal force	N
F_d	Aerodynamic drag force	N
F_r	Rolling resistance force	N
F_g	Road grade force	N
$F_{x,f}, F_{x,r}$	Longitudinal forces on each wheel at the front and rear ground contact points, respectively	N
T_f, T_r	Torque applied to each wheel at the front and rear ground contact points, respectively	Nm
R_w	Wheel radius	m
C_d	Aerodynamic drag coefficient	N·s^2/kg·m
ρ	Mass density of air	1.18 kg/m^3
A	Effective frontal vehicle cross-sectional area	m^2
V_x	Longitudinal vehicle velocity	m/s
C_r	Rolling resistance coefficient	N/A
m	Vehicle mass	kg
g	Gravitational acceleration	9.81 m/s^2
β	Incline angle	rad
$F_{z,f}, F_{z,r}$	Normal load forces on each wheel at the front and rear ground contact points, respectively	N
h	Height of vehicle CG above the ground	m
l_1, l_2	Distance of front and rear axles, respectively, from the vertical projection point of vehicle CG onto the axle-ground plane	m
μ	Coefficient of friction	N/A

Table 4.1: Vehicle Chassis Model Variables

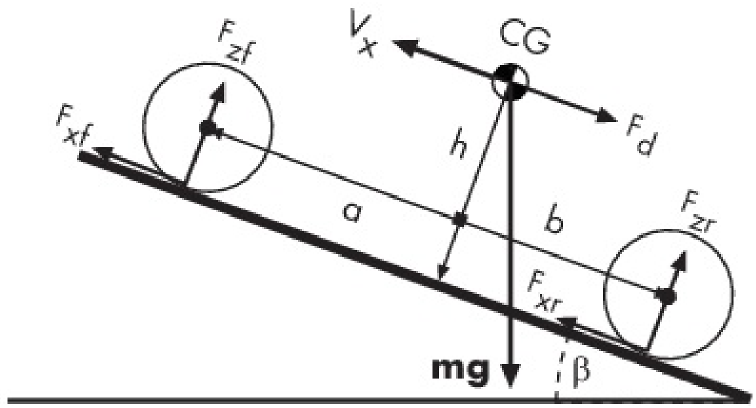

Figure 4.14: Vehicle Dynamics Free Body Diagram

The vehicle's axles are parallel and lie in a plane parallel to the ground. The longitudinal x direction exists in this plane and is perpendicular to the axles. If the vehicle is traveling on an incline with slope β, the vertical z direction is not parallel to the gravitational force but is always perpendicular to the axle-ground plane. Equation 4.3 describes how the net forces acting on the vehicle are determined based on the free body analysis.

$$F_{net} = F_x - (F_d + F_r + F_g) \tag{4.3}$$

The longitudinal tire forces are a function of the torque applied to the vehicle's wheels and the wheel radius. The aerodynamic drag force is a function of air density, the vehicle's frontal area, its coefficient of drag, and the air velocity over the chassis. The rolling resistance is calculated based on the vehicle's mass and the rolling resistance coefficient. Lastly, the grade force can be determined based on the vehicle's mass and the gradient of the road. More complex descriptions of these forces can be generated, however, these definitions are commonly accepted representations of chassis dynamics for one dimensional simulations [54]. The various forces that act on the chassis were evaluated using Equation 4.4, Equation 4.5, Equation 4.6, Equation 4.7, and Equation 4.8.

$$F_x = F_{x,f} + F_{x,r} \tag{4.4}$$

$$F_{x,f} = \frac{T_f}{R_w}, \quad F_{x,r} = \frac{T_r}{R_w} \tag{4.5}$$

$$F_d = -\frac{1}{2} C_d \rho A V_x^2 \cdot sign\,(V_x) \tag{4.6}$$

$$F_r = C_r m g \tag{4.7}$$

$$F_g = mg \cdot \sin\beta \tag{4.8}$$

Within one dimensional longitudinal chassis modelling, the dynamic weight distribution of the vehicle may be analyzed in order to to determine how much torque may be applied to each axle at any given instance without locking or spinning the tires. In order to accomplish this, the complex mass structure of the vehicle body can be simplified to the forces acting on its CG. The longitudinal weight transfer between the two axles by a given tractive force may be determined by calculating the moments about a point of reference. With the knowledge that at any given time the sum of all moments must be equal to zero, Equation 4.9 was derived.

$$F_{z,f} = \frac{-hF_{net} + l_2 \cdot mg \cdot \cos\beta}{(l_1 + l_2)}, \quad F_{z,r} = \frac{hF_{net} + l_1 \cdot mg \cdot \cos\beta}{(l_1 + l_2)} \tag{4.9}$$

The wheel normal forces must also satisfy Equation 4.10.

$$F_{z,f} + F_{z,r} = mg \cdot \cos\beta \tag{4.10}$$

Now that the normal force acting on each axle had been determined, the vehicle's maximum tractive force was calculated. To determine the traction limitation of the tires the normal force of each axle was multiplied by the coefficient of friction as shown in Equation 4.11.

$$F_{x,f,max} = \mu F_{z,f}, \quad F_{x,r,max} = \mu F_{z,r} \tag{4.11}$$

If the longitudinal tire forces being produced were in excess of their allowable limits, tire slippage occurred and resulted in wasted tractive energy.

4.5 Sensor and Actuator Models

The sensor and actuator models were used to convert the idealized signals used within the driver, powertrain, and chassis plant models into the sensed data used by the HSC model and its SoftECUs. An example of this included the position of the accelerator pedal and how this information was conveyed from the driver model to the supervisory control software.

The driver model indicated pedal position as a percentage of its depression, with 0% representing an undepressed pedal and 100% signifying full depression. The supervisory control logic, however, expected to receive an analog signal, with its voltage proportional to the pedal position. The sensor and actuator models were designed to cope with such specifications as well as to simulate any delays or latency in a signal due to a component.

4.6 Summary of Vehicle Model Development

In order to evaluate the performance of the Camaro E/28 and its control system, a mathematical representation of the vehicle was developed using MATLAB and Simulink. This model supported the development of the Camaro E/28's supervisory software, from requirements specification through design, implementation, and testing. Throughout the chapter, the segregation of the vehicle model into its component subsystems was described, and the implementation of each plant model was discussed. In Chapter 5, the method used to simulate the Camaro E/28's environmental impact and dynamic performance using the vehicle model are discussed, and the results of this analysis are presented in Chapter 10.

Chapter 5

Vehicle Testing Procedures

The vehicle model described in Chapter 4 was used to perform an analysis on the Camaro E/28 and its supervisory control system. Various features of the vehicle were evaluated, and included its energy and fuel consumption, production of GHG and criteria emission, Petroleum Energy Use (PEU), as well as its dynamic performance.

5.1 Environmental Impact Testing Procedures

One of the most significant evaluations of a vehicle's performance is to quantify its environmental impact. In order to evaluate the Camaro E/28, four categories of results were assessed, including energy and fuel consumption, GHG emissions, PEU, and criteria (regulated) emissions. GHG emissions and PEU were quantified on a Well-to-Wheels (WTW) basis, which meant both the upstream (due to fuel production, refining, and transportation) and downstream emissions were taken into consideration. This analysis was conducted from a full-fuel-cycle perspective using the Argonne National Laboratory (ANL) Greenhouse Gas, Regulated Emissions and Energy Use in Transportation (GREET) model. The 2020 assumptions provided in GREET 1 2013 for the paths associated with electricity and E/85 fuel were used in the investigation [55].

5.1.1 Standardized Driving Cycles

For the analysis of energy consumption and fuel economy to be consistent across a variety of automobiles, from multiple manufacturers, each vehicle was tested using a set of standardized driving cycles.

A driving cycle is a series of data points representing the velocity of a vehicle versus time. There exist numerous standardized driving cycles as defined by various regulatory bodies around the world for the purpose of emissions and fuel economy testing. In the United States, the EPA developed the Urban Dynamometer Driving Schedule (UDDS), Highway Fuel Economy Test (HWFET), and US06 schedules for this purpose.

In 2008, the EPA altered the emissions and energy consumption testing procedure by adding three new Supplemental Federal Test Procedures (SFTPs) to include the influence of higher driving speeds, harder acceleration, colder temperatures, and air conditioning use [56]. The new process is colloquially known as the "5-cycle" method. The 5-cycle method was introduced in response to consumer complaints of unrealistic fuel economy claims by manufacturers, in particular for hybrid electric vehicles [57].

The 5-cycle method makes use of the UDDS and HWFET driving cycles, which simulate urban and expressway driving, respectively. The procedure also takes into account aggressive driving behaviour with the US06 cycle, air conditioning with the SC03 cycle, and cold weather effects with the UDDS cycle at an ambient temperature of $-7\,^{\circ}\mathrm{C}$. Table 5.1 provides additional details on the driving cycles used in the 5-cycle method.

	City	**Highway**	**High Speed**	**A/C**	**Cold Temperature**
Cycle Name	**UDDS**	**HWFET**	**US06**	**SC03**	**UDDS**
Distance	17.8 km	16.5 km	12.9 km	5.8 km	17.8 km
Top Speed	90 km/h	97 km/h	129 km/h	88 km/h	90 km/h
Average Speed	34 km/h	78 km/h	78 km/h	35 km/h	34 km/h
Maximum Acceleration	5.3 km/h/s	5.2 km/h/s	13.6 km/h/s	8.2 km/h/s	5.3 km/h/s
Number of Stops	23	0	4	5	23
Idling Time	18%	0%	7%	19%	18%
Engine Startup	Cold	Warm	Warm	Warm	Cold
Lab Temperature	20 °C – 30 °C	20 °C – 30 °C	20 °C – 30 °C	35 °C	−6.67 °C

Table 5.1: 5-Cycle Method Driving Cycle Characteristics

Since air conditioning and cold weather effects are difficult to simulate, a novel testing procedure that mimics the results seen with the 5-cycle method was used. The "4-cycle" procedure is based on a blend of four certification cycles meant to approximate the energy use seen in EPA 5-cycle testing, without having to directly address cold weather effects or air conditioning use. The driving cycles that are used for the 4-cycle method are 505 (first 505 seconds, or Bag 1, of the UDDS cycle), HWFET, and US06 (City and Highway split into two cycles) [12]. The driving cycles that made up the 4-cycle method are illustrated in Figure 5.1, Figure 5.2, Figure 5.3, and Figure 5.4.

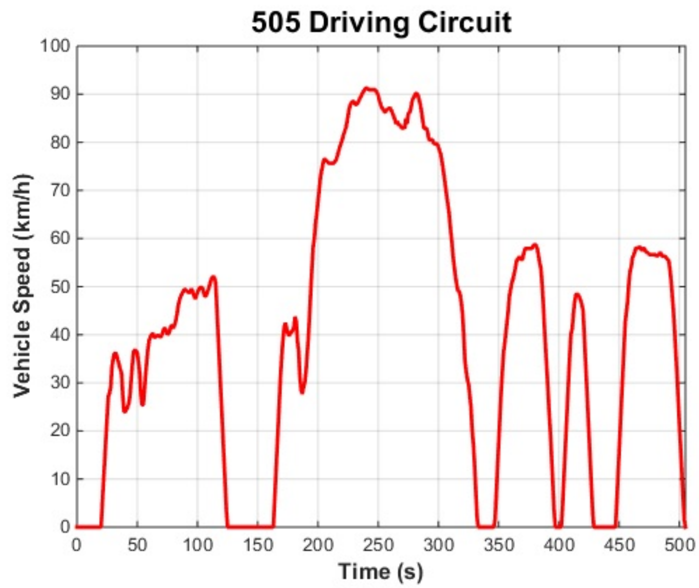

Figure 5.1: 505 Driving Cycle

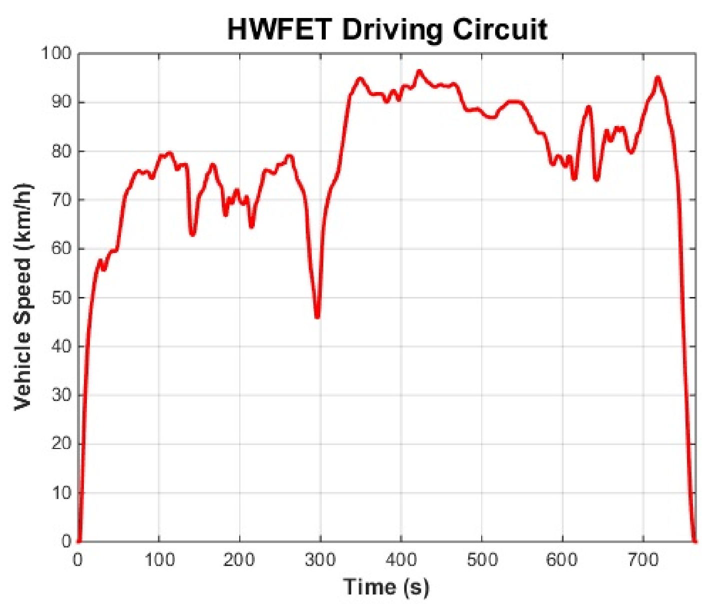

Figure 5.2: HWFET Driving Cycle

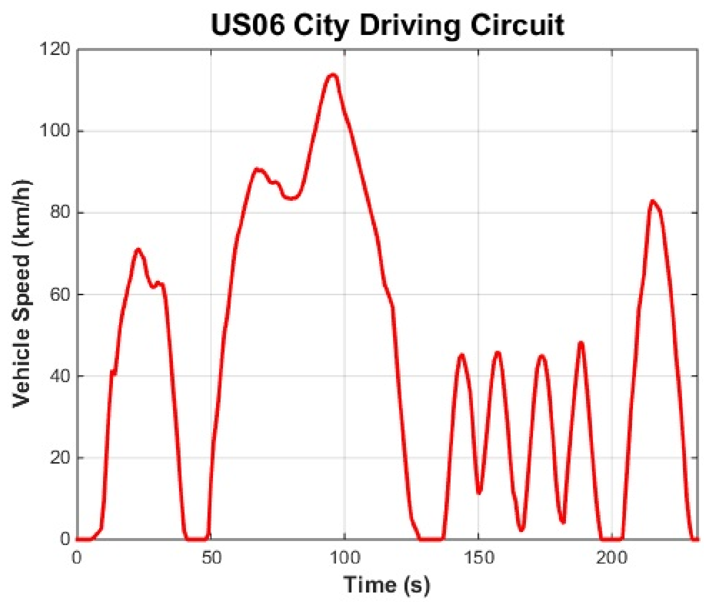

Figure 5.3: US06C Driving Cycle

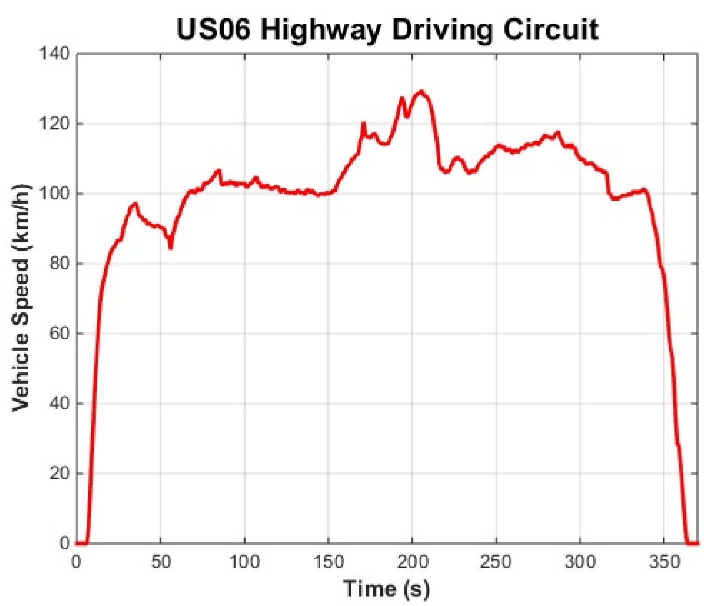

Figure 5.4: US06H Driving Cycle

Table 5.2 provides several characteristics of the driving cycles used for the 4-cycle method and describes the proportion of each which was used to calculate fuel and electric energy consumption.

	Low Speed	**Mid Speed**	**Low Speed Aggressive**	**High Speed Aggressive**
Cycle Name	**505**	**HWFET**	**US06C**	**US06H**
Distance	5.8 km	16.5 km	2.9 km	10.0 km
Top Speed	91 km/h	97 km/h	114 km/h	129 km/h
Average Speed	41 km/h	78 km/h	44 km/h	98 km/h
Maximum Acceleration	5.3 km/h/s	5.2 km/h/s	13.5 km/h/s	11.1 km/h/s
Number of Stops	4	0	4	0
Idling Time	20%	0%	15%	0%
Weighting Factor for 4-Cycle Method	29%	12%	14%	45%

Table 5.2: 4-Cycle Method Driving Cycle Characteristics

5.1.2 Utility Factor-Weighted Energy Consumption

Since the Camaro E/28 has distinct charge depleting and charge sustaining modes of operation, the vehicle's energy consumption in each mode, for every driving cycle, should be determined before applying the 4-cycle method's weighting factors. A Utility Factor (UF) must then be calculated and applied to the results of this analysis in order to arrive at the final values for the vehicle's fuel and energy consumption.

The UF represents the percentage of vehicles that will use a particular charge depleting range on any given day. The Camaro E/28's charge depleting energy consumption was weighted against this percentage, and its charge sustaining energy consumption was weighted against the remainder (1 – UF).

The vehicle's energy consumption and derivative measurements were based on the SAE J2841 definition of the UF and the SAE J1711 testing method. SAE J2841 establishes a value for the weighting of fuel and electric energy consumption for PHEVs on the basis of the National Household Travel Survey (NHTS) data [58]. SAE J1711 defines the procedure with which a PHEV's charge depleting range is measured, so that a UF may be assigned [59].

The UF for the Camaro E/28 was calculated using Equation 5.1, where x represents the vehicle's charge depleting range. The results obtained using the UF are valid through a range of 0 km to 640 km.

$$UF = 1 - \mathrm{e}^{\left[C1\left(\frac{x}{D_{norm}}\right)+C2\left(\frac{x}{D_{norm}}\right)^2+\cdots+C6\left(\frac{x}{D_{norm}}\right)^6\right]} \tag{5.1}$$

The UF curve is presented in Figure 5.5.

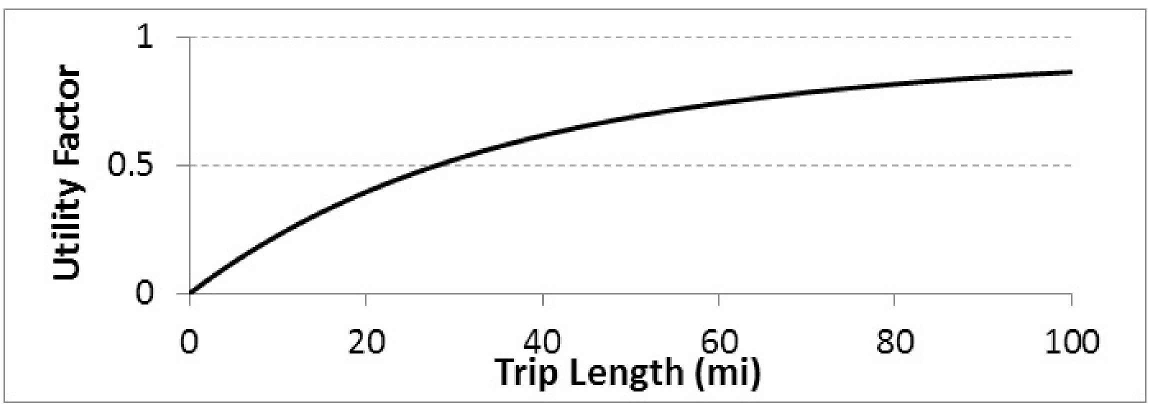

Figure 5.5: Utility Factor Plot Based on SAE J2841

The UF weighted energy consumption was used to determined the WTW GHG emissions and PEU, and was calculated using Equation 5.2.

$$EC_{UF} = EC_{CD} \times UF + EC_{CS} \times (1 - UF) \tag{5.2}$$

For PHEVs, the charge depleting energy consumption was evaluated by using Equation 5.3. The fuel energy consumed was also taken into consideration by applying the fuel's Lower Heating Value (LHV) to the volume that was consumed during the vehicle's charge depleting mode of operation.

$$EC_{CD} = EC_{elec,CD} + EC_{fuel,CD} \tag{5.3}$$

The objective of a charge sustaining operating mode is to achieve a net zero use of electrical energy. This, however, is not always the case as slight deviations in the net consumption may occur over the course of a driving cycle. The calculation for charge sustaining energy consumption must, therefore, correct for these deviations. Equation 5.4 was used to determine the energy consumption of the Camaro E/28 during its charge sustaining operating mode. The 0.25 weighting factor represents the typical efficiency associated with generating electricity through an engine and electric machine [12].

$$EC_{CS} = \frac{m_{fuel} \times LHV_{fuel} + \frac{EC_{elec,CS}}{0.25}}{d_{DC}} \tag{5.4}$$

5.1.3 Analysis of Energy Consumption

Once the Camaro E/28's UF weighted energy consumption was known, the WTW GHG emissions were estimated using Equation 5.5. For each contributing fuel, a GHG factor must be applied to the weighted energy consumption of that fuel.

$$GHG_{WTW} = C_{GHG,WTW} \times EC_{fuel,UF} \tag{5.5}$$

The approximate WTW GHG factors of each fuel used by the Camaro E/28 are provided in Table 5.3.

Factor	**E85**	**Electricity**
$\mathrm{GHG_{WTW}}$ (g/kWh)	244	489

Table 5.3: Approximate Well-to-Wheels Greenhouse Gas Factors

Much like the process used to calculate the GHG emissions, the WTW PEU was calculated by multiplying the weighted energy consumption of each contributing fuel by its corresponding PEU factor as illustrated by Equation 5.6.

$$PEU_{WTW} = C_{PEU,WTW} \times EC_{fuel,UF} \tag{5.6}$$

The PEU factors listed in Table 5.4 account for the petroleum energy used in the manufacturing and use of the fuel.

Factor	**E85**	**Electricity**
$\mathrm{PEU_{WTW}}$ (kWh PE/kWh Fuel)	0.274	0.033

Table 5.4: Approximate Well-to-Wheels Petroleum Energy Use Factors

As the analysis of the Camaro E/28 was done entirely in simulation, only the Upstream Criteria Emissions (UCEs) were evaluated. In order to determine tailpipe emissions, each criteria component would have needed to be measured modally through dynamic testing. UCEs are released as a result of producing the fuel used by the vehicle. Only the effects on urban air quality were accounted for in the upstream factors. Equation 5.7 was used to calculate the amount of UCEs that the vehicle would produce per kilometer traveled. For each criteria pollutant under consideration, a factor was applied to the UF weighted energy consumption.

$$UCE = C_{UCE} \times EC_{fuel,UF} \tag{5.7}$$

Three EPA criteria pollutants were evaluated: THC, CO, and NOx and the factors of each are provided by Table 5.5.

Factor	**E85**	**Electricity**
THC (g/kWh)	0.0488	0.0025
CO (g/kWh)	0.0078	0.0326
NOx (g/kWh)	0.0172	0.0432

Table 5.5: Approximate Upstream Criteria Emission Factors

5.2 Dynamic Testing Procedures

Since the Camaro E/28 is intended to be a high performance electrified vehicle, elements of its performance besides energy and fuel consumption were of interest. To better predict how the vehicle will operate when driven aggressively, several novel testing procedures were developed.

Traditional tests such as acceleration times, top speed, and braking distances are staples when benchmarking dynamic performance, but an increasing number of automotive manufacturers have begun to compare their vehicles based on lap times of several well-known driving circuits. For instance, lap times on the German circuit, Nürburgring, are often used to promote new, high performance, vehicles. When Porsche unveiled their new hybrid supercar, the 918 Spyder, in 2013, it announced that it had set the fastest Nürburgring lap time, reducing the previous record by fourteen seconds, and making it the first series production street legal vehicle to break the seven minute barrier [60]. This remarkable achievement immediately placed Porsche, and the 918 Spyder, in contention with Ferrari (LaFerrari) and McLaren (P1) for the title of highest performing hybrid supercar.

Driving cycles for various well-known circuits were developed using OptimumLap, a simulation tool from OptimumG, a provider of vehicle dynamic solutions for racing and commercial applications [61]. OptimumLap makes use of basic vehicle parameters such as mass, frontal area, torque curves, gearing ratios, and tire radius to calculate driving, braking and cornering forces. Decomposing a circuit into a series of segments, OptimumLap determines the vehicle's maximum velocity through corners, its acceleration out of corners, and the distance needed to decelerate the vehicle in preparation for a corner. A velocity vs. distance driving cycle may then be obtained for use with the vehicle model described in Chapter 4. The method used by OptimumLap to determine a vehicle's "ideal" driving cycle for a given circuit is represented graphically in Figure 5.6 [62].

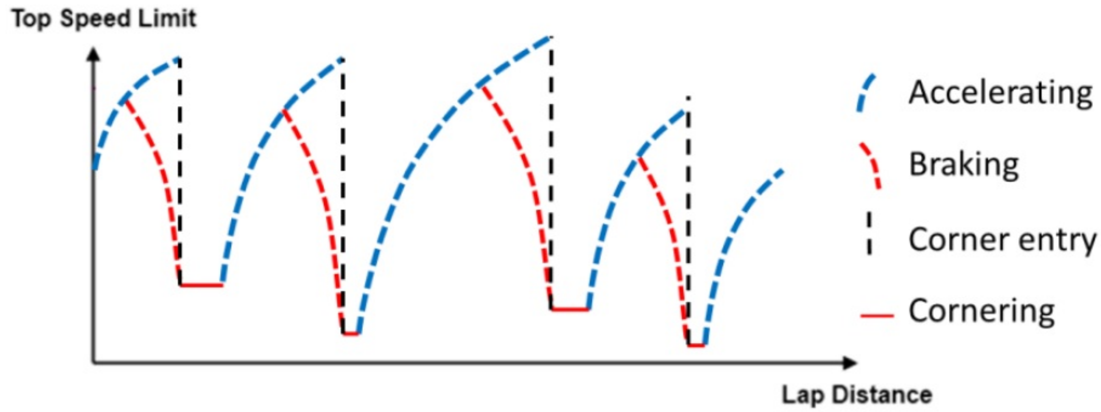

Figure 5.6: OptimumLap Calculation Method

A “performance” driver model was developed to accept the velocity vs. distance driving cycles produced by OptimumLap, as opposed to the more traditional velocity vs. time cycles used in the evaluation of a vehicle’s energy and fuel consumption. Due to the complex nature of the Camaro E/28’s powertrain, the vehicle model is not always capable of meeting the ideal driving cycle produced by OptimumLap. This is, however, not an indication that the results are invalid (as would be the case for a vehicle model not being able to follow a velocity vs. time driving cycle) since the performance metric in this evaluation was the length of time taken to traverse a distance. The performance driver model used for the analysis of the Camaro E/28’s dynamic capabilities is illustrated, below, in Figure 5.7.

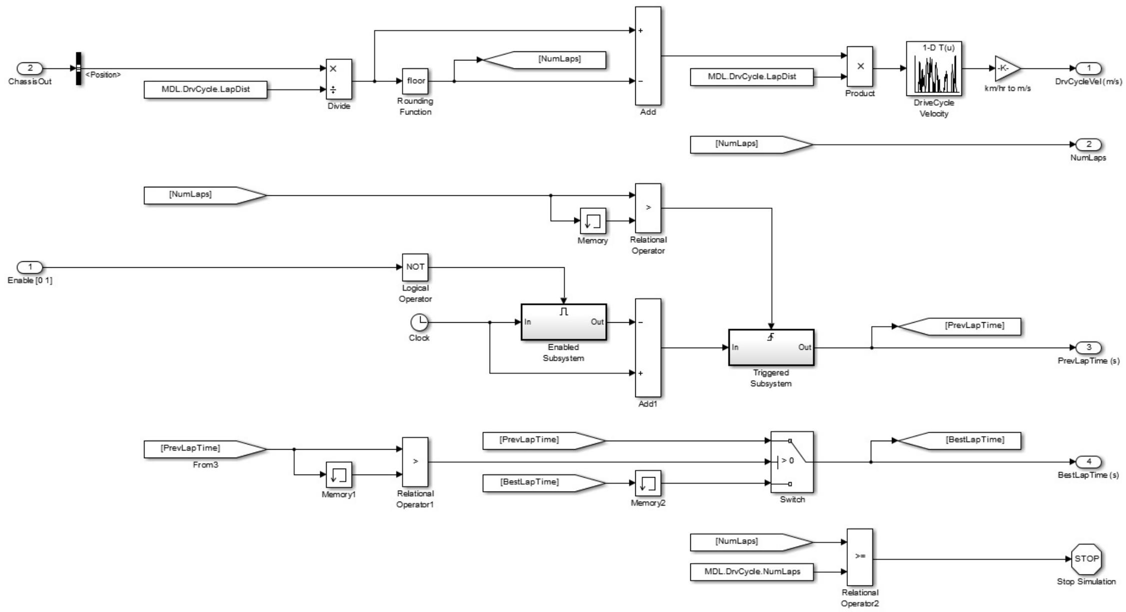

Figure 5.7: Performance Driver Plant Model

5.3 Summary of Vehicle Testing Procedures

In order to evaluate the environmental impact and dynamic performance of the Camaro E/28, several testing procedures, that utilized the vehicle model described in Chapter 4, were developed. Through the use of standardized driving cycles and the ANL GREET model, the vehicle's energy and fuel consumption, production of GHG and criteria emission, and PEU were able to be quantified on a full-fuel-cycle, or WTW, basis. A novel procedure for evaluating Camaro E/28's dynamic performance in a simulation environment was also established. This process involved having the Camaro E/28 model attempt to meet the "ideal" velocity vs. distance driving cycle produced by OptimumLap for various well-known circuits.

Chapter 6

Energy Management Problem

Supervisory control strategies can have a significant impact on the fuel economy and emissions of any hybrid electric vehicle. The use of its energy sources, both chemical and electrical, is often referred to as the “energy management problem” and has received considerable attention since the adoption of vehicle electrification [23].

Early solutions to the energy management problem were based on heuristic considerations derived from the expected behavior of the hybrid propulsion system. These methods would often result in suboptimal behaviour as they were strongly dependent on the assumptions made by control engineers. To overcome these difficulties, systematic, model-based, optimization methods using meaningful objective functions have received widespread adoption.

In the case of the Camaro E/28, the Equivalent Consumption Minimization Strategy (ECMS) and its extension, the A-ECMS, were investigated as potential solutions to the vehicle's energy management problem.

6.1 Equivalent Consumption Minimization Strategy

Optimal control policies, such as Dynamic Programming (DP), may seem well-suited for finding the solution to the supervisory control problem but require prior knowledge of the driving conditions (necessary to implement the DP backward algorithm) and are, therefore, not suitable for the real-time control of a HEV or PHEV. It is, however, possible to implement an optimal control strategy using the instantaneous minimization of a cost function which is dependent only on the system's state variables at the current time [63]. The cost function evaluates the value of electrical energy to that of fuel energy through the use of an "equivalence factor". This technique is known as an ECMS.

6.1.1 Problem Statement

It is the objective of the supervisory control strategy to minimize the vehicle's fuel consumption, and thereby, its emissions. This endeavour must be realized over the course of the vehicle's use, while the control actions that accomplish it must be made in real-time. To further complicate the matter, the control decisions are subject to several constraints including: meeting the driver's power request and respecting the limitations of the powertrain components.

The hybrid electric vehicle control problem may be expressed mathematically through Equation 6.1.

$$\left\{P_{ice}^{opt}\left(t\right),\, P_{em}^{opt}\left(t\right)\right\} = arg \min_{\left\{P_{ice}(t),\, P_{em}(t)\right\}} J_t, \quad t = 0, 1, 2, \ldots, t_f$$

$$\text{subject to} = \begin{cases} P_{req}\left(t\right) = P_{ice}\left(t\right) + P_{em}\left(t\right) \\ SOC_{min} < SOC\left(t\right) < SOC_{max} \\ 0 \leq P_{ice}\left(t\right) \leq P_{ice,max}\left(t\right) \\ P_{em,min}\left(t\right) \leq P_{em}\left(t\right) \leq P_{em,max}\left(t\right) \end{cases} \quad \forall t \tag{6.1}$$

where J_t is the ECMS's cost function, P_{req} is the driver's power request, P_{em} is the power of the electric motor(s), P_{ice} is the power of the ICE, and SOC is the HESS's SOC.

6.1.2 Cost Function

The ECMS determines the optimal power split between a hybridized vehicle's powertrain components through the evaluation of an instantaneous cost function. This function is the sum of the energy consumed by the vehicle's electric machines and the equivalent energy consumption of its engine. Equation 6.2 defines the instantaneous cost function that must be minimized as part of the ECMS.

$$J_t = \dot{m}_{ice}\left(P_{ice}\left(t\right)\right) H_{LHV} + \zeta\left(P_{em}\left(t\right)\right) \tag{6.2}$$

$m_{ice}()$ represents the fuel mass flow rate and H_{LHV} is the LHV of the fuel. The function $\zeta\left(P_{em}\left(t\right)\right)$ evaluates the equivalence between the energy being consumed (or produced) by the vehicle's electric machines to that of the fuel energy used by the ICE. Although electrical energy is not directly comparable to that of fuel energy, some form of equivalence factor is required. The equivalence between electrical energy and fuel energy is evaluated by considering the average energy paths that either source takes from storage to producing tractive power (or vice versa). Equation 6.3 and Equation 6.4 were used to determine the equivalent energy of the vehicle's electric machines.

$$\gamma\left(t\right)=\frac{1+sign\left(P_{em}\left(t\right)\right)}{2} \tag{6.3}$$

$$\begin{aligned}\zeta\left(P_{em}\left(t\right)\right)=s\left(t\right)\Bigg(&\gamma\left(t\right)\frac{1}{\eta_{batt}\left(P_{em}\left(t\right)\right)\eta_{em}\left(P_{em}\left(t\right)\right)}+\\&\left(1-\gamma\left(t\right)\right)\eta_{batt}\left(P_{em}\left(t\right)\right)\eta_{em}\left(P_{em}\left(t\right)\right)\Bigg)P_{em}\left(t\right)\end{aligned} \tag{6.4}$$

$\eta_{batt}()$ and $\eta_{em}()$ are the efficiencies of the vehicle's HESS and electric machines, respectively. $s\left(t\right)$ is what will henceforth be known as the "equivalence factor" and is a tunable control parameter. The equivalence factor is related to the overall powertrain efficiency throughout a particular time window, and therefore, it changes with the driving conditions. As a result, an equivalence factor that is suitable for one driving cycle will lead to poor performance for others. The vehicle's overall energy consumption can, therefore, be considered to be a function of the equivalence factor.

A systematic optimization can be applied in order to identify the equivalence factor that minimizes the energy and fuel consumption of the vehicle for known driving cycles. When the nature of the driving conditions change, however, so must the equivalence factor. The performance of ECMS is very sensitive to variations in the equivalence factor and a single set of control parameters cannot be applied to every situation [63]. Therefore, if the ECMS is to be applied to an actual vehicle, where the driving cycle is not inherently known, it must be able to adapt.

6.2 Adaptive Equivalent Consumption Minimization Strategy

In order to supplement the inability of the ECMS to conform to the variability of driving conditions, an A-ECMS was developed. A-ECMS implements a real-time algorithm for the estimation of an equivalence factor that best suits the current driving cycle. The control parameter will be periodically updated according to the current road load so that the fuel economy and emissions of the vehicle are minimized [63]. A high-level block diagram of the A-ECMS algorithm is provided by Figure 6.1, below.

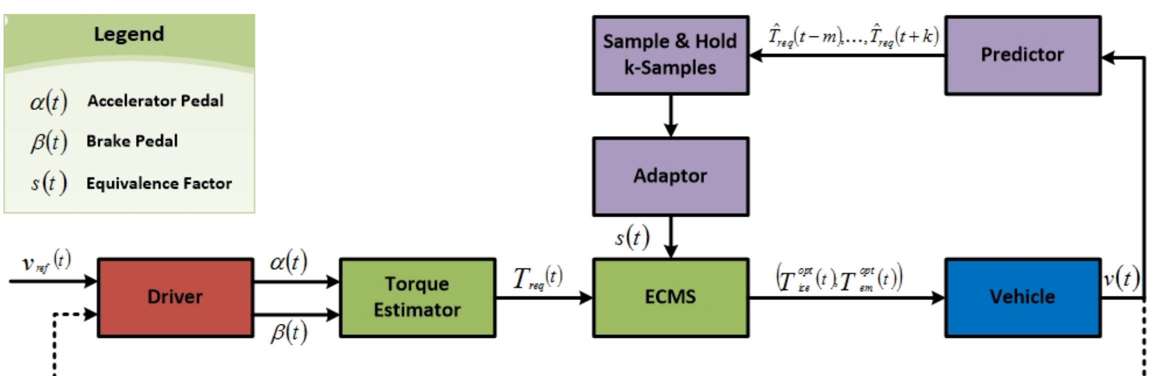

Figure 6.1: A-ECMS Control Block Diagram

The control block diagram illustrates the feedback loop introduced by an adaptation mechanism added to the ECMS framework. Without a device for the online estimation of the algorithm's control parameters, the system would operate in an open-loop manner and, consequently, could become unstable. As mentioned previously, the ECMS is highly susceptible to slight deviations in the equivalence factor and can cause unacceptable vehicle performance. The need to match the equivalent cost to that of the current driving conditions was, therefore, paramount. The A-ECMS provided the algorithm with more stability by allowing it to adopt the equivalence factor that is most appropriate for a given situation. The strategy, therefore, required no prior knowledge of the driving cycle and may still be implemented in real-time applications.

The adaptation mechanism of the A-ECMS was used to identify the vehicle's current driving conditions and to determine an equivalence factor that was suitable for that situation. The estimation was performed by combining past and predicted data so that an ideal trade-off between adaptivity and accuracy of the equivalence factor was achieved.

Several pattern recognition techniques have been proposed for the use of identifying driving conditions, including: statistical and clustering analysis techniques, stochastic process prediction techniques, and artificial neural network based techniques, among others [64]. For each method, representative driving patterns must be identified, and the control parameters tuned offline in accordance with each pattern. When a pattern is identified during the vehicle's use, the appropriate equivalence factor may be adopted. In the event that the traits of an actual driving schedule do not correspond to any of the pre-analyzed patterns, however, the adaptation mechanism will fail. In this case, it was necessary for the algorithm to adopt a set of sub-optimal control parameters that will produce suitable vehicle performance. An artificial neural network based approach for the identification of driving patterns was investigated as part of this research.

6.2.1 Driving Pattern Identification

Driving patterns exhibited by a real-world driver are the product of their instantaneous decisions to cope with the driving environment. Features such as road type, driving style, and the vehicle's mode of operation all have significant influence over a hybrid electric vehicle's fuel and energy consumption and its production of emissions [65]. An intelligent system that can accurately predict the driving patterns of the near future can, therefore, significantly benefit the control strategies of any vehicle.

For the implementation of the Camaro E/28's A-ECMS, a neural network system was developed that identified a current driving pattern as one of several representative situations. Figure 6.2 updates the control block diagram of the A-ECMS to include a neural network as the adaptation mechanism.

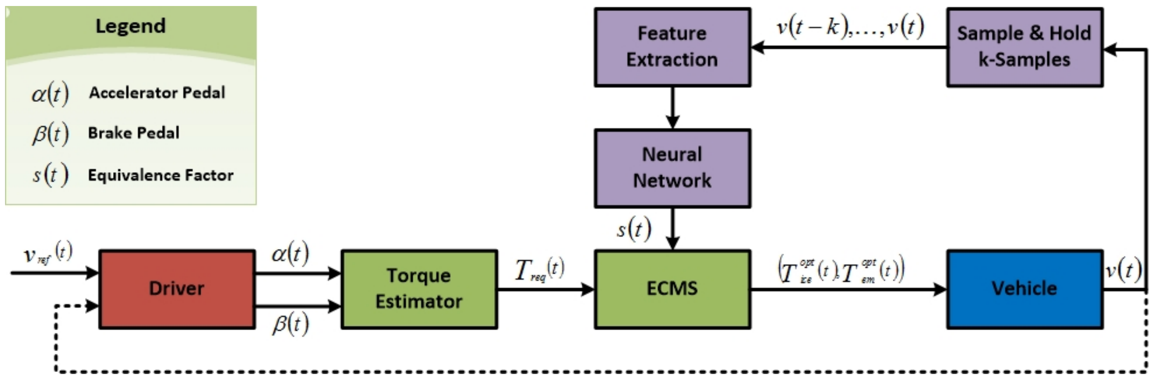

Figure 6.2: Control Block Diagram of the A-ECMS using a Neural Network

Representative Driving Cycles

Through systematic optimization, the equivalence factor that minimizes the fuel and energy consumption of the Camaro E/28 was identified for a series of known driving cycles. It was observed that the equivalence factors for similar roads types were nearly identical, and therefore, it was concluded that an adaptation mechanism needs to only identify "classes" of driving patterns and not a driving cycle itself.

Six representative driving cycles were selected and categorized into four classes, including urban, suburban, rural, and expressway patterns. These categories were selected on the basis that when the pattern recognition problem is involved, different classes are easily identifiable. Table 6.1 lists and classifies the six representative driving cycles.

Driving Pattern Type	**Driving Cycle**
Urban	UDDS NYCC
Suburban	WLTP Class 3 (590 sec – 1023 sec)
Rural	WLTP Class 3 (1024 sec – 1475 sec)
Expressway	HWFET CADC Motorway (130 km/h Variant)

Table 6.1: Representative Driving Cycles

Representative Driving Cycle Features

For the A-ECMS's adaptation mechanism to classify a driving pattern as either urban, suburban, rural, or expressway, several representative features of those driving conditions must first be recognized and observed. Driving patterns, for the most part, may be identified through the speed profile of the vehicle. In fact, it has been shown that the basic characteristics features related to fuel consumption and emissions are average cycle velocity, average running velocity, stop time/total time, and positive acceleration kinetic energy [66]. Table 6.2 describes the fourteen parameters that were chosen to characterize the representative driving patterns.

	Features	**Units**
F1	Average Cycle Velocity	km/h
F2	Average Running Velocity	km/h
F3	Stop Time/Total Time	%
F4	Positive Acceleration Kinetic Energy	m/s^2
F5	Average Acceleration	m/s^2
F6	Average Deceleration	m/s^2
F7	Number of Stops per Kilometer	Number
F8	Average Micro-Trip Time	sec
F9	Acceleration Time/Total Time	%
F10	Deceleration Time/Total Time	%
F11	Standard Deviation of Acceleration	m/s^2
F12	Standard Deviation of Deceleration	m/s^2
F13	Maximum Velocity	km/h
F14	Standard Deviation of Velocity	km/h

Table 6.2: Driving Pattern Characteristic Features

In pattern recognition, the use of additional representative features needs to be balanced with the "curse of dimensionality" where too many features may degrade system performance. Furthermore, too many parameters may cause excessive computational complexity which would result in higher hardware costs when deployed [67]. The problem of selecting a subset of optimal features is a classic research topic in pattern recognition. As the feature selection problem is computationally expensive, research has focused on finding a quasi-optimal subset of features, where quasi-optimal implies good classification performance but not necessarily the best classification performance. The fourteen parameters listed in Table 6.2 were found to produce the best results for identifying driving patterns in this application.

Before any of the characteristic features may be used with the A-ECMS's adaptation mechanism, they must first be standardized so that the features with the largest value do not distort the driving pattern recognition performance. Any of the fourteen parameters may also be weighted per its contribution in the identification of the driving pattern. Since features F1 through F6 are considered to be of more importance, their weights are larger than those of the other features.

Artificial Neural Network

The method chosen for the A-ECMS's adaptation mechanism was a three layer feedforward artificial neural network. Neural networks take a novel approach to machine learning as they employ a computational method which attempts to emulate the way the human brain solves problems. Many of the applications for neural networks have been concerned with problems in pattern recognition, and make use of feedforward network architectures to categorize inputs according to target classes. These systems are self-learning and are trained rather than explicitly programmed. Neural networks excel in areas where the solution or feature detection is difficult to express using traditional computer programming.

The neural network which was designed to be used as the A-ECMS's adaptation mechanism has three layers of successive transformations: two feedforward layers and a competition layer. The feedforward layers make use of sigmoid neurons to perform the inner product between each of the representative driving patterns and the current driving conditions and allows for the output of each layer to be interpreted as a probability. The competition layer contains softmax neurons which store the results of the feedforward layers and compete to determine a winner. After the competition, a single neuron will emerge victorious and indicates which representative driving pattern is closest to the current driving conditions. Figure 6.3 illustrates the architecture of the described neural network.

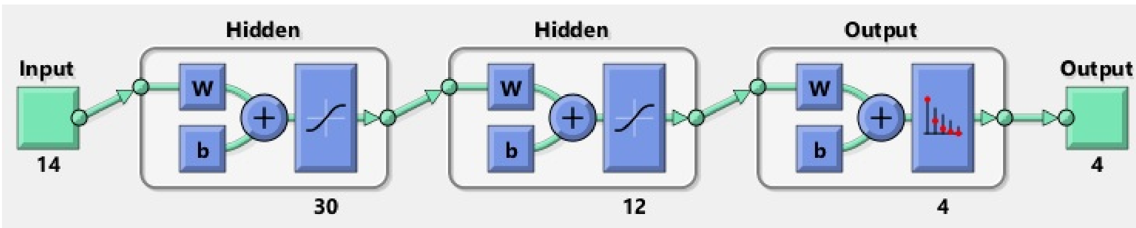

Figure 6.3: Three-Layer Feedforward Neural Network

After defining the network architecture, the representative features were extracted from the six known driving cycles and the resulting data was divided into training, validation, and testing sets. The network was trained with scaled conjugate gradient backpropagation where the forward stimulation is used to reset weights on the "front" neural units. After training, the neural network's performance was evaluated using cross-entropy and percent misclassification error, as well as with visualization tools such as confusion matrices and receiver operating characteristic curves.

Considerable thought was also put into the selection of the number of neurons in the feedforward layers in an attempt to avoid over-fitting or under-fitting the training data. Although several "rule-of-thumb" approaches have been suggested, they often do not take into account many aspects of the pattern recognition problem, and therefore, have varied results. A systematic optimization was instead adopted; the result of which found that layer sizes of thirty neurons and twelve neurons for the first and second feedforward layers, respectively, produced the best performance.

6.2.2 Algorithm Refresh Rate for Online Prediction

A critical point of consideration for an A-ECMS is the refresh rate of the equivalence factors. Although a high refresh frequency would result in a more adaptive algorithm, the computational burden that would result may jeopardize its real-time operation. In addition, if the refresh rate is too high, the segment of the vehicle's speed profile that the driving cycle's representative features are being extracted from may not contain any useful information. If the frequency is too low, however, the segment may contain obsolete data and the equivalence factors would not match the current driving conditions.

A suitable refresh rate for the A-ECMS was determined through systematic optimization. For all the frequencies under investigation, a neural network system was trained and tested using the data sets extracted from the six representative driving cycles. The representative features were extracted from each cycle's velocity profile for the time interval between successive refreshes and used as the input vector to the neural network. Figure 6.4 shows the results of this experimentation. Based on the analysis of the performances on both the training and test data, the best suited refresh rate was determined to be once every one hundred seconds.

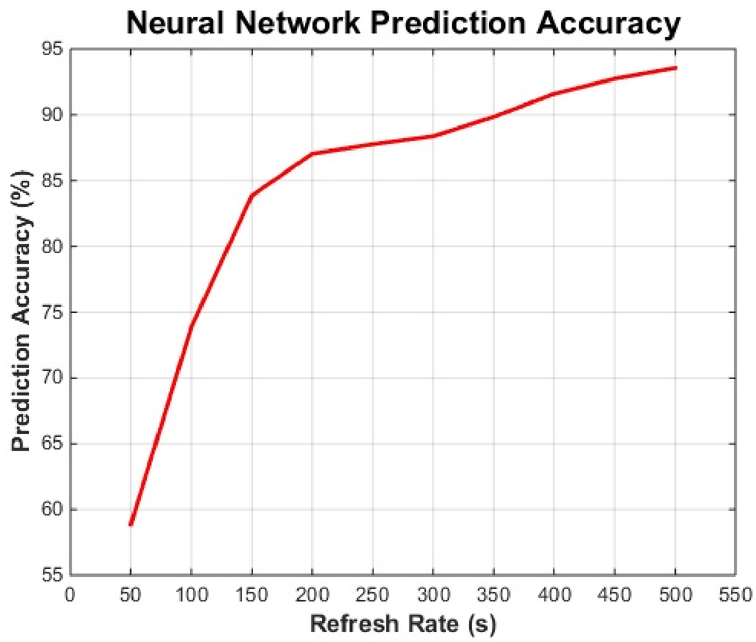

Figure 6.4: A-ECMS Predication Accuracies for Various Refresh Rates

6.2.3 Efficient Power Split

To reiterate, the A-ECMS determines a highly efficient power split at each moment based on an instantaneous minimization of a cost function that depends only on the system variables at that precise moment. The HESS's SOC, and by extension, whether the Camaro E/28 is operating per a charge depleting or charge sustaining control strategy, is one such variable. In fact, the selection of the ideal equivalence factor is determined, in equal amounts, by both the driving cycle and by the HESS's SOC. For each of the representative driving cycles there exist two equivalence factors, one for when the vehicle is operating according to a charge depleting strategy and one for when a charge sustaining strategy is being followed.

With this knowledge, the A-ECMS was able to determine the Camaro E/28's ideal power split using the following procedure:

1. The vehicle's velocity was measured and stored in the memory of the HSC.
2. Upon encountering the algorithm's refresh interval, the representative driving cycle features were extracted from the velocity profile.
3. The features were presented to the neural network, which identified it as one of the four representative driving patterns.
4. An equivalence factor was selected based upon the identified driving pattern and whether the vehicle is operating per a charge depleting or charge sustaining control strategy.
5. The ideal power split was calculated from the chosen equivalence factor.

6.2.4 A-ECMS Application

The A-ECMS factors into several aspects of the Camaro E/28's control strategies. The algorithm is not only used to determine of the ideal power split between the vehicle's engine and two electric machines during the parallel drive mode but it also aids in identifying when it is most appropriate for the vehicle to transition away from its current mode due to the present driving conditions. The exact application of the A-ECMS in these situations will be discussed further in Chapter 8.

6.3 Summary of Energy Management Problem

The method employed by a hybrid electric vehicle in the determination of how it uses its energy sources – whether it be electrical or chemical energy – is often referred to as it's solution to the supervisory control or energy management problem. An A-ECMS was developed for the Camaro E/28 and was used to determine a highly efficient power split, and thereby, provided a suitable solution to its energy management problem. The strategy's adaptation mechanism made use of an artificial neural network to identify specific driving patterns in real-time, and therefore, addressed the concerns involving the sensitivity of instantaneous minimization methods (such as the ECMS) to the driving cycle. The A-ECMS is ideal for use in hybrid vehicles as it is real-time oriented, computationally cheap, readily accounts for unexpected events, and has been shown to produce results comparable to those obtained using DP. In research conducted by Musardo, Rizzoni, Guezennec, and Staccia, it was shown that the A-ECMS was capable of achieving vehicle fuel economies within 0.4 mpg of those produced though DP [63].

Chapter 7

Vehicle Control System

With the selection of the Camaro E/28's architecture and powertrain components complete, the design of the vehicle's control system began. The ECUs that needed to be added to the Camaro's pre-existing control system were selected and the architecture of the network which they use to communicate was designed. This process was non-trivial as Camaro specific ECUs were required to function alongside both purchased and team designed embedded controllers.

7.1 Electronic Control Modules

In order to support the Camaro E/28's hybrid powertrain architecture, several ECUs were required to be purchased, or designed and manufactured by the McMaster Engineering EcoCAR 3 Team. For the control units that would be purchased from a manufacturer, the selection process involved identifying the ECUs that were either designed to accompany a specific powertrain component or to select the unit that would be most appropriate for the vehicle's high performance application. The complete list of the ECUs that were added to the Camaro's pre-existing control system is provided by Table 7.1.

Control Unit		**Manufacturer**	**Part Name**
Hybrid Supervisory Controller	HSC	dSpace	MicroAutoBox II 1401/1513
Battery Management Module	BMM	Elithion	Lithiumate Pro
Ultracapacitor Management Module	UCCM	McMaster University	N/A
Ultracapacitor Master Control Module	UMCM	JSR Micro	ULTIMO Master Control Unit
HESS DC/DC Converter Module	BBCM	BRUSA Elektronik	BDC546
P1 Motor Control Module	P1MCM	Rinehart Motion Systems	PM150DZR
P2 Motor Control Module	P2MCM	Rinehart Motion Systems	PM150DZR
Engine Control Module	ECM	General Motors	E-92 ECM
Transmission Control Module	TCM	General Motors	T87 TCM
Low-Voltage Support Front Module	LVFM	McMaster University	N/A
Low-Voltage Support Rear Module	LVRM	McMaster University	N/A
Dashboard Support Module	DSM	McMaster University	N/A
HV-to-LV DC/DC Converter Module	APM	BRUSA Elektronik	BSC623
HV Compressor Module	HVCM	Ford Motor Company	BM6Z19703A
Charger Control Module	CCM	BRUSA Elektronik	NLG513

Table 7.1: Electronic Control Modules

The MicroAutoBox II (MABXII) was selected as the vehicle's HSC due to its powerful processing capabilities, assortment of I/O and serial communication ports, and compatibility with the team's dSpace HIL simulator [68]. The dSpace ControlDesk and AutomationDesk development software were also shared between the MABXII and HIL simulator, and it was this shared platform that contributed significantly towards the selection of the HSC [69] [70].

The supervisory control system of the Camaro E/28 included several team designed control units meant to supplement the vehicle-to-controller interfaces of the MABXII. These controllers were designed to drive relays, interface with sensors, and to govern various actuators. The HSC still maintained full command of these control units through the use of a Controller Area Network (CAN). This design significantly reduced the number of digital and analog I/O required from the MABXII. Several examples of these supplemental control units included the Low-Voltage Support Front Module and the Low-Voltage Support Rear Module which aided the MABXII with power distribution for the newly introduced ECUs, and the Dashboard Support Module which provided the driver with additional vehicle interfaces specific to the Camaro E/28's hybrid systems.

The Battery Management Module (BMM), Ultracapacitor Master Control Module (UMCM), Engine Control Module (ECM), and Transmission Control Module (TCM) were all designed to function with a specific powertrain component, and as such, were selected for ease of integration. The Motor Control Modules (MCMs), on the other hand, were selected for their suitability in high performance and motorsport applications. Very few electric motor inverters would have been capable of achieving the power ratings and efficiency that were required by the Camaro E/28's powertrain architecture.

As mentioned in Chapter 3, the vehicle's HESS was designed according to the active parallel topology with the batteries and ultracapacitors existing in separate, and self-contained, accumulator packs. Each accumulator pack has its own set of contactors and appropriate fusing hardware in order to achieve safety constraints.

The BMM from Elithion was able to meet all of the requirements concerning the management of the battery pack, but the UMCM from JSR Micro was lacking some of this functionality. In order to supplement the UMCM's feature set, the Ultracapacitor Management Module (UCMM) was developed. The UCMM implements contactor control, temperature sensing, current sensing, and leakage detection within the ultracapacitor pack.

7.2 Vehicle Control Network

The next phase in the development of the Camaro E/28's control system was to identify a control network architecture that would be suitable for the vehicle. The primary issue that needed to be addressed was how to introduce the ECUs that supported the Camaro E/28's hybrid systems without interfering with the 2016 Chevrolet Camaro LT's stock control system. The proposed design of the control network is illustrated in Figure 7.1, below.

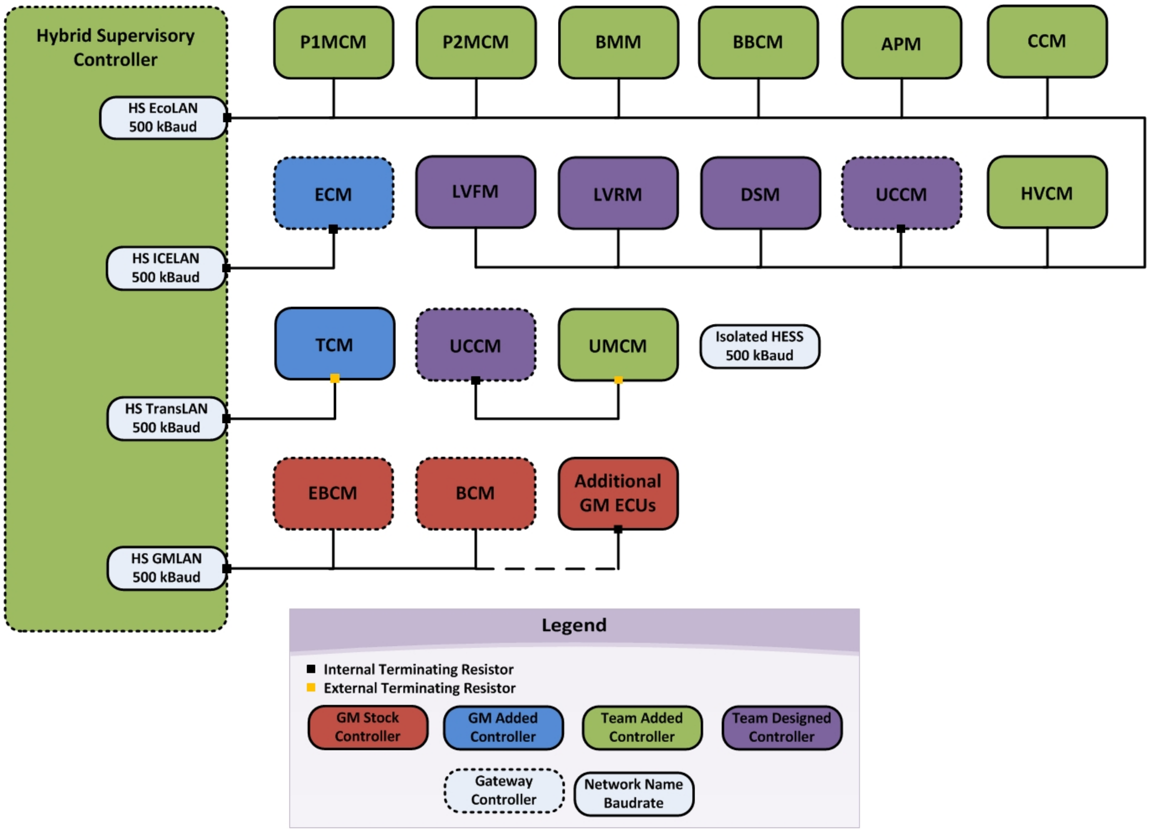

Figure 7.1: Vehicle Control Network Architecture

The HSC that was selected, the dSpace MABXII 1401/1513, has support for up to four CAN channels. All four of these channels were required by the proposed control network architecture. One channel, operating at a baud rate of 500 kBaud, supported the non-GM controllers that have been added to the vehicle. The second and third channels also function at a baud rate of 500 kBaud and belong to the ECM for the GM LTG ICE, and the TCM for the GM 8L90 transmission, respectively. The last channel interfaces with the vehicle's pre-existing High Speed GMLAN CAN network which operates at 500 kBaud.

Several factors were considered when designing the architecture of the vehicle's control network, including: message or controller identifier conflicts, baud rate compatibility, isolating components from the stock vehicle's controllers, and bus loading.

The first item under consideration was the isolation of any of the vehicle's stock components from those being added to support the hybrid powertrain. This decision will prevent any identifier conflicts between the messages being broadcast on the High Speed GMLAN network and those of the introduced control units. Any issues regarding baud rate compatibility and network loading from these additional controllers were also mitigated. The vehicle's stock ECM and TCM were removed from the High Speed GMLAN network and were instead replaced with the HSC. The HSC acts as a gateway module to the vehicle's other control networks and terminates the High Speed GMLAN network in place of the stock ECM.

Two non-stock GM powertrain controllers were also added to the vehicle, an ECM for the GM LTG ICE and a TCM for the GM 8L90 transmission. In order to achieve the level of functionality necessary from these components, the new ECUs were required to be placed on their own isolated networks, separate from each other and from the High Speed GMLAN network. As a series-parallel PHEV, the Camaro E/28 has multiple powertrain components that may meet the crankshaft torque requests sent from the driver and from the TCM, where in a traditional combustion vehicle it would only be met by the ICE. The HSC must, therefore, intercept all CAN signals to, and from, the ECM in order to command the required torque from the engine and to satisfy the requests from the vehicle's other stock controllers. Similarly, in order for the HSC to command an appropriate gear from the transmission (during the vehicle's manual gear selection mode using the paddle shifters), the TCM must also exist independently from the rest of the vehicle's control network. The HSC will, once again, terminate the High Speed ICELAN network with the help of the internal terminating resistor of the ECM, and the High Speed TransLAN network with a resistor external to the TCM.

In order to electrify the 2016 Chevrolet Camaro LT, numerous additional components and control units were introduced to the vehicle. These control units exist on their own network and use the HSC as a gateway module to gain access to pertinent information provided by the vehicle's stock controllers. Message identifier conflicts, baud rate compatibility, and bus loading were all considered when deciding which control units would be able to exist on this network. All of the controllers that were added were able to configure their baud rate and CAN message identifiers. The control units that were designed by the McMaster Engineering EcoCAR 3 Team operate at a baud rate of 500 kBaud and were programmed to use a CAN protocol with identifiers that do not conflict with those of the purchased components. The HSC and the team designed UCMM are used to terminate the bus.

The bus loading due to the team added control units was put into consideration when designing the High Speed EcoLAN network. If the bus loading of the network exceeded approximately 80%, messages may be dropped or lower priority messages may have to wait an unacceptable amount of time to be transmitted [71]. Approximate bus loading was determined through simulation and CAN bus logs of the stock vehicle, the results of which are provided by Table 7.2. The complete analysis of the Camaro E/28's control networks is available in Appendix A. From these tests, it was determined that all of the non-GM, newly introduced control units may exist on a single CAN channel.

Network Name	Baud Rate	Network Loading
High Speed EcoLAN	500 kBaud	62.50%
High Speed ICELAN	500 kBaud	40.50%
High Speed TRANSLAN	500 kBaud	44.60%
High Speed GMLAN	500 kBaud	56.70%

Table 7.2: Vehicle Control Network Bus Loading Estimates

An additional isolated control network was required to be added to the vehicle. This network allows the JSR Micro UMCM to convey information concerning the ultracapacitor modules to the team designed UCMM. The UCMM then functions as the single point of contact between the Camaro E/28's control system and the ultracapacitor pack.

7.3 Summary of Vehicle Control System

To support the Camaro E/28's hybrid powertrain, several supplemental ECUs were added to the 2016 Chevrolet Camaro LT and a new control network architecture was defined. It was necessary that these new control units did not interfere with the operation of the vehicle's other systems and, it was for this reason, they were isolated on an independent CAN channel. Several factors contributed to the design of the vehicle's control network, including: message or controller identifier conflicts, baud rate compatibility, isolating components from the stock vehicle's controllers, and bus loading.

Chapter 8

Vehicle Control Algorithms

The design and implementation of the Camaro E/28's supervisory control algorithms was approached with the intent of following a rational and systematic process. Although it is unrealistic to derive a design in a totally rational and error-free way from a statement of requirements, an attempt was made and the documentation that makes it appear as though it had, was produced. The following sections outline the development of requirements, modular structure, module interfaces, dataflow dependency, and internal structures and implementation for the vehicle's supervisory control software.

8.1 Software Requirements

The first step in the rational design process of safe and functional software is to develop and document the requirements for the desired behaviour of the system. These requirements may take one of two forms: existing as a system-level requirement or as a component-level requirement.

System-level requirements are a set of statements that identify the functions which the system should fulfill to satisfy the stakeholder's desires, and are expressed using an appropriate combination of textual statements, views, and non-functional requirements. In the case of the Camaro E/28, the system-level requirements state how the vehicle is meant to function and specifies the levels of safety, security, and reliability that will be necessary. Conversely, component-level requirements define the behaviour of each of the vehicle's principal components with the objective of meeting the system-level requirements. Component-level requirements may specify hardware, input/output interfaces, timing and accuracy constraints, normal operational behaviour, and undesired event handling.

Table 8.1 provides examples of several component-level requirements for the software associated with the P1/P2 MCM. Every requirement entry has a unique identification number, a list of test cases used to verify the requirement, and the requirement's author. The identification numbers are used to relate a component-level requirement to a corresponding system-level requirement.

Req. ID	Requirement	Test Case	Author
2.1.1	The HSC must begin broadcast of the MCM Command message before the MCM is supplied with LV power.	2.1.1.1 2.1.1.2	AML
2.1.2	The HSC must broadcast the MCM Command message cyclically every 500ms (or sooner).	2.1.2.1	AML
2.2.1	The HSC must first enable the inverter interlock before attempting to enable the MCM using the Command message.	2.1.1.1 2.1.1.2	AML
2.3.1	The HSC must first disable the MCM using the Command message to remove the inverter lockout. Once removed, the MCM may be enabled.	2.3.1.1 2.3.1.2	AML

Table 8.1: Motor Control Module Component-Level Requirements

Although a system-level and component-level requirements specification has been completed for the Camaro E/28's supervisory control system, the full documents are only available under a non-disclosure agreement due to the proprietary nature of the project and of the EcoCAR 3 competition. The examples provided by Table 8.1 do not include any confidential information.

8.2 Software Modular Structure

After defining the requirements for the Camaro E/28's supervisory control system, the next phase of the rational design process is to establish the methodology for the decomposition and modularization of the software. The approach which was adopted was based upon a philosophy described in Gouthier and Pont's 1970 textbook "Designing Systems Programs" [72]. Their method is characterized by the following concepts:

1. Each task forms a separate, distinct program module.

2. Each module's inputs and outputs are well-defined, there is no confusion in the intended interface with other system modules.
3. The integrity of each module is tested independently.
4. The system is maintained in a modular fashion; system errors and deficiencies can be traced to specific system modules, thus limiting the scope of detailed error searching.

Gouthier and Pont's approach to software decomposition on the basis of responsibility is often abandoned in favor of modularization according to "information hiding". This method, developed by David Parnas, is characterized by software modules that conceal knowledge of a design decision from all others [73]. Module interfaces and definitions are chosen so as to reveal as little as possible about its implementation. David Parnas' approach, however, is difficult to apply to dataflow programming languages such as Simulink. Since software decomposition according to concerns was more easily applied, this was the method used in the development of the Camaro E/28's supervisory control software.

Despite the difficulties of its use in dataflow programing languages, the benefits of modular decomposition are many and are worth pursuing. Software development times can be drastically shortened as separate programmers may work on each module with little need for communication, product flexibility is increased as drastic changes can be made to one module without requiring to change others, and system errors can be easily identified and traced back to specific modules.

With the intent of decomposing the Camaro E/28's supervisory control software according to responsibility, the vehicle's modules were selected so that each governs a single powertrain component or provides a specific service. The documentation produced through this process is known as a module guide. A module guide defines the responsibilities of each of the modules by stating the design decisions that will be encapsulated by it. A module guide is needed to avoid duplication, to avoid gaps, and to achieve separation of concerns. Table 8.2 provides a simplified module guide for the Camaro E/28's supervisory control system.

Software Module		**Responsibility**
Power Mode Selection Ring	PMR	Control vehicle startup and shutdown
Drive Mode Selection Ring	DMR	Determine vehicle drive mode and driver torque request
P1 Motor Control Ring	P1MR	Control the P1 electric motor and series mode operation
P2 Motor Control Ring	P2MR	Control the P2 electric motor and regenerative braking
Internal Combustion Engine Control Ring	ICER	Control the engine and series mode operation
Transmission Control Ring	TCR	Control the transmission and torque converter
HESS Control Ring	HESSR	Control the HESS (ultracapacitors batteries, DC/DC)
HV-to-LV DC/DC Converter Control Ring	APMR	Control the HV-to-LV DC/DC converter
On-Board Charger Control Ring	CCR	Control the on-board charger
HV Compressor Control Ring	HVCR	Control the HV compressor
Thermal Management Ring	THMR	Control the vehicle's thermal management systems
Torque Security Ring	TSR	Ensure vehicle torque security is maintained
ECMS Control Ring	ECMSR	Determine the vehicle's ideal torque split

Table 8.2: Supervisory Control Software Module Guide

Software modules such as P1MR, ICER, and TCR are designed to interact with and control specific powertrain components; in this case, the P1 electric motor, the ICE, and the transmission, respectively. These modules contain the software to communicate with the component's ECU (or to command the HSC's I/O), perform diagnostics, and to implement the control logic involving the component. The diagnostics performed involve ensuring that the feedback from each component meets plausibility and timeliness constraints (signal diagnostics), as well as to determine the status and overall effectiveness of the component (component diagnostics). If the diagnostics indicate that the component is experiencing some form of failure, its capabilities may be reduced, or it may be taken offline entirely.

Modules such as PMR, DMR, and TSR are not responsible for controlling a component of the powertrain, but instead provide a service to the supervisory control system. PMR is accountable for overseeing the startup and shutdown of the vehicle while DMR determines the drive mode, or powertrain configuration, that is most suitable at a given instance. TSR is what has been identified as a "system diagnostics" module. It does not concern itself with a particular component or service, but instead ensures that the vehicle is functioning as intended.

8.3 Software Module Interfaces

The third stage of the rational design process is to specify the Module Interface Specifications (MISs). MISs are formal documentation that dictate the externally observable behaviour of each software module as well as the required interfaces. An MIS contains no information on the module's implementation, but is instead intended as a guide for its use. MISs are of importance to designers that may require the use of a software module but are not necessarily responsible for its implementation. MISs are also indispensable in the design of the dataflow dependency between each software module. An MIS was developed for each of the thirteen modules that make up the Camaro E/28's supervisory control system.

To further facilitate the uniformity between the software modules, a naming convention for the input and output signals was established. This resolution was developed with the intent of making every signal unique and easily identifiable. The convention indicates the signal's source, data type, measurement unit, and range. Table 8.3 illustrates several examples of the signal naming convention.

Signal Name	Signal Origin	Signal Type	Unit	Range
BMM_b_VehicleMonitor_[0 1]	BMU	Boolean	None	[0 – 1]
BMM_d_DischargeMax_Amp_[0 300]	BMU	Double	A	[0 – 300]
BMM_d_DischargeBuffer_Pct_[0 100]	BMU	Double	%	[0 – 100]

Table 8.3: Vehicle Model Signal Naming Convention

8.4 Software Dataflow Dependency

The fourth step in the rational design process is to establish the "uses" hierarchy of each software module. In dataflow programming languages such as Simulink, however, a hierarchy does not exist in the traditional sense, and instead, the relation between modules must be viewed as a "dataflow dependency". In the case of the Camaro E/28's supervisory control system, structured dependencies exist within each software module in addition to between the modules themselves.

Each software module was divided into several subsystems according to the level of abstraction that was required from the actual vehicle. Modules may include the software to interface with a physical component, signal and component level diagnostics, and the logic which implements the module's functional specifications. Dataflow dependencies are formed as each of these subsystems is dependent upon the output of another. The structure of several software modules within the supervisory controller is demonstrated by Figure 8.1, below.

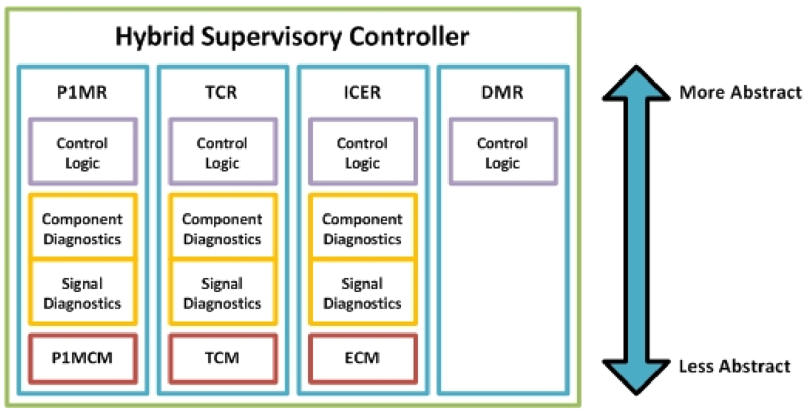

Figure 8.1: Supervisory Control Software Module Decomposition

As mentioned earlier, dependencies also exists between the software modules themselves as they may use outputs derived from one another. It was necessary to be aware of the relation between modules as it was imperative in meeting the staged deliveries of the EcoCAR 3 competition, the development of fail soft systems, and in the verification and validation of the Camaro E/28's control system. The dataflow dependencies of the HSC's thirteen software modules is provided by Table 8.4. A checkmark within the table indicates that the corresponding *Input Module* (horizontal axis) was reliant upon the data provided by the intersecting *Output Module(s)* (vertical axis). The software module DMR, for instance, produced data which was then used as input to PMR, P2MR, TCR, HESSR, and ECMSR.

Output Module \ Input Module	PMR	DMR	P1MR	P2MR	ICER	TCR	HESSR	APMR	CCR	HVCR	THMR	TSR	ECMSR
PMR			✓	✓	✓	✓	✓	✓	✓	✓		✓	
DMR	✓			✓		✓	✓						✓
P1MR	✓	✓		✓	✓		✓						✓
P2MR	✓	✓	✓		✓	✓	✓						✓
ICER	✓	✓	✓	✓			✓						✓
TCR	✓	✓	✓		✓								
HESSR	✓	✓	✓	✓				✓	✓	✓			
APMR	✓						✓						
CCR	✓						✓						
HVCR	✓						✓						
THMR	✓	✓	✓	✓									
TSR			✓	✓	✓	✓							
ECMSR		✓					✓						

Table 8.4: Supervisory Control Software Dataflow Dependencies

8.5 Software Internal Structures and Implementation

The final two stages in the rational design process of the Camaro E/28's supervisory control system was to design and implement the internal structure of each software module. The HSC's software encompasses thirteen modules and numerous unique control strategies, but in the interest of conciseness, only four will be discussed in detail. These control strategies include the vehicle's startup procedure, drive mode selection, powertrain torque production, and optimal shift schedules.

8.5.1 Vehicle Startup

Being a hybrid electric vehicle, the process of starting the Camaro E/28 is complicated by the existence of its multiple torque producing components and ESSs. The 2016 Chevrolet Camaro LT's keyless entry feature was used to detect the presence of the driver, and preemptively begin the vehicle's startup procedure. The keyless entry module was used to wakeup the team designed LVSR control unit from a low-power state, and it in turn provides power to the HSC and the vehicle's other ECUs. The HSC will then wait until the driver has chosen to start the vehicle before continuing with the startup process. If the vehicle's battery pack or HV-to-LV DC/DC converter are unable to be enabled, the vehicle will be rendered inoperable as the low-voltage battery cannot sustain the low-voltage power demands of the vehicle. If the ultra-capacitor pack, HV-to-HV DC/DC converter, or P2 electric motor are unable to be brought online, the vehicle will be unable to produce tractive power. Additionally, if the P1 electric motor is inoperable, the ICE will be unable to be started (the vehicle lacks a starter motor). The system-level vehicle startup procedure is illustrated by Figure 8.2.

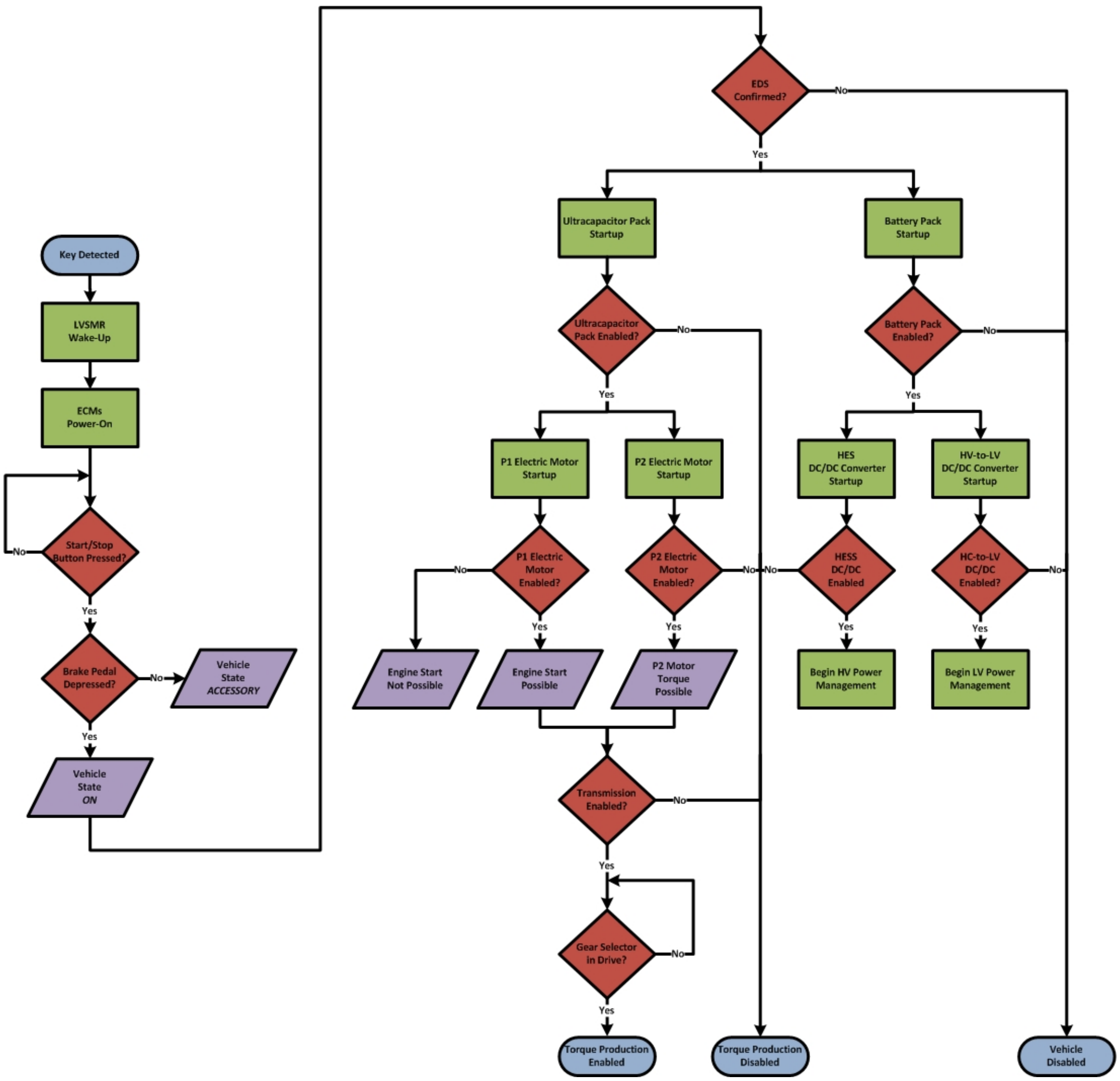

Figure 8.2: Vehicle Startup Procedure

The startup procedure, as described, was implemented using Simulink Stateflow within the PMR control module. An image of the implemented startup logic is provided by Figure 8.3, below.

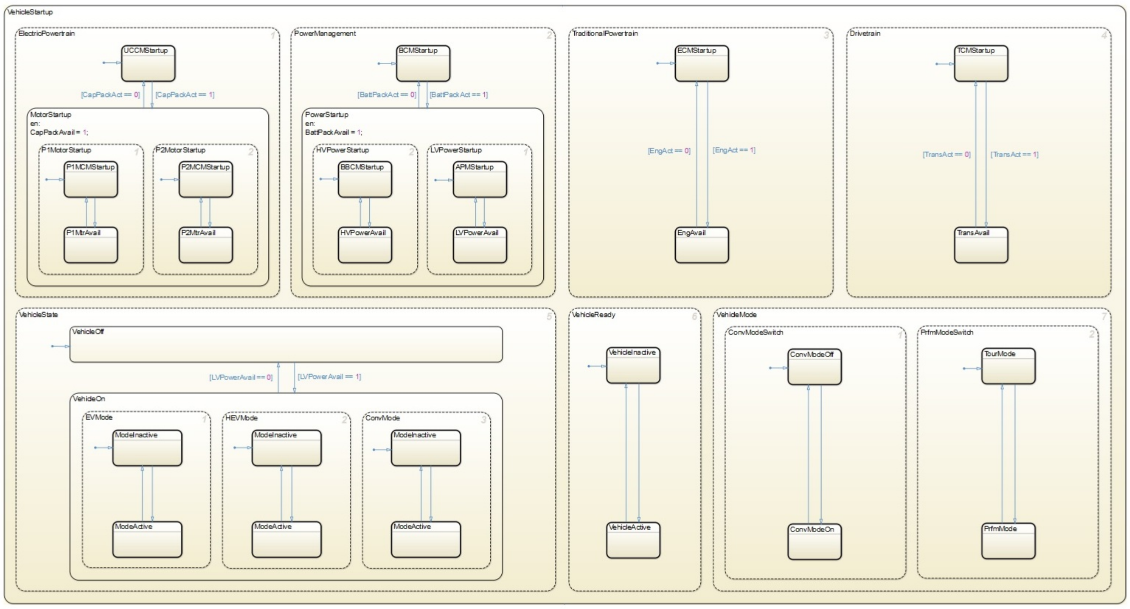

Figure 8.3: Vehicle Startup Control Software

Many aspects of the Camaro E/28's startup procedure may occur in parallel; as illustrated by Figure 8.2. These concurrent operations are necessary to achieve rapid vehicle startup and to meet the two second requirement that the EcoCAR 3 competition has for achieving propulsion readiness. A startup procedure with concurrent elements was able to be implemented in Simulink Stateflow using a combination of parallel (AND) and exclusive (OR) states.

Although the PMR software module is accountable for when aspects of the vehicle's powertrain should be brought online, it is the responsibility of the module which governs that component to be concerned with how it is brought online. P1MR, for instance, encapsulates the information on how to communicate with the electric motor's inverter and how to achieve propulsion readiness with it. PMR simply informs P1MR when to bring the P1 electric motor on or offline, and what the remediating actions are if there is an issue while performing either operation.

Electric Motor Startup Procedure Example

The process that the P1MR (or P2MR) software module takes while enabling the torque production capabilities of the P1 (or P2) electric motor involves a "hand-shaking" procedure between the HSC and the MCM. The PM150DZR MCM from Rinehart Motion Systems has an enable lockout safety feature that must be disabled before any torque requests can be sent to the electric motor [74]. Several CAN messages are exchanged between the two ECUs.

The *Internal States* CAN message is transmitted by the MCM and is used to indicate the status of the inverter as well as the state of the torque production lockout safety feature. The format of the *Internal States* CAN message is shown in Table 8.5, below. To avoid confusion, only the pertinent aspects of CAN messages are provided throughout this document.

CAN ID	Byte.Bit	Name	Format	Description
0x1AA	6.0	Inverter Enable State	Enumerated Type	0 = Disabled 1 = Enabled
	6.7	Inverter Enable Lockout	Enumerated Type	0 = Inverter can be Enabled 1 = Inverter cannot be Enabled
	7.0	Direction Command	Enumerated Type	0 = Reverse 1 = Forward

Table 8.5: P1/P2 MCM Internal States CAN Message

The HSC sends the *Command* CAN message that is used to request a torque and direction from the electric motor in addition to enabling its torque production. The format of the *Command* CAN message used is provided in Table 8.6.

CAN ID	Byte.Bit	Name	Format	Description
0x1C0	0.7 – 1.0	Torque Command	Signed Integer E = N * 0.1	Torque command.
	4.0	Direction	Boolean	0 = CW 1 = CCW
	5.0	Enable	Boolean	0 = Inverter Off 1 = Inverter On

Table 8.6: P1/P2 MCM Command CAN Message

The exchange of the *Internal States* and *Command* CAN messages between the HSC and the MCM during the process of enabling the torque production of the P1 (or P2) electric motor is illustrated in Table 8.7. Values of "X" indicate a "Don't Care" scenario and the significance of the highlighted values are explained further in the table's "Description" column.

		Byte								
Message Sender	**CAN ID**	**0**	**1**	**2**	**3**	**4**	**5**	**6**	**7**	**Description**
MCM	0x1AA	0x04	0x00	0x09	0x00	0x00	0x00	0x80	0x00	MCM lockout is enabled.
HSC	0x1C0	0x00	0x00	0x00	0x00	0x00	0x00	X	X	Send out inverter disable command to release lockout.
MCM	0x1AA	0x04	0x00	0x09	0x00	0x00	0x00	0x00	0x00	MCM lockout is disabled.
HSC	0x1C0	0x00	0x00	X	X	0x01	0x01	X	X	Enable the MCM in the forward direction.
MCM	0x1AA	0x05	0x00	0x08	0x00	0x00	0x00	0x01	0x01	The MCM is enabled and ready to run in the forward direction.

Table 8.7: P1/P2 MCM Enabling Procedure

8.5.2 Drive Mode Selection

As a series-parallel PHEV, the Camaro E/28 is capable of several drive modes, including:

1. An Electric Drive Mode
2. A Series Drive Mode,
3. A Parallel Drive Mode, and
4. An Engine-Only Drive Mode

The supervisory control software will transition the vehicle between these four drive modes depending upon several factors. These factors consist of meeting the driver's power request, the HESS's SOC, the vehicle's desired performance mode, the status of the various powertrain components, and the current driving pattern.

The driver commands tractive power from the vehicle using the accelerator pedal. This command, is in turn, converted into a torque requested from the Camaro E/28's powertrain. If the torque request exceeds what the vehicle is capable of producing in its current configuration, the supervisory control logic will select the drive mode that will best suit the driver's needs. The torque that the powertrain is capable of producing is dependent upon the driveline speed, powertrain component temperatures, and the discharge limit of the HESS, among other factors.

The HESS's SOC also contributes significantly to how the supervisory control logic selects the vehicle's drive mode. Since the Camaro E/28 is a PHEV, its HESS may be recharged by an external power source, unlike a HEV which must generate its electrical energy through the use of an ICE or regenerative braking. The greater capacity of the HESS and the ability to recharge from the power grid allows the Camaro E/28 to operate as an electric vehicle (and be gasoline-independent) for significant distances, with the extended range of an engine for longer trips. In order to maximize its fuel economy, the Camaro E/28 will operate according to a charge depleting control strategy, where it will function as an electric vehicle, before transitioning to a charge sustaining strategy after the HESS's SOC reaches a minimum allowable level. While in the charge sustaining mode, the vehicle will use its P1 electric motor and ICE as a generator (series drive mode) to power its primary traction motor (P2 electric motor) and recharge the HESS. The Camaro E/28 may also enter its parallel drive mode while adhering to a charge sustaining strategy in order to meet the power requests from the driver that exceed the performance capabilities of the P2 electric motor. Figure 8.4 illustrates how the transition between a charge depleting and charge sustaining control strategy is dependent upon the HESS's SOC.

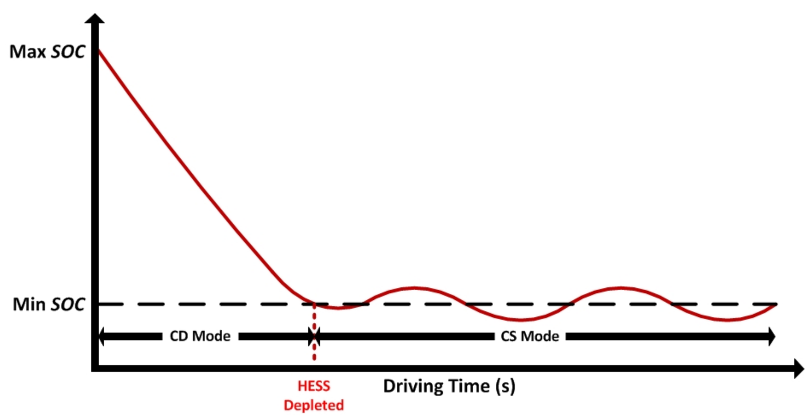

Figure 8.4: Transition between Charge Depleting/Charge Sustaining Strategies

The Camaro E/28 comes equipped with two performance modes: a touring mode and a sport mode. The touring mode is primarily concerned with maximizing the fuel economy and drivability of the vehicle, while the sport mode allows the driver to unleash its full dynamic capabilities.

The sport mode alters how the position of the accelerator pedal correlates to the power requested from the powertrain, allowing for more torque to be available to the driver than in touring mode. The gear selection schedules are also altered to permit the ICE to operate at higher speeds, and thereby, produce more power but at the cost of a lower operating efficiency. Lastly, sport mode has the Camaro E/28 transition more quickly to, and spend more time in, its parallel drive mode.

Since the transition from the vehicle's electric drive mode is an elaborate process which involves starting the ICE, matching its speed to that of the P2 electric motor and closing a clutch, a method to limit the frequent switching of drive modes was implemented. Time dependent logic was developed to ensure that the need to alter the current drive mode was not fleeting and would benefit the vehicle in the long-term. In the sport performance mode, the supervisory control software will allow for a dramatically quicker transition to the parallel drive mode and will prevent it from leaving this mode for an extended period of time. The time dependent logic acts as a low-pass filter, and prevents frequent, and potentially unnecessary, mode switching. The drive mode selection logic is featured in Figure 8.5 and the time dependent logic for the transition between the electric and series/parallel drive modes is illustrated in Figure 8.6.

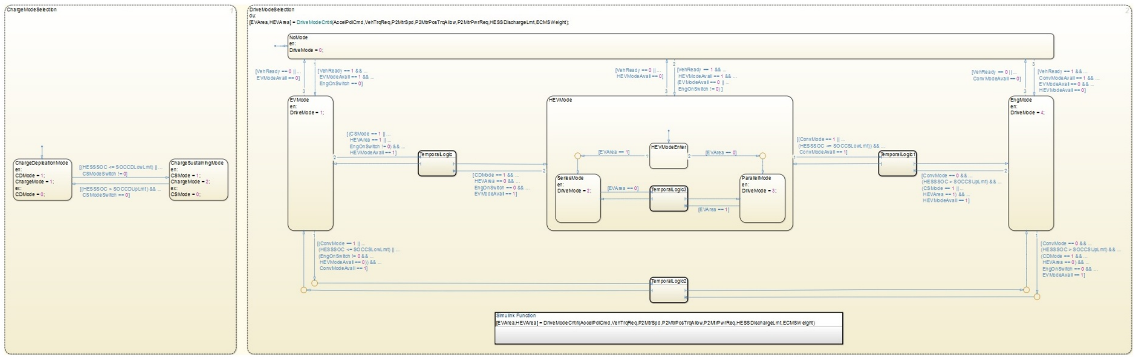

Figure 8.5: Drive Mode Selection Software

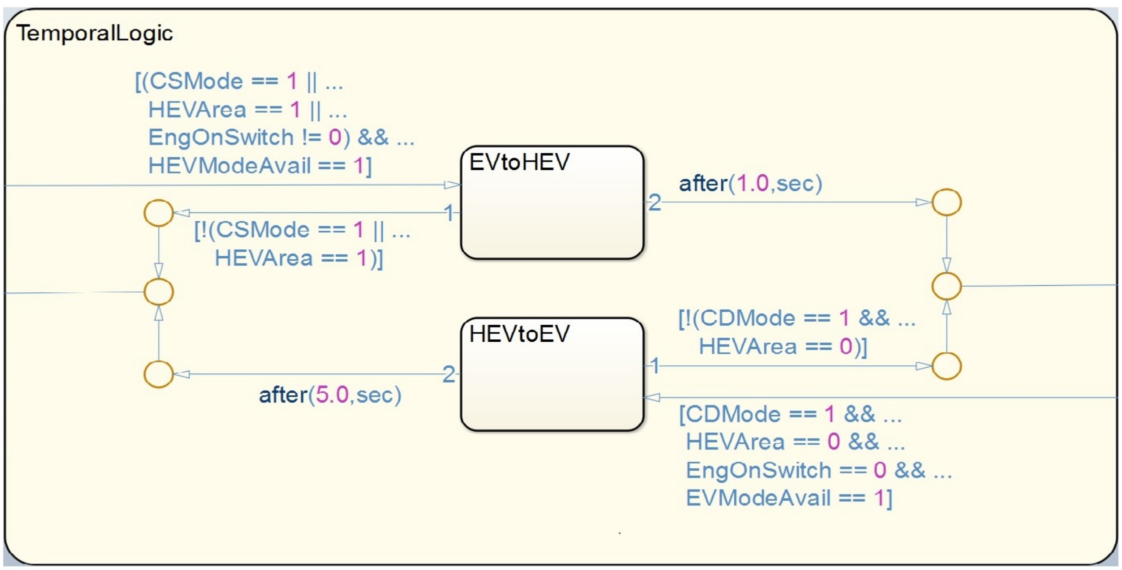

Figure 8.6: Time Dependent Logic used when Switching between Drive Modes

Component failure, or unavailability, also affects which of the drive modes the Camaro E/28 may enter. Table 8.8 demonstrates how the selection of a drive mode is affected by a fault in a component or subsystem either during the vehicle's startup or operation. The supervisory control software will select the drive mode that best suits the driver's needs without violating these constraints.

Component Failure	Electric Mode	Series Mode	Parallel Mode	Engine Mode
P1 Motor or Inverter	Available	Unavailable	Limited	Unavailable
P2 Motor or Inverter	Unavailable	Unavailable	Limited	Available
Engine	Available	Unavailable	Unavailable	Unavailable
Transmission	Unavailable	Unavailable	Unavailable	Unavailable
HESS	Unavailable	Unavailable	Unavailable	Unavailable
Clutch (Open)	Available	Available	Unavailable	Unavailable
Clutch (Closed)	Unavailable	Unavailable	Available	Available

Table 8.8: Drive Mode Availability Logic

Lastly, the vehicle's current driving pattern also influences which drive mode the supervisory control software selects. The A-ECMS classifies the driving pattern and identifies the power split between the engine and the two electric machines which yields the minimum energy consumption. If the power split has the P2 electric motor meeting the driver's requests, the electric drive mode would be chosen as the most suitable. Conversely, if the split has the P1 electric motor and ICE acting as a generator or as a source of tractive power it would dictate that the series and parallel drive modes are required, respectively.

The A-ECMS is only used to determine when the supervisory control software should transition the vehicle away from the electric drive mode to either the series or parallel modes. If the driver's power request, the HESS's SOC, or the status of the various powertrain components necessitate a change in the drive mode, this adjustment will be made in potential opposition to the suggestion made by the A-ECMS. This guideline is necessary to ensure the safety and drivability of the Camaro E/28.

8.5.3 Drive Mode Control Logic

Each of the Camaro E/28's four drive modes uses a unique approach in determining the power split between the its engine and two electric machines. The following sections provide a brief description of the approach taken for the vehicle's electric, series, parallel, and engine-only drive modes.

Electric Drive Mode

While in its electric drive mode, the Camaro E/28's P2 electric motor is used to meet all of the driver's tractive power requests. The clutch that exists between the ICE and the motor is opened and the engine is not used. If the driver's power request exceeds the capabilities of the P2 electric motor, the supervisory control software will transition the vehicle into an alternate drive mode where the request may be fulfilled. The temperature of the motor's rotor, core, windings, and inverter, as well as the discharge limits of the HESS will all contribute to the performance capabilities of the vehicle's electric drive mode.

Series Drive Mode

In the series drive mode, the clutch that exists between the engine and P2 electric motor is opened and the vehicle is driven entirely using its electric propulsion system while the ICE and P1 electric motor function as a generator. Since there exists no mechanical connection between the ICE and the transmission, the engine speed may be set independently from that of the vehicle. The ICE may, therefore, function along its Optimal Operating Line (OOL) where the speed and torque are chosen so as to maximize its efficiency for a given output power.

The efficiencies and operating characteristics of both the ICE and P1 electric motor were considered when determining the OOL for the Camaro E/28's series drive mode. The OOL is displayed alongside the efficiency maps of both the P1 electric motor and the engine in Figure 8.7 and Figure 8.8, respectively. The star in either figure represents the Optimal Operating Point (OOP), or the setpoint which yields the highest generator efficiency. The P1 electric motor and ICE will operate at this setpoint given that the HESS may accept the energy being generated and that power being consumed by the P2 electric motor is less. If either of these constraints are violated the setpoint will deviate away from the OOP and along the OOL so that more, or less, power is generated.

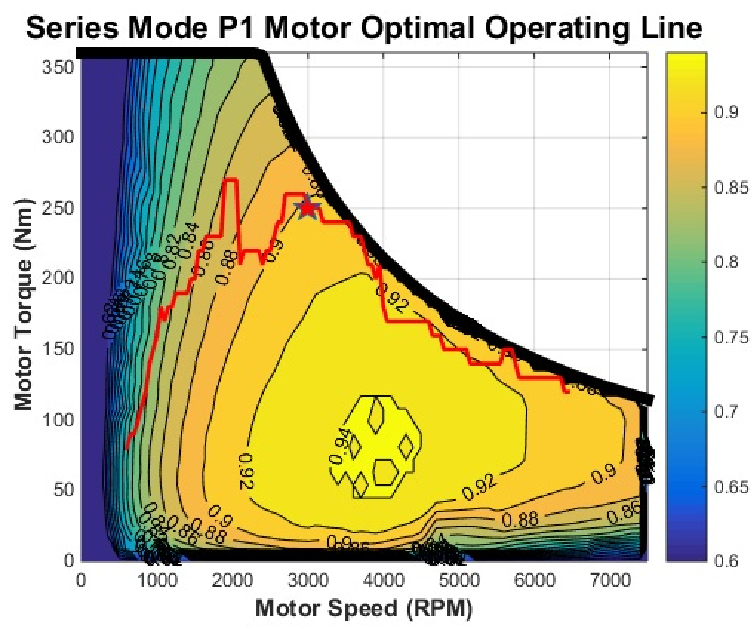

Figure 8.7: Series Drive Mode P1 Motor Optimal Operating Line

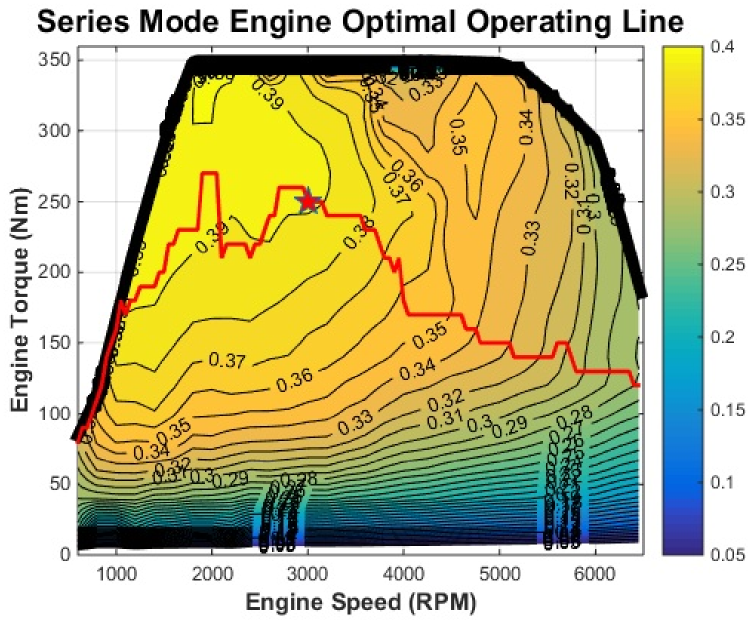

Figure 8.8: Series Drive Mode Engine Optimal Operating Line

In the series drive mode, it is necessary to directly equate the power that will be generated by the P1 electric motor and engine to a speed and torque setpoint. The generator speed at which a specific power request would be most efficiently met is demonstrated in Figure 8.9. The OOL can then be used to identify the torque which would produce the desired power.

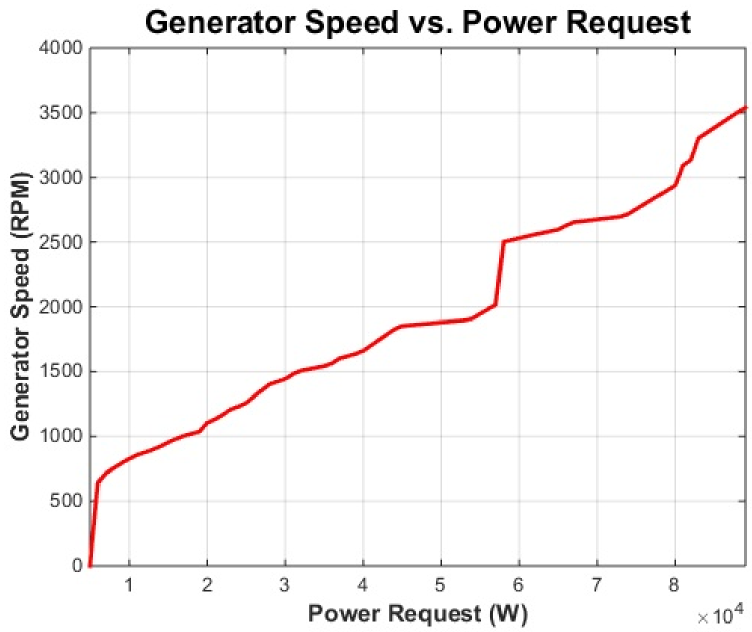

Figure 8.9: Generator Speed for a Given Power Request

The series drive mode is necessary when the power provided by the HESS is insufficient to meet the driver's requests. This is often the case during the vehicle's charge sustaining operating mode, where the HESS has reached its minimum allowable SOC. Without a series drive mode, the Camaro E/28 would be unable to recharge the HESS, forcing the vehicle to use its ICE to meet all tractive power requests. Without its electric propulsion system, the vehicle's fuel economy and dynamic performance would significantly decrease, which in turn, would adversely affect its drivability.

Parallel Drive Mode

In the parallel drive mode, the Camaro E/28's engine and two electric machines may all be used to meet the driver's tractive power requests. The power split between these three components is determined using the A-ECMS, and therefore, may change due to the current driving pattern.

The power split as determined by the A-ECMS represents the ideal solution to the energy management problem. In the event that the power request made to either of the electric machines cannot be fulfilled due to the thermal constraints of the motors or due to the charge/discharge limits of the HESS, the ICE will attempt to close the performance gap so that the driver's power request will still be met.

Figure 8.10, Figure 8.11, and Figure 8.12 demonstrate the torque requests made to the P1 electric motor, the P2 electric motor, and the engine while the vehicle is in its parallel drive mode, respectively. The power split shown was determined using the ECMS for an equivalence factor of 2.0.

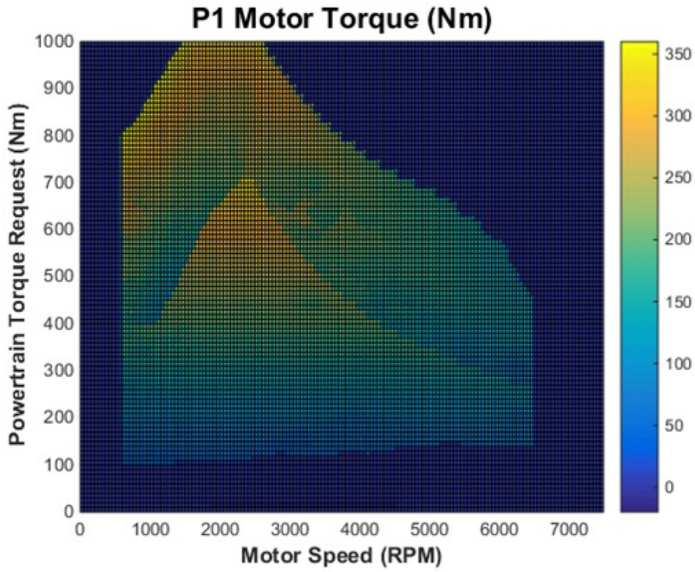

Figure 8.10: Parallel Drive Mode P1 Motor Torque Request

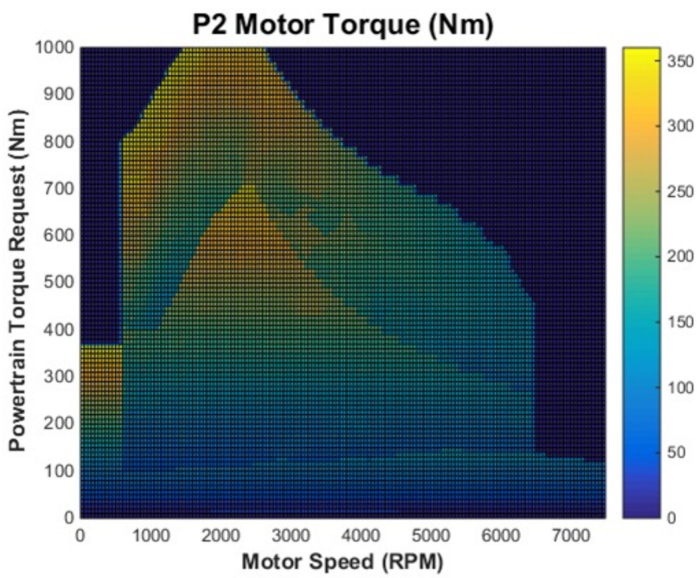

Figure 8.11: Parallel Drive Mode P2 Motor Torque Request

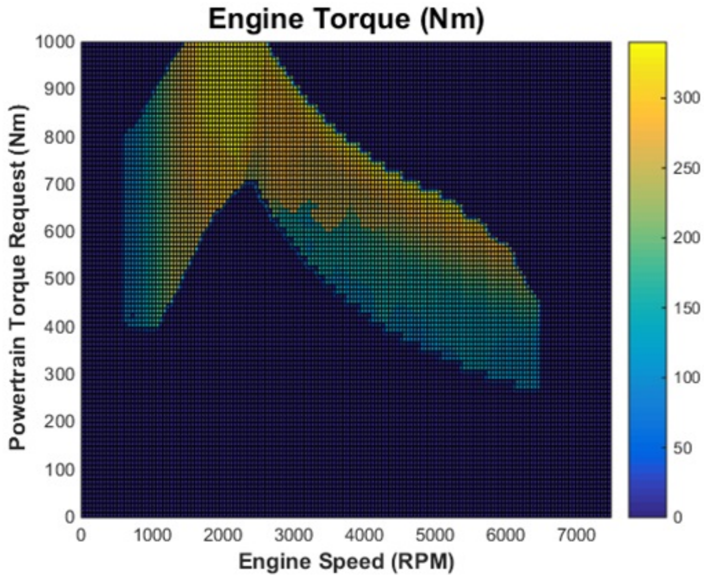

Figure 8.12: Parallel Drive Mode Engine Torque Request

Engine-Only Drive Mode

The engine-only drive mode becomes available as a remediating action to a fault in the vehicle's high-voltage electrical system. All power requests made by the driver are fulfilled exclusively by the ICE, much like a traditional, non-electrified vehicle. The engine-only drive mode is undesirable, and typically goes unused, since the performance of the Camaro E/28 would actually be worse than that of the stock 2016 Chevrolet Camaro LT. The cause of the reduced performance is the added weight of the Camaro E/28's electrified powertrain components and the decreased power of its GM LTG ICE in comparison to the 2016 Chevrolet Camaro LT's 3.6L LGX V6 engine.

8.5.4 Transmission Optimal Gear Selection Schedule

The need for a transmission in a traditional combustion automobile is a consequence of the characteristics of the ICE. Engines need to operate at a relatively high rotational velocity, which is inappropriate in many situations. A transmission adapts the higher speed of the ICE to the drive wheels, increasing torque in the process. Electric machines, on the other hand, may operate at very low rotational velocities, producing their maximum achievable torque within this range. In either case, both engines and electric machines benefit from the use of a transmission since it allows their operating points to be adapted in order to achieve greater efficiencies.

The Camaro E/28 is capable of operating in numerous drive modes each of which uses electric machines, an ICE, or both. The transmission's gear selection schedule must, therefore, be optimized for each drive mode in order to achieve its maximum efficiency, and thereby, reduce fuel and energy consumption, reduce the production of emissions, and increase the utility of the HESS's stored electrical energy.

The vehicle's optimal gear selection schedules were developed by determining which of the transmission's gears would result in the powertrain's most efficient use of electrical and fuel energy for every possible combination of torque and speed setpoints. In order to accomplish this, efficiency maps of each of the four drive modes were derived and used for the optimization. Figure 8.13, Figure 8.14, and Figure 8.15 illustrate the optimal gear selection schedules for the electric/series, parallel, and engine-only drive modes, respectively.

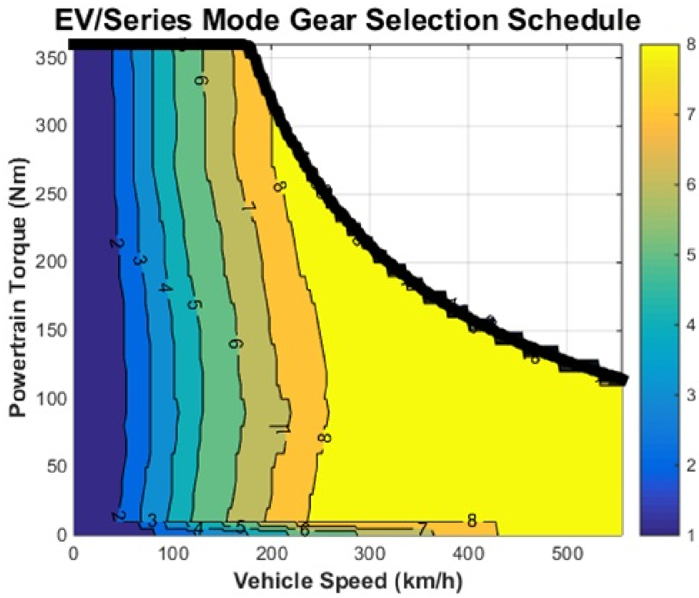

Figure 8.13: EV/Series Drive Mode Gear Selection Schedule

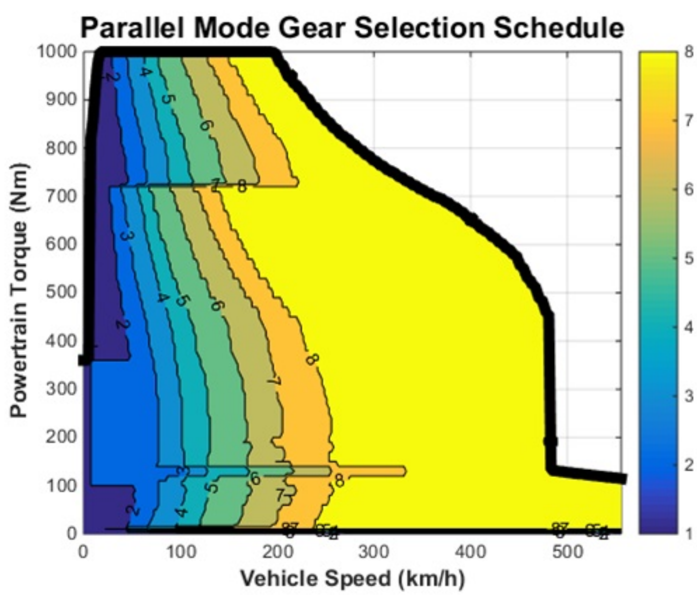

Figure 8.14: Parallel Drive Mode Gear Selection Schedule

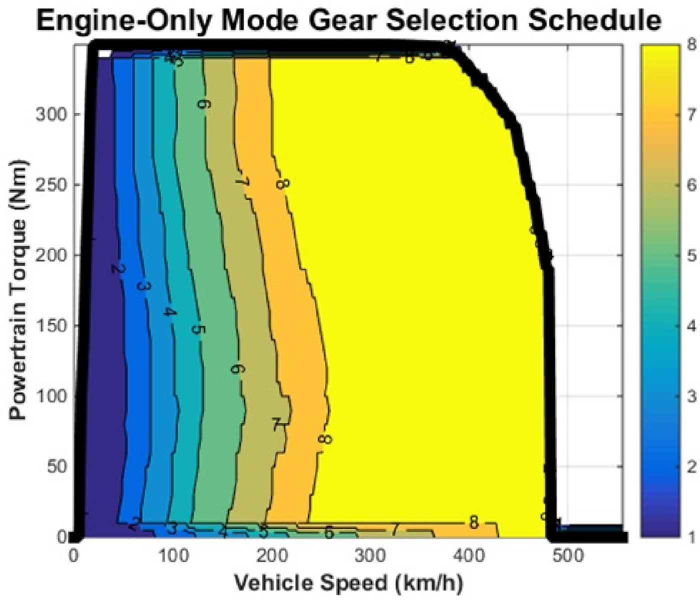

Figure 8.15: Engine-Only Drive Mode Gear Selection Schedule

8.6 Summary of Vehicle Control Algorithms

The design and implementation of the Camaro E/28's supervisory control algorithms occurred according to a rational and systematic process. Software requirements were developed, the modular structure and interfaces were defined, the dataflow dependencies were established, and the internal structures were fashioned as part of the control system's development. The vehicle's supervisory software was decomposed into thirteen modules and encompassed numerous control strategies. Only four strategies, however, were discussed in detail throughout the chapter. These areas of focus included the vehicle's startup procedure, drive mode selection, powertrain torque production, and optimal shift schedules.

The Camaro E/28's startup procedure took advantage of the fact that many of the aspects of the process may occur in parallel. This concurrency was implemented in Simulink Stateflow using a combination of parallel (AND) and exclusive (OR) states, and was instrumental in achieving the two second requirement that the EcoCAR 3 competition had for achieving propulsion readiness.

The Camaro E/28 was a series-parallel PHEV, and as such, was capable of operating in several drive modes, including: an electric drive mode, a series drive mode, a parallel drive mode, and an engine-only drive mode. The vehicle's supervisory control software selected from among these four modes depending upon a number of factors. The driver's power request, the HESS's SOC, the vehicle's performance mode, the status of the various powertrain components, and the current driving pattern all influenced which drive mode was ultimately chosen by the HSC.

Each of the vehicle's drive modes had a unique approach in determining how the driver's power request was met. In the electric and engine-only drive modes, for instance, the solution was trivial as the request was fulfilled entirely by the Camaro E/28's primary traction motor and ICE, respectively. The series and parallel drive modes, however, were much more complex as they required the supervisory control software to produce a solution to the vehicle's energy management problem.

For each of the Camaro E/28's drive modes, the transmission's gear selection schedule was required to be optimized so that the vehicle may achieve a high level of efficiency. For each mode of operation, the gear selection schedule was developed by determining which of the transmission's gears would result in the powertrain's most efficient use of energy for every possible combination of torque and speed setpoints.

Chapter 9

Control System Verification

Within the V-Model development cycle, the process of verification and calibration occurs following the design and implementation of the supervisory control software. This process is, however, iterative as testing exposes flaws and faults within the system that then require modifications to its design and/or implementation. To facilitate the verification of the Camaro E/28's control system, SoftECUs were developed and several features were built into the simulation tool described in Chapter 4 in order to facilitate the testing activities.

9.1 SoftECU Development

To support the development of control algorithms and to facilitate testability across the SIL and HIL environments, several SoftECUs, or software representations of the vehicle's ECUs, were developed. The SoftECUs that were chosen to be modelled are based upon the vehicle's control system architecture. The SoftECUs that were chosen for development are listed in Table 9.1.

SoftECU		**Function**
Battery Management Module	BMM	Monitor and management the HESS battery pack
Ultracapacitor Management Module	UCCM	Monitor and management the HESS ultracapacitor pack
HESS DC/DC Converter Module	BBCM	Transfer energy between the battery and ultracapacitor pack
P1 Motor Control Module	P1MCM	Control, and provide power to, the P1 electric motors
P2 Motor Control Module	P2MCM	Control, and provide power to, the P2 electric motors
Engine Control Module	ECM	Control the internal combustion engine
Transmission Control Module	TCM	Control the transmission
Low-Voltage Support Front Module	LVFM	Provides power to the added control modules (front)
Low-Voltage Support Rear Module	LVRM	Provides power to the added control modules (rear)
Dashboard Support Module	DSM	Supports added switches, buttons, and telemetry
HV-to-LV DC/DC Converter Module	APM	Provide power to the LV system
HV Compressor Module	HVCM	Control the HV compressor for air conditioning
Charger Control Module	CCM	Control the on-board charger

Table 9.1: Vehicle Model SoftECUs

The approach that was used in the development of the SoftECUs was one of accurate representation. Where possible, the manufacturer of each of the control units was contacted to obtain interfacing documentation and CAN databases. The interface between the HSC and the SoftECUs were then modelled as accurately as possible to ensure a seamless transition between the SIL and HIL testing environments.

The SoftECUs were also modelled to allow for the insertion of both simple and complex faults. This permitted the design and validation of the supervisory control software's remediating actions. Faults that may be simulated by the SoftECUs range from implausible/intermittent accelerator and brake pedal positions to HESS contactor faults (positive/negative contactor welds, precharge relay failure, HV interlock failure, etc.). The Soft BMM is illustrated in Figure 9.1, below.

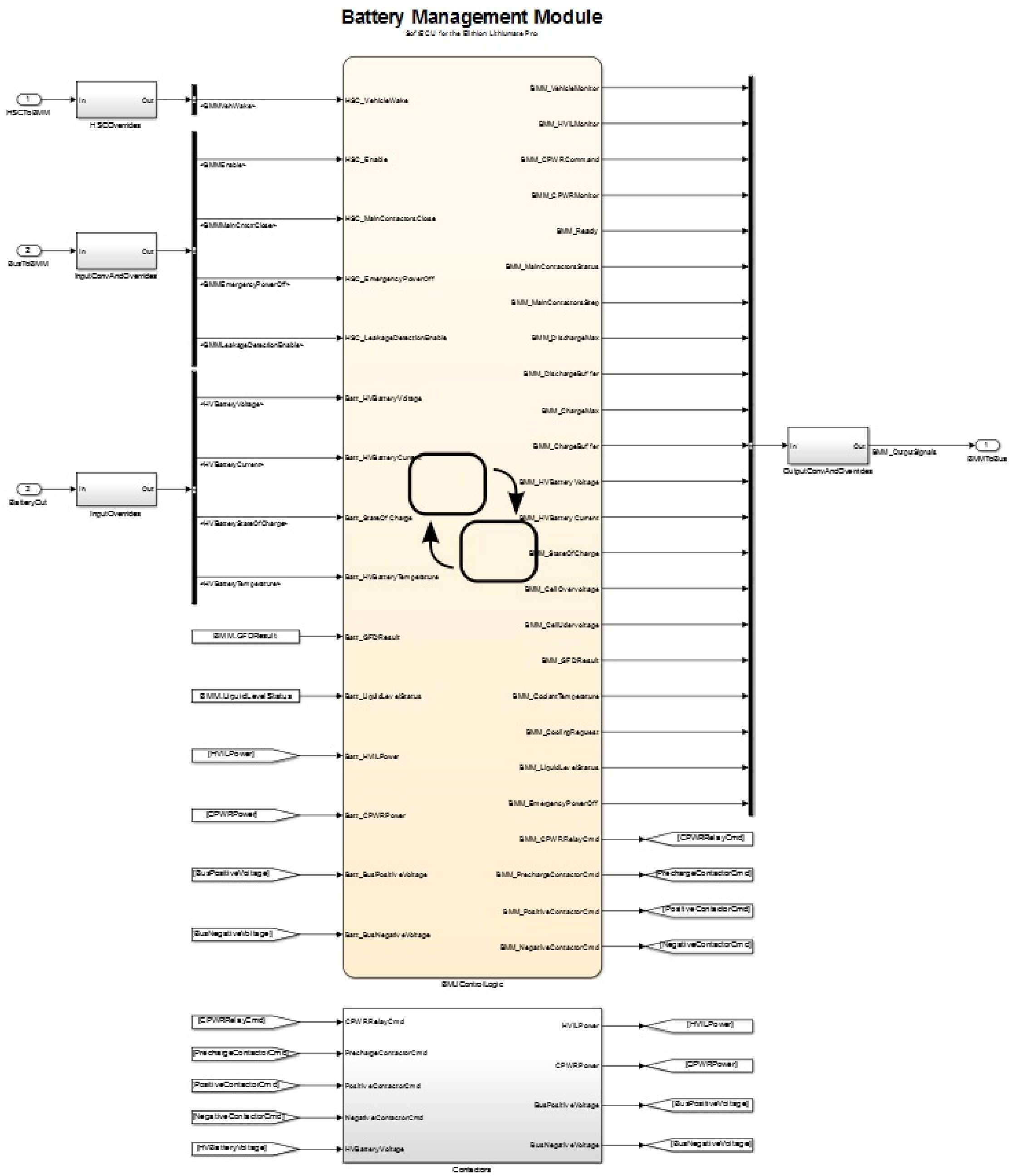

Figure 9.1: Soft BMM Model

Using time dependent logic in Stateflow, the SoftECUs are able to replicate the performance of the actual ECUs. Startup and shutdown procedures were accurately reproduced, outputs were updated accordingly, and expectations concerning the timeliness of inputs were maintained.

Much like how the HSC interacts with the vehicle through the ECUs, the SoftECUs have been developed to provide a similar interface to the vehicle model. During SIL and HIL verification, the SoftECUs acted as an intermediary between the supervisory control software and the vehicle model. They provided the control logic with realistic interactions, yet at the same time, allowed for the same interface to the vehicle model that existed during MIL development.

The supervisory control software may interface with the SoftECUs using the Simulink Vehicle Network Toolbox and a Vector Virtual CAN Channel instead of through a direct connection using Simulink signals [75] [76]. This is a more realistic means of modelling the transfer of data across the vehicle. Variables will be updated at the same rate as in the actual vehicle, and the control logic concerning the handling of dropped/inconsistent CAN messages may be implemented and tested during SIL development. The virtual CAN network interface between the control logic and the SoftECUs is shown below in Figure 9.2.

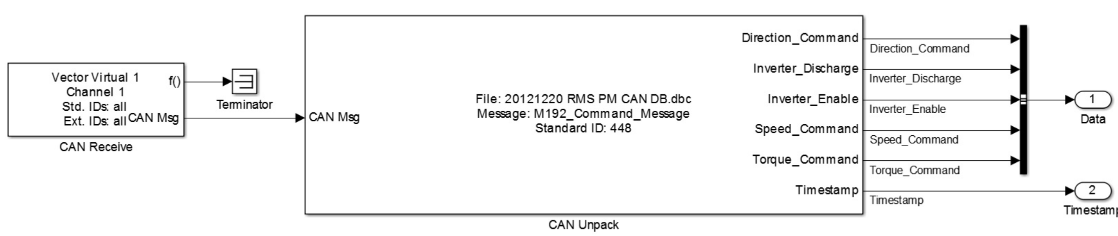

Figure 9.2: Virtual CAN Network Interface

9.2 Support for Testing Activities

One of the fundamental objectives for the development of the vehicle model was to maintain its ability to simulate the Camaro E/28 over a driving cycle regardless of the work being done in plant model or controller development. Several tools and practices were employed to meet this goal including model referencing, model variants, revision control, and Simulink Projects.

The simulation tool made extensive use of model referencing in order to achieve the parallel development of plant and controller models. Each component was created as an independent model that may be simulated and tested for validity separately from the full vehicle model. Each component was then referenced from within the simulation tool and used to perform analyses of the vehicle over a number of driving cycles. Model referencing also made revision control using Git a possibility.

In addition to model referencing, model variants were used to simulate the vehicle using higher/lower fidelity models (thermal models, etc.) and to seamlessly transition between the controllers used for testing in the MIL, SIL, and HIL environments. Higher fidelity models, specifically thermal models, caused the overall performance of the simulation tool to decrease, making it unsuitable for testing in the SIL and HIL environments where the tool is expected to run in real-time. Nevertheless, the information provided by these higher fidelity models were invaluable and having the ability to transition between models of varying fidelity was indispensable.

MATLAB's integrated support for version control, which helps to better manage the development of the vehicle models, was also used extensively. Git, a distributed version control system, was used to manage both the vehicle plant models as well as the supervisory control software. GitLab, a web-based Git repository manager, was also maintained in order to make the creation and merging of parallel development streams as seamless as possible [77].

Finally, Simulink Projects was used to view and label modified files and to help guide the peer review workflow. The projects helped monitor model and software change requests, and ultimately, allowed for projected milestones and software releases to be met [78].

9.2.1 Transition between Testing Environments

In addition to maintaining consistent model interfaces, both model referencing and model variants were used to seamlessly transition between the different testing environments. These tools allowed the controller model to be easily switched between the MIL controller, which uses simple heuristics to determine the power split between the electric machines and ICE and uses idealized signals; the SIL controller, which incorporated additional control and diagnostic logic and is representative of the actual vehicle's software; and the HIL controller, which allowed the vehicle model to interface with a HIL simulator. No changes, beyond that being made to the controller model variant, were required to be made to the vehicle model when transitioning between different testing environments. The interface used to transition the controller model's variant is illustrated in Figure 9.3.

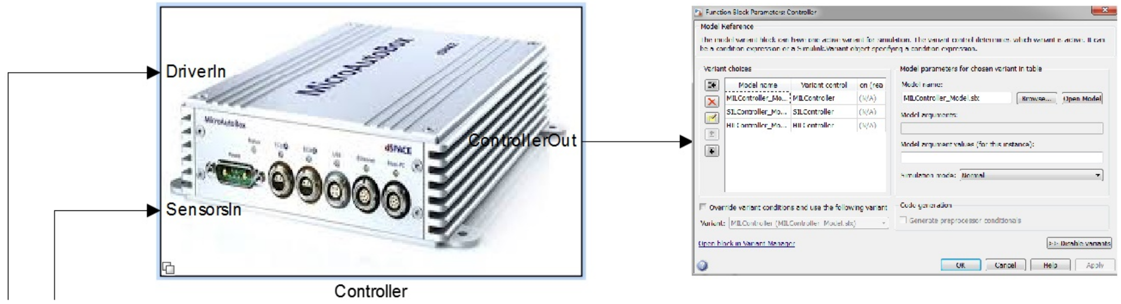

Figure 9.3: Controller Model Variant Transition Mechanism

9.2.2 Fault Insertion

Throughout its development process, several hazard analysis techniques helped guide the design and implementation of the Camaro E/28. The hazard analysis consisted of identifying which components and interfaces may fail and the remediating actions that must occur in response to each fault. The detection and appropriate response to these faults were required to be addressed when the control algorithms for the vehicle were being developed. In order to verify the correct operation of these algorithms, the vehicle model was required to be able to simulate each of these failures.

The three techniques that were used to conduct the hazard analysis were Systems Theoretic Process Analysis (STPA), Failure Mode and Effects Analysis (FMEA), and Fault Tree Analysis (FTA). The STPA was used to generate a set of control requirements, and the FMEA and FTA guided the production of test cases. FTA was of particular use when trying to identify the causes that may lead to failure of a particular component or subsystem. For this reason, FTA was used extensively when establishing the plant model requirements that would be used to support the testing activities.

Table 9.2 illustrates a test case developed from the aforementioned hazard analysis. The following test case was used to verify the ability of the HSC to identify the permanent loss of the accelerator pedal signal and perform the appropriate remediating actions.

Test Case Overview	
Test Identification Number:	2.0 Version: 1.0
Last Updated (mm/dd/yyyy):	01/01/2015
Author(s):	Alexander Lebel
System/Component:	Accelerator Pedal
Test Case Domain:	SIL/HIL
Test Case Description	
Test Case Name:	Permanent Loss of Accelerator Pedal Signal
Functionality Validated:	The test is used to validate the ability of the HSC to identify the permanent loss of the accelerator pedal signal and perform the appropriate remediating actions.
Components Involved:	The components involved in the test are: 1) The accelerator pedal, and 2) the HSC.
Process:	The test will be performed by removing the accelerator pedal signal from the HSC.
Test Case Procedure	
Test Initialization:	**SIL Testing Environment** 1) Load the vehicle model by executing the SimStartup script. By default, both accelerator pedal signals should be connected to the HSC controller. 2) Run the vehicle model, having the driver model follow any appropriate driving cycle. **HIL Testing Environment**

	1) Ensure that both of the accelerator pedal's analog signal wires are connected to the HSC as specified in the _MABXII_PinOut document. 2) Ensure that the HSC is connected to the HIL simulator as specified in the Control_dSpaceHIL_PinOut document. The HIL simulator will be used to provide power to both the accelerator pedal and the HSC. An analog output from the HSC will be used to request torque from the ECM SoftECU and a CAN channel will be used to request torque from the P1/P2 MCM SoftECUs.
Test Body:	**SIL Testing Environment** The permanent loss of the accelerator pedal signal may be simulated by inserting the fault within the driver model. 1) Navigate to MEE3T_SimulationTool/DriverModel/AutomatedDriver. 2) The fault may be inserted by setting APPFailureMode/Value to 4. **HIL Testing Environment** The permanent loss of the accelerator pedal signal may be simulated by either: 1) Preventing the HIL simulator from providing power to the accelerator pedal, or 2) Permanently interrupting one/both of the analog signals from the accelerator pedal to the HSC.
Test Completion:	**SIL Testing Environment** In order to return the vehicle model back to its original state, the model must be stopped and the permanent loss of the accelerator pedal fault must be removed from within the driver model. 1) Navigate to MEE3T_SimulationTool/DriverModel/AutomatedDriver. 2) The fault may be removed by setting APPFailureMode/Value to 0. 3) Navigate to MEE3T_SimulationTool/SILController/HSC/ SignalDiag/DriverInput_SignalDiag. 4) The fault may be cleared by setting AccelPdlFltClr/Value to 1 while the model is running. 5) AccelPdlFltClr /Value must be set to 0 after the fault has been cleared.

	HIL Testing Environment In order to return the vehicle model back to its original state, the model must be stopped and the functionality of the accelerator pedal restored. 1) Ensure that the accelerator pedal functionality is restored.
Test Case Summary	
Test Date (mm/dd/yyyy):	10/12/2015
Tested By:	Himesh Kurera
Expected Results:	In response to the permanent loss of the accelerator pedal signal, the HSC must: 1) prevent any further torque requests from being fulfilled, 2) alert the driver that the fault has occurred, and 3) prevent the fault from being cleared until the vehicle has been repaired by a qualified technician. • Once the HSC has permanently lost the accelerator pedal signal, the HSC will register the fault within 500 ms. • The analog signals to the ECM SoftECU and the CAN messages to the P1/P2 MCM SoftECUs will indicate a torque request of 0 Nm. • The TFM_FaultMsg CAN message will be transmitted periodically at a rate of 1 Hz by the HSC. This message is used to notify the driver of the fault.
Actual Results	• Fault was identified by the HSC within 500 ms. • The HSC prevented further torque requests from being fulfilled. • TFM_FaultMsg CAN message transmitted periodically at a rate of 1 Hz by the HSC.
Pass/Fail	Pass

Table 9.2: Permanent Loss of Accelerator Pedal Signal Test Case

The faults were modelled in either the vehicle's plant models or SoftECUs, and the necessary control strategies were developed. These faults ranged from the failure of a powertrain component to the loss of CAN messages on the vehicle's control networks. These faults were inserted into the vehicle model during testing in either the SIL or HIL environments.

Figure 9.4 illustrates how various faults associated with the vehicle's control networks were inserted into the vehicle model.

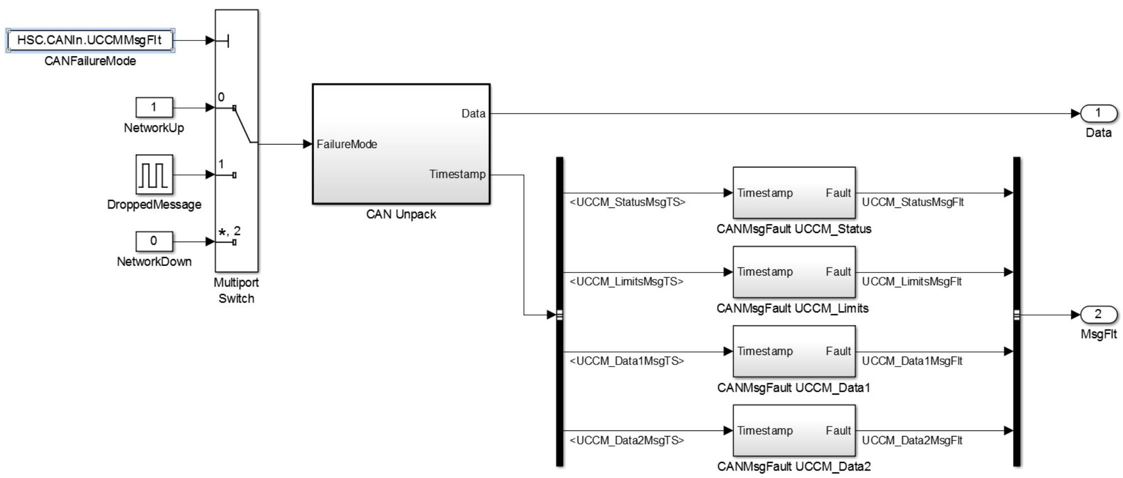

Figure 9.4: Insertion of CAN Network Faults into the Vehicle Model

The automated execution of testing routines was accomplished using MATLAB scripts and Report Generator, and dSpace AutomationDesk in the SIL and HIL testing environments, respectively [79]. These tools allowed the entire suit of test cases to be conducted automatically on every iteration of the vehicle's supervisory control logic. The results were recorded and reviewed by both the McMaster Engineering EcoCAR 3 Team's System Modeling and Simulation Subteam and its System Safety Subteam. Any issues that are discovered are submitted as a change request for the next version of the vehicle's software.

9.3 Summary of Control System Verification

The verification of the Camaro E/28's supervisory control system was an iterative process and required substantial consideration towards the facilitation of testing activities. SoftECUs were developed to permit the vehicle's software to interface with the simulation tool described in Chapter 4 in a realistic manner and allowed for faults to be inserted in both the SIL and HIL environments. Model referencing, model variants and Simulink Projects were employed alongside practices from software engineering, like revision control and continuous integration, to support collaboration, guide the peer review workflow, and ensured that projected milestones were met. Several hazard analysis techniques, including STPA, FMEA, and FTA, were involved in the generation of control requirements and in the identification of the Camaro E/28's failure modes. Test cases were then produced and used to ensure that the vehicle's control algorithms were able to detect and appropriately respond to these fault scenarios.

Chapter 10

Analysis of Control Strategies and Vehicle Electrification

One of the most significant indicators of the performance of a vehicle's control strategy is to evaluate its environmental impact over a set of regulatory driving cycles that reproduce common situations and are used for official estimates. The Camaro E/28's supervisory control software was assessed using the simulation tool described in Chapter 4 and the methods outlined in Chapter 5. Several noteworthy parameters used in the simulation of the Camaro E/28 are provided in Appendix B and Appendix C contains supplementary results to those presented in this chapter.

10.1 Analysis of A-ECMS

The impact that the A-ECMS has on the Camaro E/28, and the potential for its introduction into the energy management strategies of hybrid electric vehicles, was assessed by comparing its performance against that of a purely thermal control strategy as well as against the results obtained using the non-adaptive ECMS (perfectly tuned). Table 10.1 illustrates the outcome of this analysis and the improvements achieved for the vehicle's energy consumption, fuel consumption, and emissions.

	Pure Thermal	Optimal ECMS		A-ECMS	
Specification	**Value**	**Value**	**Improv. (%)**	**Value**	**Improv. (%)**
UF-Weighted Fuel Energy Consumption	643 Wh/km (32.4 mpg)	491 Wh/km (42.5 mpg)	23.6%	491 Wh/km (42.5 mpg)	23.6%
UF-Weighted Electric Energy Consumption	58 Wh/km	86 Wh/km	-48.3%	86 Wh/km	-48.3%
UF-Weighted Total Energy Consumption	701 Wh/km (29.8 mpg)	577 Wh/km (36.1 mpg)	17.7%	577 Wh/km (36.1 mpg)	17.7%
UF-Weighted WTW Petroleum Energy Use	176 Wh PE/km	137 Wh PE/km	22.2%	137 Wh PE/km	22.2%
UF-Weighted WTW Greenhouse Gas Emissions	187 g GHG/km	162 g GHG/km	13.4%	162 g GHG/km	13.4%

Table 10.1: Performance Estimates Using Regulatory Driving Cycles

Although it has been proven that the A-ECMS achieves a sub-optimal solution when compared to other power management techniques such as DP, it will produce the best results among any approach that may be implemented in practice and used in every situation [63]. The estimated improvement of 18% to the Camaro E/28's fuel economy illustrates the impact of the strategy.

As further proof of the effectiveness of the A-ECMS, the algorithm was tested on a real-world driving cycle that does not belong to the regulatory cycles usually taken as reference. The cycle was obtained by measuring the velocity and elevation data of a route including urban, suburban, rural, and expressway driving throughout Hamilton, Ontario, Canada. The map of the driving cycle is illustrated in Figure 10.1

and its velocity and elevation profiles are provided by Figure 10.2 and Figure 10.3, respectively.

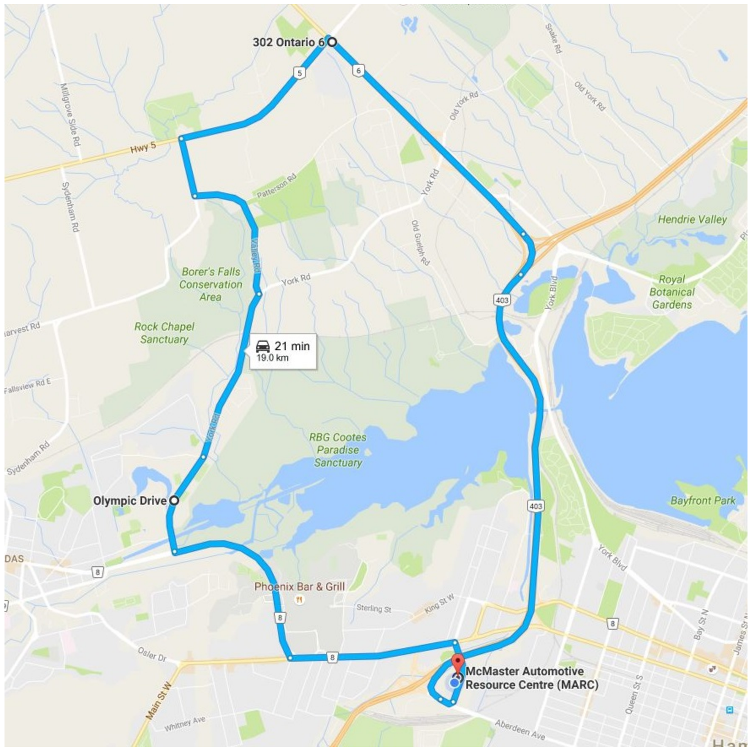

Figure 10.1: Real-World Driving Cycle Map

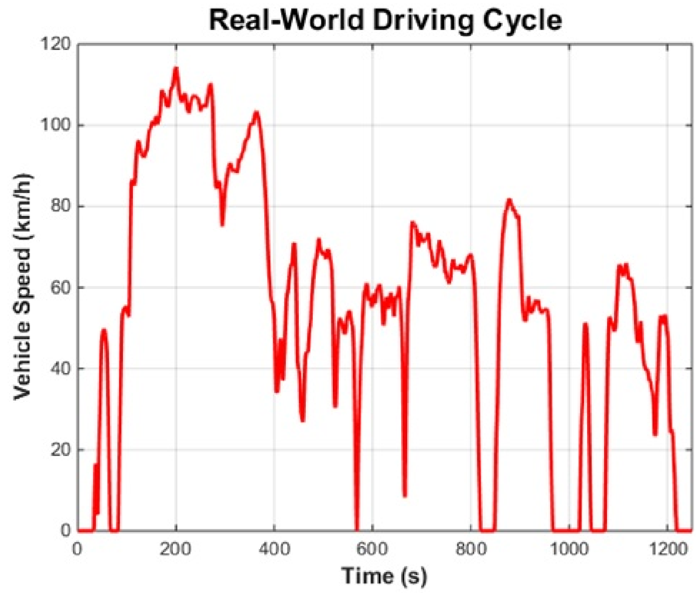

Figure 10.2: Real-World Driving Cycle

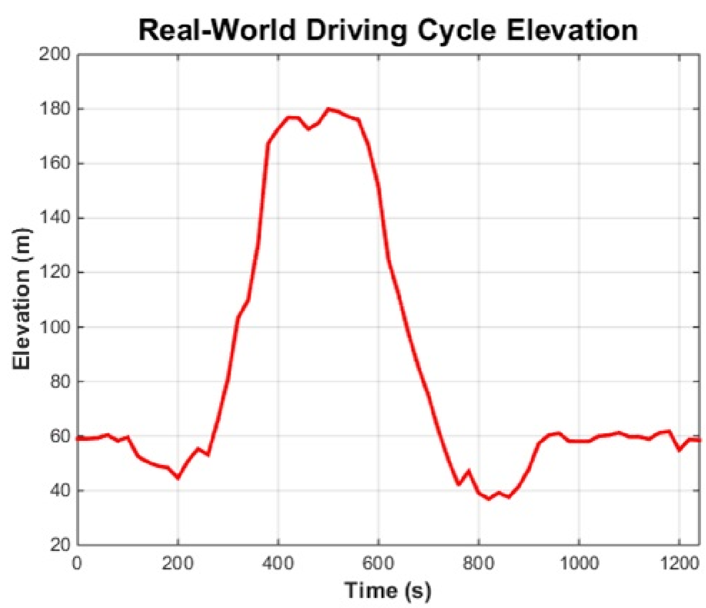

Figure 10.3: Real-World Driving Cycle Elevation

The analysis was performed and Table 10.2 compares the fuel and energy consumption, PEU, and emissions produced with the purely thermal control strategy, ECMS, and A-ECMS. Even in a driving cycle that was very different from the ones used to train and initially test the A-ECMS, the results are encouraging, with the control algorithm increasing the vehicle's fuel economy by more than 13 mpg over the purely thermal strategy.

	Pure Thermal	Optimal ECMS		A-ECMS	
Specification	**Value**	**Value**	**Improv. (%)**	**Value**	**Improv. (%)**
UF-Weighted Fuel Energy Consumption	356 Wh/km (58.6 mpg)	219 Wh/km (95.2 mpg)	38.5%	219 Wh/km (95.2 mpg)	38.5%
UF-Weighted Electric Energy Consumption	112 Wh/km	143 Wh/km	-27.7%	143 Wh/km	-27.7%
UF-Weighted Total Energy Consumption	468 Wh/km (44.6 mpg)	362 Wh/km (57.6 mpg)	22.6%	362 Wh/km (57.6 mpg)	22.6%
UF-Weighted WTW Petroleum Energy Use	126 Wh PE/km	64 Wh PE/km	49.2%	64 Wh PE/km	49.2%
UF-Weighted WTW Greenhouse Gas Emissions	157 g GHG/km	123 g GHG/km	21.6%	123 g GHG/km	21.6%

Table 10.2: Performance Estimates Using a Real-World Driving Cycle

Figure 10.4 shows the results of the A-ECMS's adaptation mechanism in recognizing the patterns contained within the real-world driving cycle. The patterns were categorized according to the observations of the passenger when the cycle data was recorded and were used to determine that the algorithm was capable of identifying the correct driving pattern 92% of the time.

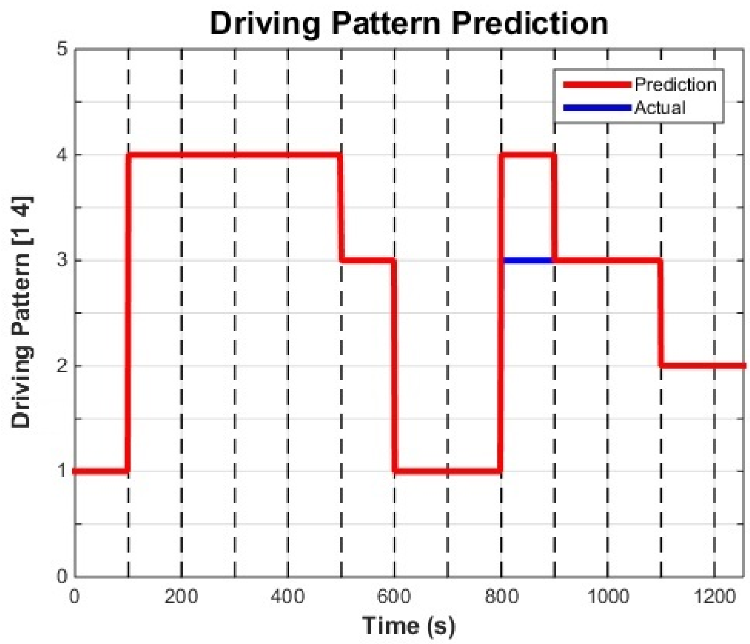

Identifier	Driving Pattern
1	Urban
2	Suburban
3	Rural
4	Expressway

Figure 10.4: Results of Driving Pattern Recognition

The distribution of the operating points for the Camaro E/28's two electric machines and its ICE were also used to confirm the results obtained using the A-ECMS. As shown by the clustering of dots in Figure 10.5 and Figure 10.6, the P1 electric motor is often used as a variable load for the engine, so that the latter can work in the highest efficiency regions. Moreover, the ICE's lower efficiency operating points are almost completely avoided, as the power requests are satisfied instead by an electric machine in these situations. The P2 electric motor also primarily operates in its most efficient regions due to the optimization of the Camaro E/28's gear selection schedules, as illustrated by the clustering of dots in Figure 10.7.

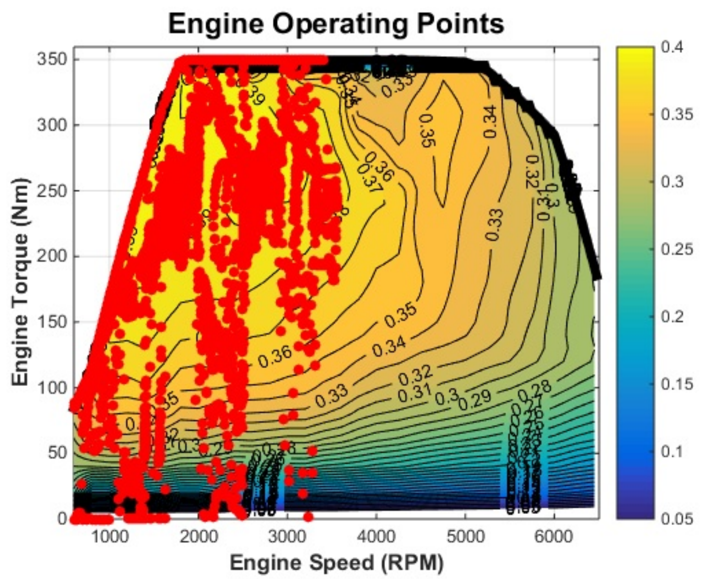

Figure 10.5: Internal Combustion Engine Operating Region

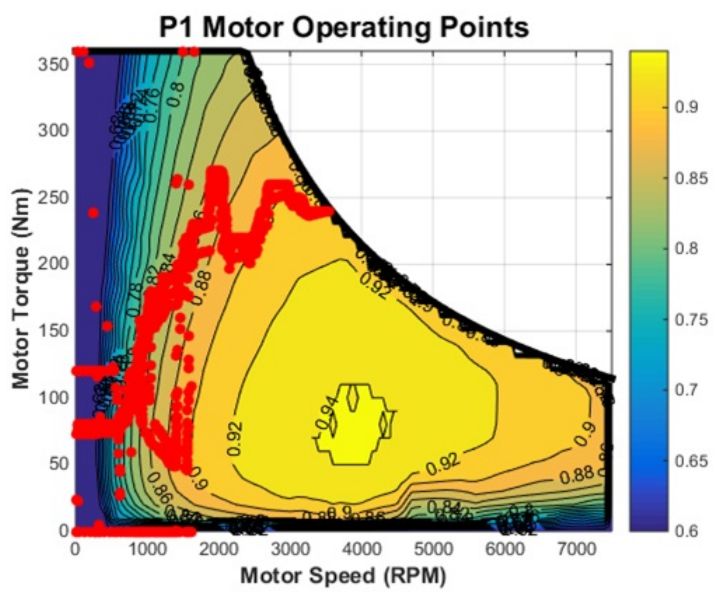

Figure 10.6: P1 Electric Motor Operating Region

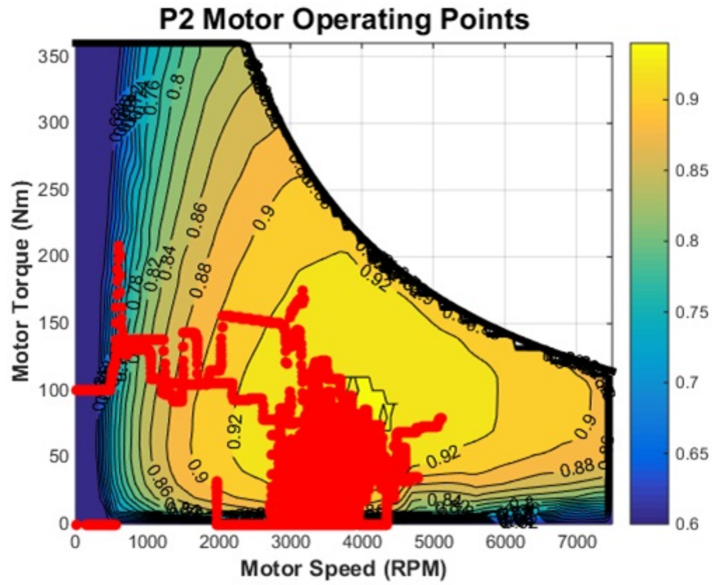

Figure 10.7: P2 Electric Motor Operating Region

10.2 Analysis of Vehicle Electrification

Although the A-ECMS was shown to improve the performance of the Camaro E/28, the impact that electrification had on the vehicle is also of interest. To assess the benefits, a model of the 2016 Chevrolet Camaro LT was developed. The methods outlined in Chapter 5 were used to approximate the energy and fuel consumption, PEU, and emissions produced by both vehicles, and it is these properties that are compared in Table 10.3 along with their respective technical specifications.

Specification	2016 Camaro LT	Camaro E/28	Improv. (%)
Total Power	250 kW	410 kW	64.0%
Curb Mass	1565 kg	1931 kg	-23.4%
Power-to-Weight Ratio	160 W/kg	212 W/kg	32.5%
Engine Displacement	3640 cc	1998 cc	45.1%
Acceleration, IVM – 100 km/h	5.3 s	4.6 s	13.2%
Acceleration, 80 – 110 km/h	3.4 s	2.2 s	35.3%
Braking, 100 – 0 km/h	38 m	39 m	-2.6%
Total Vehicle Range	673 km	402 km	-40.3%
UF-Weighted Fuel Energy Consumption	935 Wh/km (22.3 mpg)	491 Wh/km (42.5 mpg)	47.5%
UF-Weighted Electric Energy Consumption	0 Wh/km	86 Wh/km	N/A
UF-Weighted Total Energy Consumption	935 Wh/km (22.3 mpg)	577 Wh/km (36.1 mpg)	38.3%
UF-Weighted WTW Petroleum Energy Use	255 Wh PE/km	137 Wh PE/km	46.3%
UF-Weighted WTW Greenhouse Gas Emissions	229 g GHG/km	162 g GHG/km	29.3%

Table 10.3: 2016 Chevrolet Camaro LT and the E/28 Camano Comparison

The electrification of the 2016 Camaro LT was found to improve its fuel economy by approximately 38% and decrease its emissions by almost 30%.

10.3 Analysis of Dynamic Performance

The driving circuit selected to evaluate the dynamic performance of the Camaro E/28 was the Toronto Motorsport Park, located in Ontario, Canada. The circuit is 2.3 km in length and has an adequate combination of straights and corners so that a vehicle may experience a variety of dynamic events. The layout of the Toronto Motorsport Park, and the maximum velocity which the Camaro E/28 would be able achieve at various positions along the circuit, is illustrated by Figure 10.8.

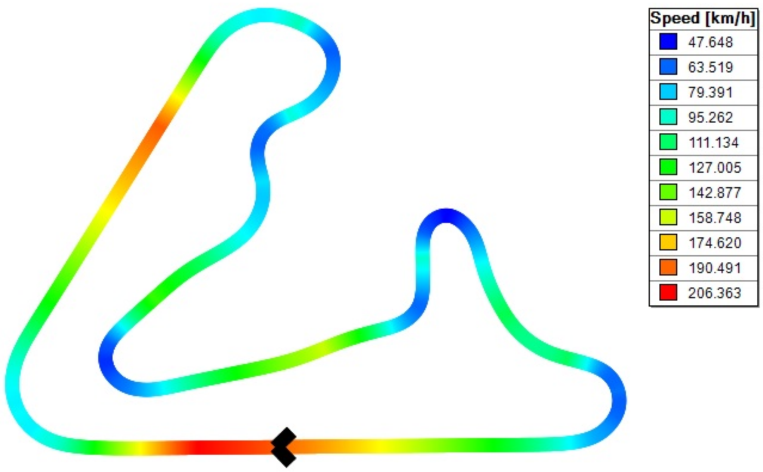

Figure 10.8: Toronto Motorsport Park Driving Circuit with Vehicle Speed

The velocity vs. distance driving cycle for the Toronto Motorsport Park is provided by Figure 10.9. It may be observed that the maximum velocity achievable by the Camaro E/28 along the circuit is 206 km/h and the slowest corner is taken at 47 km/h.

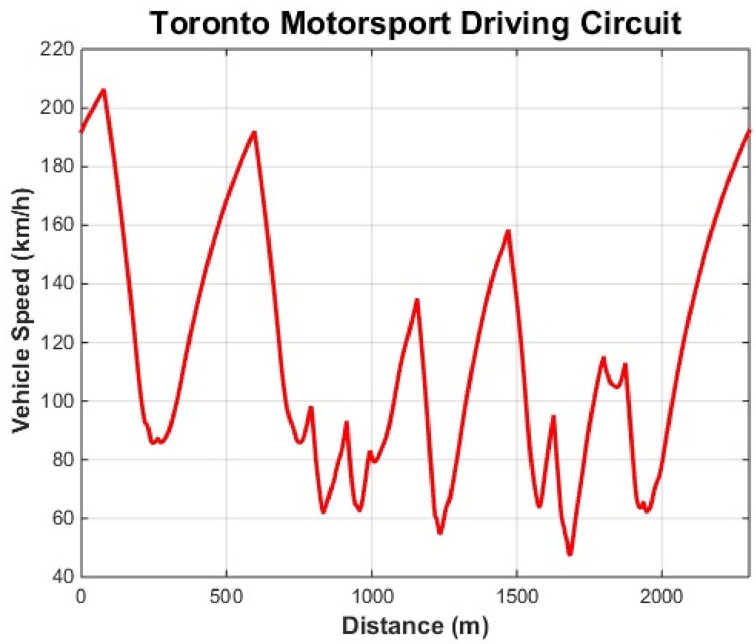

Figure 10.9: Toronto Motorsport Park Driving Cycle

The Camaro E/28 was simulated over fifteen laps on the Toronto Motorsport Park driving circuit and its lap times are displayed in Figure 10.10. Each stem of the plot represents a lap time with the vehicle starting from a complete stop for the first lap. It may be observed that the vehicle's lap times begin to increase after lap nine. The longer lap times are due to the increase in cell temperature of the HESS's battery pack which lowers the unit's discharge limit, and in turn, restricts the Camaro E/28's use of its electric propulsion system.

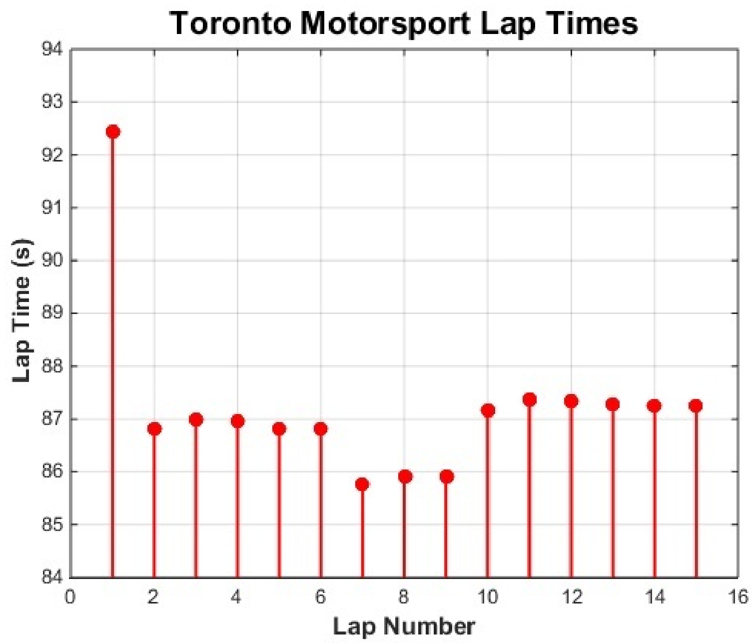

Figure 10.10: Toronto Motorsport Park Driving Cycle Lap Times

The dynamic performance of the vehicle was then compared against that of the 2015 Chevrolet Camaro Z/28, the performance benchmark for the Camaro E/28, as well as the 2016 Chevrolet Camaro LT, the platform from which the Camaro E/28 was developed. Each vehicle was simulated over several laps on Toronto Motorsport Park and their best lap times are provided in Table 10.4.

Vehicle	**Best Lap Time**
Camaro E/28	85.7 s
2015 Chevrolet Camaro Z/28	85.0 s
2016 Chevrolet Camaro LT	87.1 s

Table 10.4: Toronto Motorsport Park Driving Cycle Lap Time Comparison

Although the Camaro E/28 is capable of outperforming the 2016 Chevrolet Camaro LT, it is still marginally slower than the 2015 Chevrolet Camaro Z/28 around the Toronto Motorsport Park driving circuit. This deficiency may be explained by the increased weight of the Camaro E/28's electrified powertrain. Although the Camaro E/28 is expected to be slower than its intended benchmark vehicle, its dynamic performance has still been deemed as more than satisfactory.

10.4 Summary of Analysis of Control Strategies and Vehicle Electrification

The impact that the Camaro E/28's supervisory control algorithms have on the environment were evaluated using the simulation tool described in Chapter 4 and the methods outlined in Chapter 5. It was revealed that the estimated improvement to the vehicle's fuel economy due to the A-ECMS was approximately 18% greater than for a purely thermal control strategy. To further solidify these findings, the effectiveness of the A-ECMS was evaluated using a real-world driving cycle that does not belong to the regulatory set usually taken as reference. The algorithm's adaptation mechanism was able to identify the correct driving pattern 92% of the time and effectively improved the vehicle's total energy consumption for the trip by 13 mpg.

As the Camaro E/28 was developed from the 2016 Chevrolet Camaro LT, it was of interest to identify the improvement that electrification had on the vehicle. It was estimated that the introduction of the Camaro E/28's hybrid powertrain improved the fuel economy of the original vehicle by 14 mpg and decreased its production of emissions by almost 30%.

Lastly, the dynamic performance of the Camaro E/28 was evaluated by comparing its simulated lap times to those of other reference vehicles. The analysis was performed over fifteen laps on the Toronto Motorsport Park driving circuit and it was discovered that, although marginally slower than the Chevrolet Camaro Z/28, the Camaro E/28 was capable of outperforming the 2016 Chevrolet Camaro LT by 1.4 seconds.

Chapter 11

Future Research

As demonstrated throughout this research, the A-ECMS is ideal for use in a hybrid electric vehicle's energy management strategy. The algorithm is real-time oriented, computationally cheap, readily accounts for unexpected events, and has been shown to produce results comparable to those obtained using DP [63]. These results, however, may only be achieved with the reliable identification of the driving pattern and the perfect tuning of the equivalence factors.

Due the limited number of driving cycles available to researchers and automobile manufacturers, the variability of driving situations that an actual production vehicle is subject to is impossible to be captured within an A-ECMS. The utility of such a control strategy in practice is, therefore, questionable. The algorithm, if deployed in a real-world scenario, would ultimately need to adapt to new conditions as they are encountered if optimality is to be attained. Since the systematic optimization that is required to identify the equivalence factor that minimizes the vehicle's energy and fuel consumption for a given driving pattern is computationally intensive, such a process is not able to be feasibly performed using an automobile's control units.

A topic of future research, therefore, would be the use of a cloud computing service and remote software updates to achieve a vehicle (or a fleet of vehicles) that would learn from its surroundings and become more fuel efficient and produce less emissions as it is driven.

Using a Global Positioning System (GPS) and wireless connectivity, a vehicle would be able to record the velocity and grade for any given section of road (driving cycle) and transfer this data to a cloud computing service which would be able to handle the computational burden of identifying a suitable equivalence factor for that situation. Using the velocity and grade profiles, the driving cycle coordinates, and the newly identified control parameters, more accurate adaptation mechanisms for the A-ECMS may be developed and trained. The results of these calculations would then be used to remotely update the vehicle's control strategies. Figure 11.1 is a control block diagram for a A-ECMS which includes periodic remote updates to continuously improve the effectiveness of the algorithm.

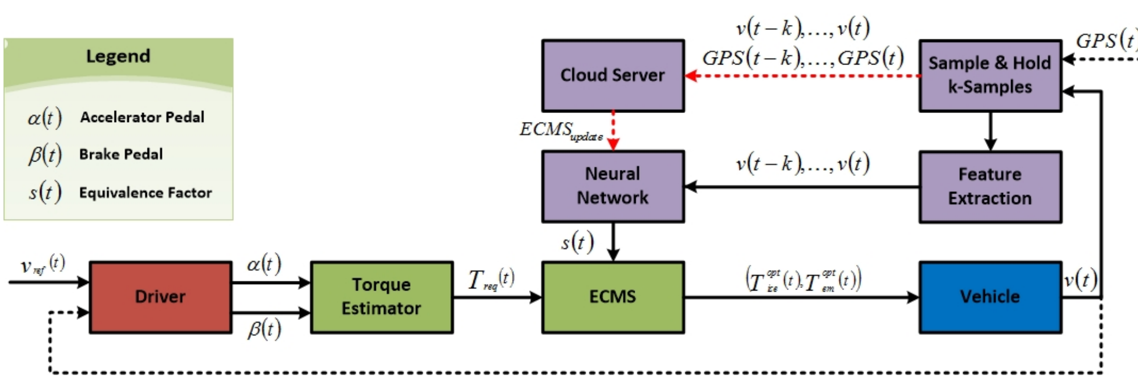

Figure 11.1: Control Block Diagram of the A-ECMS using Remote Updates

Although remote software updates for vehicles have traditionally been vilified as they are thought to introduce vulnerabilities, automobile manufacturers such as Tesla, BMW, Mercedes-Benz, and Volvo are beginning to introduce the technology as a means to add new features to their vehicles and to avoid costly recalls for issues that could have otherwise been corrected through software [80]. These same systems, ultimately, may be utilized to continuously improve a vehicle's performance over the course of their lifetime. This concept appears to be a natural progression for the automobile as an increasing number of technologies have already begun their integration into the internet of things.

Chapter 12

Conclusion

In order to curb the rampant progression of climate change, governing bodies from across the globe have placed restrictions on petroleum usage and on the production of criteria emissions. These regulations have presented a significant obstacle to the transportation sector which produces 14% of the global GHG emissions resulting from the burning of petroleum-based fuels, largely gasoline and diesel. In fact, the fuel economy of vehicles sold within the United States are required to increase incrementally from 35.5 mpg in 2016 to 54.5 mpg by 2025 [4]. The CAFE regulations enforce these limits with a fine of $5.50 per vehicle for every 0.1 mpg (or $55 per 1 mpg) by which a manufacturer's fleet falls short of the standard [81]. To avoid costly penalties, automobile manufacturers have invested significant resources into the research and development of EVs that meet these environmental regulations.

The presence of a bidirectional ESS and one or more electric machines within a vehicle allows for the reduction, or even elimination, of tailpipe emissions, but at the cost of increased control complexity. A solution to the energy management problem, a control strategy which seeks to minimize fuel consumption and emissions within a HEV or a PHEV, is a topic of intense and continuing research within the field of automotive engineering.

McMaster University, through competing in the AVTC program, EcoCAR 3, designed and implemented a high performance, fuel efficient, hybrid powertrain for the 2016 Chevrolet Camaro LT. The resulting vehicle, known as the Camaro E/28, was the platform for which the design and implementation of a control system was the basis for this research.

Throughout this thesis, the design of the Camaro E/28's control system and the implementation of its supervisory algorithms were presented. A solution to the vehicle's energy management problem was proposed and involved an A-ECMS that makes use of an artificial neural network to identify representative driving patterns. In order to evaluate the effectiveness of the control algorithms, a model of the Camaro E/28 was developed and used to approximate the vehicle's energy consumption, fuel consumption, and emissions. It was discovered that the A-ECMS was able to improve the performance of the vehicle by 18% over a purely thermal control strategy and that the vehicle's electrification improved the 2016 Chevrolet Camaro LT's fuel economy by 13.8 mpg.

It is obvious that the development of EVs and their software will play a significant role in curtailing petroleum usage within the transportation sector. As vehicles become increasingly intelligent the need for new and progressively more advanced control systems will endure.

Appendix A

Analysis of Control Network Loading

Control Unit		**Network Loading**
Battery Management Module	BMM	0.5%
Ultracapacitor Management Module	UCCM	3.3%
HESS DC/DC Converter Module	BBCM	10.5%
P1 Motor Control Module	P1MCM	19.9%
P2 Motor Control Module	P2MCM	19.9%
Low-Voltage Support Front Module	LVFM	0.5%
Low-Voltage Support Rear Module	LVRM	0.5%
Dashboard Support Module	DSM	1.2%
HV-to-LV DC/DC Converter Module	APM	5.7%
HV Compressor Module	HVCM	0.5%
Total Network Loading		62.5%

Table A.1: High Speed EcoLAN CAN Network Bus Loading Estimates

Control Unit		**Network Loading**
Engine Control Module	ECM	40.5%
Total Network Loading		40.5%

Table A.2: High Speed ICELAN CAN Network Bus Loading Estimates

Control Unit		**Network Loading**
Transmission Control Module	TCM	44.6%
Total Network Loading		44.6%

Table A.3: High Speed TransLAN CAN Network Bus Loading Estimates

Control Unit		**Network Loading**
Hybrid Supervisory Controller	HSC	30.0%
Stock Vehicle Controllers	GMLAN	26.7%
Total Network Loading		56.7%

Table A.4: High Speed GMLAN CAN Network Bus Loading Estimates

Appendix B

Camaro E/28 Simulation Parameters

N·s^2/kg·m

Component	Simulation Parameters	Value
Fuel (E85)	Fuel-Specific Energy by Mass (kWh/kg)	7.96
	Fuel Density (kg/L)	0.7871
Internal Combustion Engine (GM LTG)	Displacement (L)	2
	Peak Torque (Nm)	400
	Peak Power (kW)	184
	Idle Speed (RPM)	640
	Max Speed (RPM)	6500
Electric Motors (YASA-P400)	Peak Power (kW)	145 (400V)
	Continuous Power (kW)	100
	Max Torque (Nm)	390
	Continuous Torque (Nm)	300
	Max Speed (RPM)	8,000

Transmission (GM 8L90)	Ratios	1st Gear	4.56
		2nd Gear	2.97
		3rd Gear	2.08
		4th Gear	1.69
		5th Gear	1.27
		6th Gear	1
		7th Gear	0.85
		8th Gear	0.65
	Efficiency (%)		92
Wheels	Rolling Resistance ($C1 + C2 \cdot V_{veh}$)	$C1$ (N)	0.00757
		$C2$ (N·s/m)	0.00012
	Coefficient of Friction		0.97
	Dynamic Radius (m)		0.355
Electrical Accessory	Constant Load (W)		200
Vehicle	Frontal Area (m^2)		2.165
	Coefficient of Drag		0.35
	Center of gravity height (m)		0.35
	Wheelbase (m)		2.85
	Front Weight Bias		0.52
Final Drive	Ratio		2.77
	Efficiency (%)		96

Table B.1: Camaro E/28 Simulation Parameters

Appendix C

Analysis of Control Strategies and Vehicle Electrification

	Pure Thermal	**Optimal ECMS**		**A-ECMS**	
Specification	**Value**	**Value**	**Improv. (%)**	**Value**	**Improv. (%)**
UF-Weighted Fuel Energy Consumption	543 Wh/km (38.4 mpg)	229 Wh/km (91.0 mpg)	57.8%	229 Wh/km (91.0 mpg)	57.8%
UF-Weighted Electric Energy Consumption	52 Wh/km	114 Wh/km	-119.2%	114 Wh/km	-119.2%
UF-Weighted Total Energy Consumption	595 Wh/km (35.0 mpg)	343 Wh/km (60.8 mpg)	42.4%	343 Wh/km (60.8 mpg)	42.4%
UF-Weighted WTW Petroleum Energy Use	151 Wh PE/km	66 Wh PE/km	56.3%	66 Wh PE/km	56.3%
UF-Weighted WTW Greenhouse Gas Emissions	158 g GHG/km	112 g GHG/km	29.1%	112 g GHG/km	29.1%

Table C.1: Performance Estimates Using the 505 Driving Cycle

	Pure Thermal	Optimal ECMS		A-ECMS	
Specification	**Value**	**Value**	**Improv. (%)**	**Value**	**Improv. (%)**
UF-Weighted Fuel Energy Consumption	478 Wh/km (43.6 mpg)	178 Wh/km (117.2 mpg)	62.8%	178 Wh/km (117.2 mpg)	62.8%
UF-Weighted Electric Energy Consumption	47 Wh/km	136 Wh/km	-189.4%	136 Wh/km	-189.4%
UF-Weighted Total Energy Consumption	525 Wh/km (39.7 mpg)	314 Wh/km (66.4 mpg)	40.2%	314 Wh/km (66.4 mpg)	40.2%
UF-Weighted WTW Petroleum Energy Use	133 Wh PE/km	53 Wh PE/km	60.2%	53 Wh PE/km	60.2%
UF-Weighted WTW Greenhouse Gas Emissions	139 g GHG/km	110 g GHG/km	20.9%	110 g GHG/km	20.9%

Table C.2: Performance Estimates Using the HWFET Driving Cycle

	Pure Thermal	Optimal ECMS		A-ECMS	
Specification	**Value**	**Value**	**Improv. (%)**	**Value**	**Improv. (%)**
UF-Weighted Fuel Energy Consumption	978 Wh/km (21.3 mpg)	660 Wh/km (31.6 mpg)	32.5%	660 Wh/km (31.6 mpg)	32.5%
UF-Weighted Electric Energy Consumption	75 Wh/km	101 Wh/km	-34.7%	101 Wh/km	-34.7%
UF-Weighted Total Energy Consumption	1053 Wh/km (19.8 mpg)	761 Wh/km (27.4 mpg)	27.7%	761 Wh/km (27.4 mpg)	27.7%
UF-Weighted WTW Petroleum Energy Use	270 Wh PE/km	184 Wh PE/km	31.9%	184 Wh PE/km	31.9%
UF-Weighted WTW Greenhouse Gas Emissions	275 g GHG/km	211 g GHG/km	23.3%	211 g GHG/km	23.3%

Table C.3: Performance Estimates Using the US06C Driving Cycle

	Pure Thermal	Optimal ECMS		A-ECMS	
Specification	**Value**	**Value**	**Improv. (%)**	**Value**	**Improv. (%)**
UF-Weighted Fuel Energy Consumption	604 Wh/km (34.5 mpg)	375 Wh/km (55.6 mpg)	37.9%	375 Wh/km (55.6 mpg)	37.9%
UF-Weighted Electric Energy Consumption	60 Wh/km	148 Wh/km	-146.7%	148 Wh/km	-146.7%
UF-Weighted Total Energy Consumption	664 Wh/km (31.4 mpg)	523 Wh/km (39.9 mpg)	21.2%	523 Wh/km (39.9 mpg)	21.2%
UF-Weighted WTW Petroleum Energy Use	168 Wh PE/km	107 Wh PE/km	36.3%	107 Wh PE/km	36.3%
UF-Weighted WTW Greenhouse Gas Emissions	177 g GHG/km	164 g GHG/km	7.3%	164 g GHG/km	7.3%

Table C.4: Performance Estimates Using the US06H Driving Cycle

	Driving Cycle			
Specification	**505**	**HWFET**	**US06C**	**US06H**
UF-Weighted Fuel Energy Consumption	995 Wh/km (21.0 mpg)	792 Wh/km (26.3 mpg)	1,111 Wh/km (18.8 mpg)	880 Wh/km (23.7 mpg)
UF-Weighted WTW Petroleum Energy Use	272 Wh PE/km	216 Wh PE/km	303 Wh PE/km	240 Wh PE/km
UF-Weighted WTW Greenhouse Gas Emissions	243 g GHG/km	194 g GHG/km	272 g GHG/km	215 g GHG/km

Table C.5: Performance Estimates for the 2016 Chevrolet Camaro LT

Bibliography

[1] Wirasingha, Sanjaka G.; Schofield, Nigel; Emadi, Ali. Plug-in hybrid electric vehicle developments in the US: trends, barriers, and economic feasibility. Harbin, China, 2008. IEEE Vehicle Power and Propulsion Conference.

[2] Office of the Press Secretary. Obama Administration National Fuel Efficiency Policy: Good For Consumers, Good For The Economy And Good For The Country. Online, May 2009. URL https://www.whitehouse.gov/the-press-office/fact-sheet-and-particpants-todays-rose-garden-event. Accessed 10 October 2016.

[3] National Highway Traffic Safety Administration. Obama Administration Finalizes Historic 54.5 mpg Fuel Efficiency Standards. Online, August 2012. URL http://www.nhtsa.gov/About-NHTSA/Press-Releases/2012/Obama-Administration-Finalizes-Historic-54.5-mpg-Fuel-Efficiency-Standards. Accessed 10 October 2016.

[4] United States Enviromental Protection Agency. EPA and NHTSA Set

Standards to Reduce Greenhouse Gases and Improve Fuel Economy for Model Years 2017-2025 Cars and Light Trucks. Online, August 2012. URL https://www3.epa.gov/otaq/climate/documents/420f12051.pdf. Accessed 9 October 2016.

[5] Center for Climate and Energy Solutions. Comparison of Actual and Projected Fuel Economy for New Passenger Vehicles. Online, June 2014. URL http://www.c2es.org/federal/executive/vehicle-standards/fuel-economy-comparison. Accessed 9 October 2016.

[6] Bossel, Ulf. Does a Hydrogen Economy Make Sense? *Proceedings of the IEEE*, 94(10):1826 – 1837, 2006.

[7] Markus, Frank; Brantley, Brian; Lutz, Cory. 2017 Tesla Model S P100D First Test: A New Record - 0 - 60 mph in 2.28 seconds! Online, February 2017. URL http://www.motortrend.com/cars/tesla/model-s/2017/2017-tesla-model-s-p100d-first-test-review/. Accessed 22 February 2017.

[8] Roper, David L. Tesla Model S. Online, September 2016. URL http://www.roperld.com/science/TeslaModelS.htm. Accessed 22 February 2017.

[9] Sorokanich, Bob. The Tesla Model S P100D Is Not the "Fastest Car in the World". Online, August 2016. URL http://www.roadandtrack.com/new-cars/news/a30536/tesla-model-s-p100d-quickest-not-fastest/. Accessed 22 February 2017.

[10] Ford, Tom; Turner, Charlie; Marriage, Ollie. LaFerrari vs McLaren P1 vs Porsche 918. Online, November 2014. URL `http://www.topgear.com/car-news/supercar/laferrari-vs-mclaren-p1-vs-porsche-918`. Accessed 22 February 2017.

[11] Argonne National Laboratory. Homepage: Advanced Vehicle Technology Competitions. Online, 2016. URL `http://avtcseries.org/`. Accessed 1 April 2016.

[12] Argonne National Laboratory. *EcoCAR 3: Non-Year-Specific Rules.* Argonne, Illinois, G edition, March 2016.

[13] Government of Canada. Ali Emadi: Canada Excellence Research Chair in Hybrid Powertrain. Online, March 2014. URL `http://www.cerc.gc.ca/chairholders-titulaires/emadi-eng.aspx`. Accessed 1 April 2016.

[14] Stiene, Tyler. Analysis of a Hybrid Energy Storage System and Electrified Turbocharger in a Performance Vehicle. Masters thesis, McMaster University, 2017 January.

[15] Parnas, David Lorge; Clements, Paul C. A Rational Design Process: How and Why to Fake It. *IEEE Transactions on Software Engineering*, 12(2):251 – 257, 1986.

[16] Forsberg, Kevin; Mooz, Harold. The Relationship of System Engineering to the Project Cycle. Chattanooga, TN, 1991. Joint Conference of National

Council On Systems Engineering and the American Society for Engineering Management.

[17] MathWorks. Simulink: Simulation and Model-Based Design. Online, 2016. URL https://www.mathworks.com/products/simulink.html. Accessed 4 November 2016.

[18] IBM. Rational Statemate: Rapidly develop complex embedded systems with prototypes. Online, 2016. URL http://www-03.ibm.com/software/products/en/ratistat. Accessed 4 November 2016.

[19] National Instruments. LabVIEW: System Design Software. Online, 2016. URL http://www.ni.com/labview/. Accessed 4 November 2016.

[20] Sangiovanni-Vincentelli, Alberto; Di Natale, Marco. Embedded System Design for Automotive Applications. *Computer*, 40(10):42 – 51, 2007.

[21] MathWorks. Model-Based Design. Online, 2016. URL https://www.mathworks.com/help/simulink/gs/model-based-design.html. Accessed 15 October 2016.

[22] Jaikamal, Vivek. Model Based ECU Development: An Integrated MIL, SIL, HIL Approach. Detroit, MI, 2009. SAE World Congress.

[23] Sciarretta, Antonio; Guzzella, Lino. Control of Hybrid Electric Vehicles. *IEEE Control Systems Magazine*, 27(2):60 – 70, 2007.

[24] Serrao, Lorenzo; Onori, Simona; Rizzoni, Giorgio. A Comparative Analysis of Energy Management Strategies for Hybrid Electric Vehicles. *Journal of Dynamic Systems, Measurement, and Control*, 133(3):1 – 9, 2011.

[25] General Motors. 2014 Camaro Z/28 the Most Track-capable Camaro Ever. Online, March 2013. URL http://media.gm.com/media/us/en/gm/news.detail.html/content/Pages/news/us/en/2013/Mar/nyas/27mar-chevrolet/0327-2014-camaro-z28.html. Accessed 10 October 2016.

[26] Motor Trend Channel. Talking 2014 Chevrolet Camaro Z/28 with Chief Engineer Al Oppenheiser! Wide Open Throttle Ep. 74. Online, July 2013. URL https://www.youtube.com/watch?v=jCnbwm4dcFs. Accessed 10 October 2016.

[27] YASA Motors. Homepage: YASA Motors. Online, 2016. URL http://www.yasamotors.com/. Accessed 1 April 2016.

[28] YASA Motors. P400 Series: Compact Axial Flux Motors and Generators. Online, Milton Park, Abingdon, UK, October 2016. URL http://www.yasamotors.com/wp-content/uploads/2015/09/YASA_P400_Product_Sheet.pdf. Accessed 1 April 2016.

[29] Rinehart Motion Systems, LLC. Homepage: Rinehart Motion Systems, LLC. Online, 2015. URL http://www.rinehartmotion.com/. Accessed 19 September 2016.

[30] Rinehart Motion Systems, LLC. PM100 and PM150 Family Propulsion Inverters. Online, Wilsonville, OR, 2016. URL http://www.rinehartmotion.com/uploads/5/1/3/0/51309945/pm100-150datasheet_2.pdf. Accessed 1 April 2016.

[31] GM Authority. GM 2.0 Liter Turbo I4 Ecotec LTG Engine. Online, 2016. URL http://gmauthority.com/blog/gm/gm-engines/ltg/. Accessed 19 September 2016.

[32] U.S. Department of Energy. Flex-fuel Vehicles. Online, 2016. URL https://www.fueleconomy.gov/feg/flextech.shtml. Accessed 19 September 2016.

[33] Vermont Tuning. Camaro 2.0T Performance. Online, 2016. URL http://www.vermonttuning.com/products/chevrolet/chevrolet-camaro-2-0t/. Accessed 19 September 2016.

[34] GM Authority. GM 8-Speed 8L90 M5U Hydra-Matic Automatic Transmission. Online, 2016. URL http://gmauthority.com/blog/gm/gm-transmissions/m5u/. Accessed 19 September 2016.

[35] Lukic, Srdjan M.; Cao, Jian; Bansal, Ramesh C.; Rodriguez, Fernando; Emadi, Ali. Energy Storage Systems for Automotive Applications. *IEEE Transactions on Industrial Electronics*, 55(6):2258 – 2267, 2008.

[36] Cao, Jian; Emadi, Ali. A New Battery/UltraCapacitor Hybrid Energy Storage System for Electric, Hybrid, and Plug-In Hybrid Electric Vehicles. *IEEE Transactions on Power Electronics*, 27(1):122 – 132, 2012.

[37] Skeleton Technologies. Skelcap: High Energy Ultracapacitor. Online, Bautzen, Germany, 2016. URL http://skeletontech.com/datasheets/skelcap-energy-en.pdf. Accessed 3 October 2016.

[38] Berkeley Energy and Resources Collaborative. The Promise of Energy Storage. Online, January 2016. URL https://www.studentenergy.org/posts/529-the-promise-of-energy-storage. Accessed 3 October 2016.

[39] LG Chem. Product Specification: Rechargeable Lithium Ion Battery Model: INR18650HG2 3000mAh. Online, October 2014. URL https://www.imrbatteries.com/content/lg_INR18650HG2.pdf. Accessed 3 October 2016.

[40] BJM Energy Corporation. Lithium Ion Capacitor ULTIUMO. Online, May 2012. URL http://jsr-nv.savvybyte.com/docs/ULTIMO%20Brocure-en.pdf. Accessed 3 October 2016.

[41] BRUSA Elektronik AG. BDC546-Bidirectional 750V DC/DC-Converter. Online, 2016. URL http://www.brusa.biz/fileadmin/template/

Support-Center/Datenbl%C3%A4tter/BRUSA_DB_EN_BDC546.pdf. Accessed 3 October 2016.

[42] AllCell Technologiesy. Phase Change Composite (PCC) Thermal Management Material. Online, 2014. URL https://www.allcelltech.com/index.php/products/thermal-management-material. Accessed 4 November 2016.

[43] AllCell Technologies. PCC: Thermal Management Material. Online, Chicago, IL, 2014. URL https://www.allcelltech.com/images/datasheets/pcc/AllCell_PCC.pdf. Accessed 3 October 2016.

[44] MathWorks. MATLAB: The Language of Technical Computing. Online, 2016. URL https://www.mathworks.com/products/matlab.html. Accessed 4 November 2016.

[45] MathWorks. Simulink: Simulation and Model-Based Design. Online, 2016. URL https://www.mathworks.com/products/simulink.html. Accessed 4 November 2016.

[46] MathWorks. Simscape: Model and simulate multidomain physical systems. Online, 2016. URL https://www.mathworks.com/products/simscape.html. Accessed 4 November 2016.

[47] Argonne National Laboratory. Autonomie. Online, 2016. URL http://www.autonomie.net/. Accessed 25 October 2016.

[48] MathWorks. Model and Simulate a Complete Car. Online, 2016. URL http://www.mathworks.com/help/physmod/sdl/drive/modeling-and-simulating-a-complete-car.html. Accessed 19 September 2016.

[49] MathWorks. Torque Converter. Online, 2016. URL http://www.mathworks.com/help/physmod/sdl/ref/torqueconverter.html. Accessed 19 September 2016.

[50] Irimescu, A.; Mihon, L.; Pdure, G. Automotive Transmission Efficiency Measurement Using a Chassis Dynamometer. *International Journal of Automotive Technology*, 12(4):555 – 559, 2011.

[51] MathWorks. Simscape Power Systems: Model and simulate electrical power systems. Online, 2016. URL https://www.mathworks.com/products/simpower.html. Accessed 8 November 2016.

[52] Siemens. Thermal Analysis. Online, 2016. URL https://www.plm.automation.siemens.com/en_us/products/simcenter/3d/thermal-analysis/. Accessed 4 November 2016.

[53] MathWorks. Statistics and Machine Learning Toolbox. Online, 2016. URL https://www.mathworks.com/products/statistics.html. Accessed 4 November 2016.

[54] MathWorks. Vehicle Body. Online, 2016. URL `http://www.mathworks.com/help/physmod/sdl/ref/vehiclebody.html#zmw`. Accessed 26 October 2016.

[55] Argonne National Laboratory. GREET Model: The Greenhouse gases, Regulated Emissions, and Energy use in Transportation Model. Online, 2016. URL `https://greet.es.anl.gov/`. Accessed 2 October 2016.

[56] U.S. Department of Energy. Detailed Test Information. Online, 2016. URL `http://www.fueleconomy.gov/feg/fe_test_schedules.shtml`. Accessed 2 October 2016.

[57] United States Enviromental Protection Agency. Fuel Economy Labeling of Motor Vehicles: Revisions To Improve Calculation of Fuel Economy Estimates. *Federal Register*, 71(248), 2006.

[58] Hybrid - EV Committee. Utility Factor Definitions for Plug-In Hybrid Electric Vehicles Using Travel Survey Data. *SAE International*, 2010.

[59] Hybrid - EV Committee. Recommended Practice for Measuring the Exhaust Emissions and Fuel Economy of Hybrid-Electric Vehicles, Including Plug-in Hybrid Vehicles. *SAE International*, 2010.

[60] Garrett, Jerry. Frankfurt Motor Show: The Record-Breaking Porsche 918 Spyder Has Arrived. Online, September 2013. URL `http://wheels.blogs.nytimes.com/2013/09/10/`

frankfurt-motor-show-the-record-breaking-porsche-918-spyder-has-arrived/?ref=automobiles&_r=1. Accessed 3 November 2016.

[61] OptimumG. OptimumLap: Vehicle Dynamics Simulation, Simplified. Online, 2016. URL http://www.optimumg.com/software/optimumlap/. Accessed 3 November 2016.

[62] OptimumG. OptimumLap v1.4 Documentation. Denver, CO, 2016.

[63] Musardo, Cristian; Rizzoni, Giorgio; Guezennec, Yann; Staccia, Benedetto. A-ECMS: An Adaptive Algorithm for Hybrid Electric Vehicle Energy Management. *European Journal of Control*, 11(4):509 – 524, 2005.

[64] Wang, Rui; Lukic, Srdjan M. Review of Driving Conditions Prediction and Driving Style Recognition Based Control Algorithms for Hybrid Electric Vehicles. Chicago, IL, 2011. IEEE Vehicle Power and Propulsion Conference.

[65] Jeon, Soon-il; Jo, Sung-tae; Park, Yeong-il; Lee, Jang-moo. Multi-Mode Driving Control of a Parallel Hybrid Electric Vehicle Using Driving Pattern Recognition. *Journal of Dynamic Systems, Measurement, and Control*, 124(1): 141 – 149, 2002.

[66] Bata, Reda; Yacoub, Yasser; Wang, Wenguang; Lyons, Donald; Gambino, Michele; Rideout, Greg. Heavy Duty Testing Cycles: Survey and Comparison. *SAE International*, pages 29 – 41, 1994. SAE Technical Paper.

[67] Murphey, Yi L.; Chen, ZhiHang; Kiliaris, Leo; Park, Jungme; Kuang, Ming; Masrur, Abul; Phillips, Anthony. Neural Learning of Driving Environment

Prediction for Vehicle Power Management. Hong Kong, 2008. IEEE International Joint Conference on Neural Networks (IEEE World Congress on Computational Intelligence).

[68] dSpace. MicroAutoBox II: Compact and robust prototyping system for in-vehicle applications. Online, 2016. URL `https://www.dspace.com/en/pub/home/products/hw/micautob.cfm`. Accessed 27 October 2016.

[69] dSpace. ControlDesk: Universal modular experiment and instrumentation software for electronic control unit (ECU) development. Online, 2016. URL `https://www.dspace.com/en/inc/home/products/sw/experimentandvisualization/controldesk.cfm`. Accessed 27 October 2016.

[70] dSpace. AutomationDesk: Powerful test authoring and automation tool. Online, 2016. URL `https://www.dspace.com/en/pub/home/products/sw/test_automation_software/automdesk.cfm`. Accessed 27 October 2016.

[71] CANbus Academy. CAN Bus Load Calculator. Online, 2016. URL `https://www.canbusacademy.com/resources/can-bus-load-calculator/`. Accessed 15 November 2016.

[72] Gauthier, Richard; Pont, Stephen. *Designing Systems.* Prentice-Hall, TEnglewood Cliffs, NJ, 1970.

[73] Parnas, David Lorge. On the Criteria To Be Used in Decomposing Systems into Modules. *Communications of the ACM*, 15(12):1053 – 1058, 1972.

[74] Chris Brune. *RMS CAN Protocol*. Rinehart Motion Systems, LLC, Wilsonville, OR, revision 4.1 edition, November 2015.

[75] MathWorks. Vehicle Network Toolbox. Online, 2016. URL `http://www.mathworks.com/help/releases/R2016b/vnt/index.html`. Accessed 26 October 2016.

[76] Vector. XL-Driver-Library. Online, July 2016. URL `http://vector.com/portal/medien/cmc/factsheets/XL_Driver_Library_Factsheet_EN.pdf`. Accessed 26 October 2016.

[77] GitLab. Homepage: GitLab. Online, 2016. URL `https://about.gitlab.com/`. Accessed 27 October 2016.

[78] MathWorks. Simulink Projects: Simulink in Teams. Online, 2016. URL `https://www.mathworks.com/discovery/simulink-projects.html`. Accessed 27 October 2016.

[79] MathWorks. MATLAB Report Generator. Online, 2016. URL `https://www.mathworks.com/help/rptgen/`. Accessed 27 October 2016.

[80] Taub, Eric A. Your Cars New Software Is Ready. Update Now? Online, September 2016. URL `http://www.nytimes.com/2016/09/09/automobiles/your-cars-new-software-is-ready-update-now.html`. Accessed 3 November 2016.

[81] United States Government Accountability Office. Vehicle Fuel Economy: Reforming Fuel Economy Standards Could Help Reduce Oil Consumption by

Cars and Light Trucks, and Other Options Could Complement These Standards. Online, Washington, D.C., August 2007. URL http://www.gao.gov/assets/270/265059.pdf. Accessed 4 November 2016.